ATTACHMENT 5 TO C1101-05

WESTINGHOUSE ELECTRIC CORPORATION
AFFIDAVIT FOR WITHHOLDING FROM PUBLIC DISCLOSURE

ATTACHMENT 6 TO C1101-05

WCAP-15753 NON-PROPRIETARY VERSION OF WCAP-14118,
"STRUCTURAL INTEGRITY EVALUATION OF REACTOR VESSEL UPPER HEAD
PENETRATIONS TO SUPPORT CONTINUED OPERATION:
D. C. COOK UNITS 1 AND 2"

ATTACHMENT 7 TO C1101-05

INDIANA MICHIGAN POWER COMPANY (I&M) SUMMARY OF
WESTINGHOUSE ELECTRIC CORPORATION
WCAP-14118, REVISION 4

To address flaws that may be discovered during the Vessel Head Penetration (VHP) inspections at Donald C. Cook Nuclear Plant (CNP) Units 1 and 2, Westinghouse Electric Corporation (Westinghouse) prepared and issued Revision 4 to WCAP – 14118, "Structural Integrity Evaluation of Reactor Vessel Upper Head Penetrations to Support Continued Operation: D. C. Cook Units 1 and 2." This document is unique to the CNP units and specifically addresses axial, circumferential, and lack of fusion flaws including:

- Acceptance criteria
- Flaw tolerance
- Material properties, fabrication history and crack growth prediction
- Stress analysis
- Industry experience

This analysis specifically addresses the stresses from fabrication as well as operational stresses using CNP-specific data and does not rely upon the less comprehensive EPRI susceptibility model (which only considered time-at-temperature). Instead, a detailed three dimensional elastic-plastic finite element analysis was used. Also, unlike the EPRI model which considers susceptibility only for the penetration base metal, all crack locations are addressed including the weld.

I&M intends to use the criteria in this document to evaluate flaws for continued service should any be discovered during VHP inspections. The analysis is very conservative and is intended to be such to account for uncertainties and provide a significant margin against reactor coolant leakage or an extremely unlikely rod ejection event. For example, the estimate for a circumferential flaw growing to a critical flaw size is at least 38 Effective Full Power Years (EFPY) and does not credit the time for a crack to grow through-wall from an axial flaw to allow primary water into the annulus area. CNP 2 presently has accumulated less than 15 EFPY. Therefore, even if a through-wall crack had developed for CNP 2 early in its plant life, the model predicts a substantial additional amount of operating time before any potential safety issue would be presented.

The cracking in VHP tubes has now been confirmed to be Primary Water Stress Corrosion Cracking (PWSCC). Important factors which affect this process are: a) relatively high residual stresses that are produced in the outermost penetrations due to fabrication and welding processes; b) operating temperature of the reactor vessel head; and c) length of operating time. Higher temperatures and longer time are more detrimental to the process of PWSCC. The current EPRI model for calculating the susceptibility ranking considers only time and temperature effects and does not consider effect of residual stresses developed by the construction and welding process.

I&M currently understands that a significant contribution to the leakage of VHP penetrations at other stations is directly attributable to cold working during rotary straightening of the penetration prior to or during installation. It must be noted that neither of the CNP unit's VHP penetrations were subjected to the same degree of cold working during fabrication or installation. Domestic industry experience with leakage to date seems to support this distinction in fabrication and construction practices as a likely contributor to VHP leakage.

Westinghouse Non-Proprietary Class 3

WCAP - 15753

Structural Integrity Evaluation of Reactor Vessel Upper Head Penetrations to Support Continued Operation: D. C. Cook Units 1 and 2

Westinghouse Electric Company LLC

WCAP-15753

Structural Integrity Evaluation of Reactor Vessel Upper Head Penetrations to Support Continued Operation: D. C. Cook Units 1 and 2

W. H. Bamford
K. R. Hsu

October 2001

Reviewed by: _____
P. L. Strauch

Approved by: _____
S. A. Swamy, Manager
Structural Mechanics Technology

Westinghouse Electric Company LLC
P.O. Box 355
Pittsburgh, PA 15230-0355

TABLE OF CONTENTS

SECTION 1.0
INTRODUCTION

In September of 1991, a leak was discovered in the reactor vessel control rod drive head penetration region of an operating plant. This has led to the question of whether such a case could occur at D. C. Cook Unit 1 or 2. The geometry of interest is shown in Figure 1-1.

The leak resulted from cracking which occurred in the outermost penetrations of a number of operating plants, as discussed in Section 2. This outermost location, as well as the center penetration, was chosen for fracture mechanics analyses to support continued safe operation of D. C. Cook Unit 1 or 2 if such cracking were to be found.

The basis of the analyses was a detailed three dimensional elastic-plastic finite element analysis of the two penetration locations, as described in detail in Section 5. The geometry of the hillside penetration analyzed is shown in Figure 1-2.

The fracture analyses were carried out using reference crack growth rates developed from the literature and from service experience. The results are presented in the form of flaw evaluation charts for both surface and through wall flaws, to determine the allowable time of safe operation if indications are found. All the times calculated in this handbook are effective full power years.

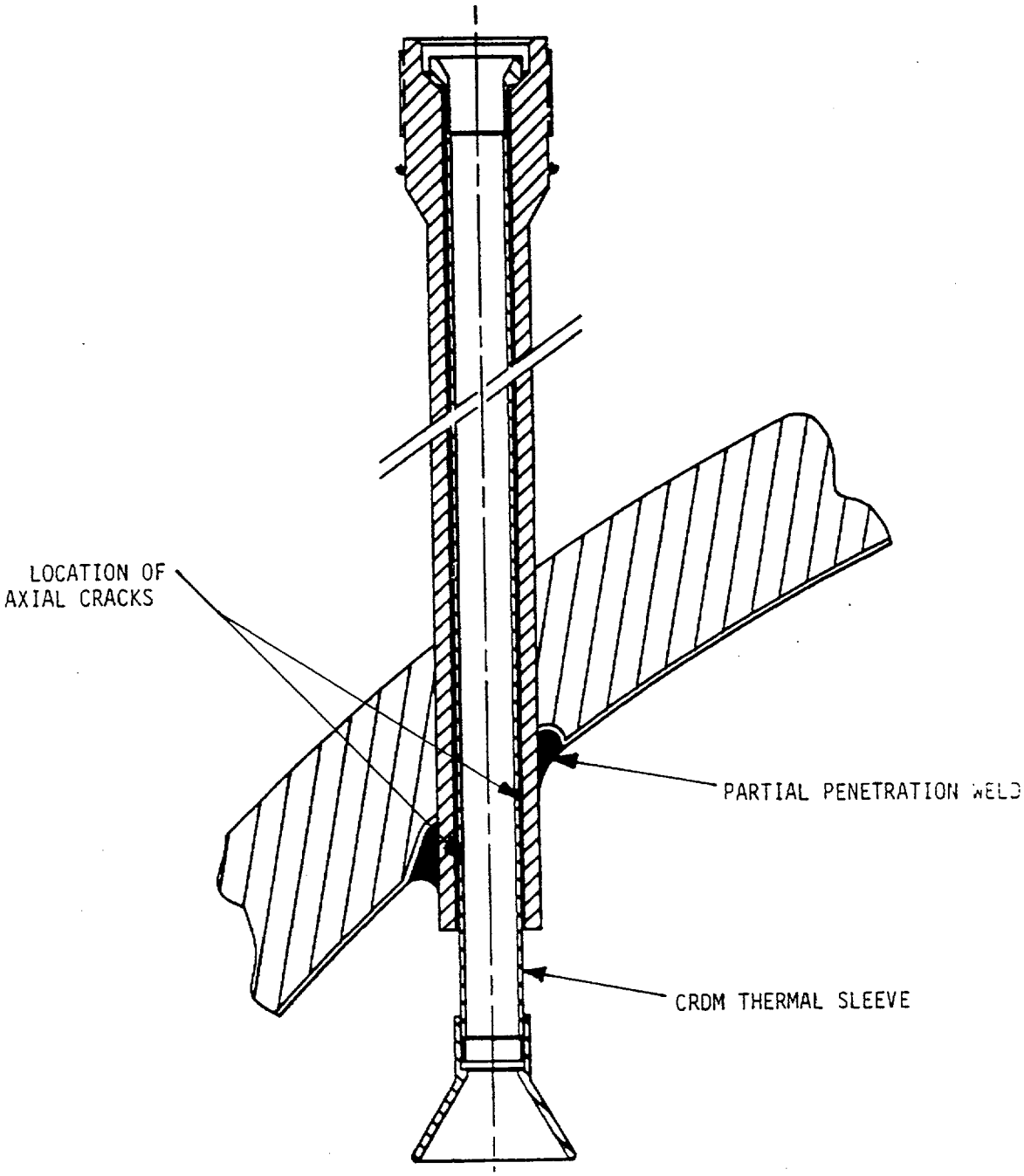

FIGURE 1-1

REACTOR VESSEL HEAD ADAPTER PENETRATION TUBE, SHOWING LOCATIONS OF AXIAL CRACKS FOUND IN SOME PLANTS

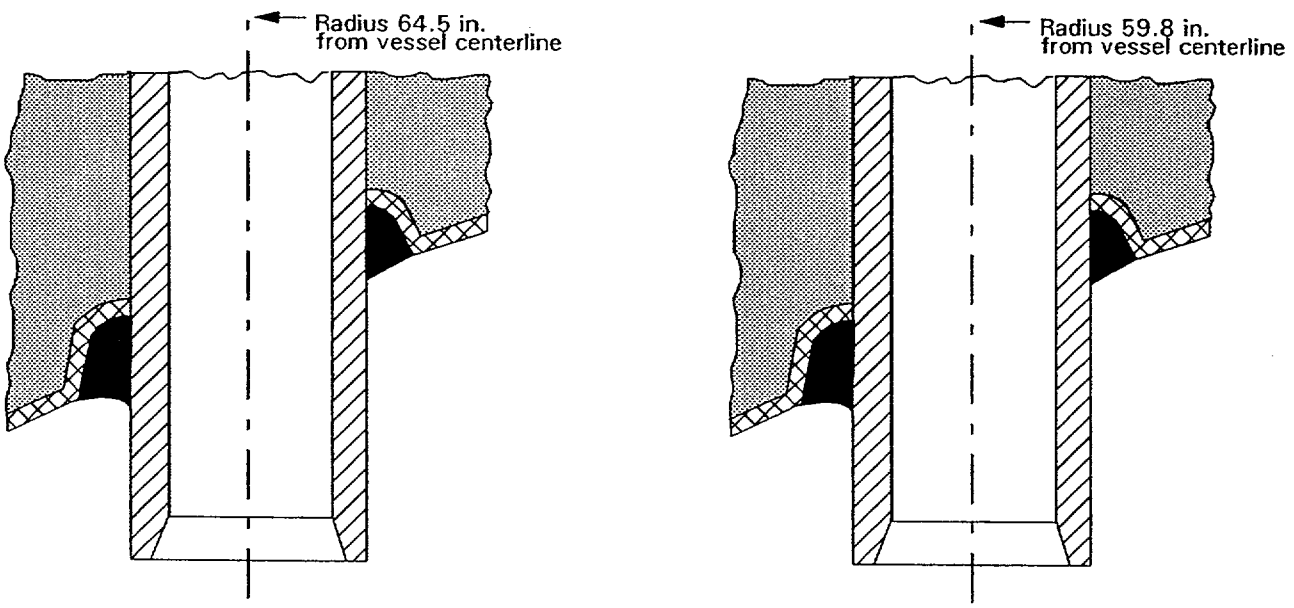

FIGURE 1-2

GEOMETRY OF THE HILLSIDE PENETRATIONS ANALYZED

SECTION 2.0
HISTORY OF CRACKING IN HEAD PENETRATIONS

In September of 1991, leakage was reported from the reactor vessel head penetration region of a French plant, Bugey Unit 3. Bugey 3 is a 920 megawatt three-loop PWR which had just completed its tenth fuel cycle. The leak occurred during a post ten year hydrotest conducted at a pressure of approximately 3000 psi (204 bar) and a temperature of 194°F (90°C). The leak was detected by metal microphones located on the top and bottom heads, and the leak rate was estimated to be approximately 0.7 liter/hour. The location of the leak was subsequently established on a peripheral penetration with an active control rod (H-14), as seen in Figure 2-1.

The control rod drive mechanism and thermal sleeve were removed from this location to allow further examination. Further study of the head penetration revealed the presence of longitudinal cracks near the head penetration attachment weld. Penetrant and ultrasonic testing confirmed the cracks. The cracked penetration was fabricated from Alloy 600 bar stock (SB-166), and has an outside diameter of 4 inches (10.16 cm) and an inside diameter of 2.75 inches (7.0 cm).

As a result of this finding, all of the control rod drive mechanisms and thermal sleeves at Bugey 3 were removed for inspection of the head penetrations. Only two penetrations were found to be cracked, as shown in Figure 2-1.

An inspection of a sample of penetrations at three additional plants were planned and conducted during the winter of 1991-92. These plants were Bugey 4 , Fessenheim 1, and Paluel 3. The three outermost rows of penetrations at each of these plants were examined, and further cracking was found in two of the three plants.

At Bugey 4, eight of the 64 penetrations examined were found to contain axial cracks, while only one of the 26 penetrations examined at Fessenheim 1 was cracked. The locations of all the cracked penetrations are shown in Figure 2-1. None of the 17 penetrations inspected at Paluel 3 showed indications of cracking, at the time, but further inspection of the French plants have confirmed at least one crack in each operating plant.

Thus far, the cracking has been consistent in both its location and extent. All cracks discovered by nondestructive examination have been oriented axially, and have been located in the bottom portion of

the penetration in the vicinity of the partial penetration attachment weld to the vessel head as shown schematically in Figure 1-1.

[

]a,c,e

Non-destructive examinations of the leaking CRDM nozzles showed that most of the cracks originated on the outside surface of the nozzles below the J-groove weld, were axially oriented, and propagated primarily in the nozzle base material to an elevation above the top of the J-groove weld where leakage could then pass through the annulus to the top of the head where it was detected by visual inspection. In some cases the cracks initiated in the weld metal or propagated into the weld metal, and in a few cases the cracks propagated through the nozzle wall thickness to the inside surface.

[

]a,c,e

[

]a,c,e

The cracking has now been confirmed to be primary water stress corrosion cracking. Relatively high residual stresses are produced in the outermost penetrations due to the welding process. Other important factors which affect this process are temperature and time, with higher temperatures and longer times being more detrimental. The inspection findings for the plants examined thus far are summarized in Table 2-1.

TABLE 2-1
OPERATIONAL INFORMATION AND INSPECTION RESULTS FOR UNITS EXAMINED
(RESULTS TO APRIL 30, 2001)

Country	Plant Type	Units Inspected	K Hours	Head Temp. (°F)	Total Penetrations	Penetrations Inspected	Penetrations With Indications
France	CPO	6	80-107	596-599	390	390	23
	CPY	28	42-97	552	1820	1820	126
	1300MW	20	32-51	558-597	1542	1542	95
Sweden	3 Loop	3	75-115	580-606	195	190	8
Switzerland	2 Loop	2	148-154	575	72	72	2
Japan	2 Loop	7	105-108	590-599	276	243	0
	3 Loop	7	99	610	455	398	0
	4 Loop	3	46	590	229	193	0
Belgium	2 Loop	2	115	588	98	98	0
	3 Loop	5	60-120	554-603	337	337	6
Spain	3 Loop	5	65-70	610	325	102	0
Brazil	2 Loop	1	25	NA	40	40	0
South Africa	3 Loop	1	NA	NA	65	65	6
Slovenia	2 Loop	1	NA	NA	49	49	0
South Korea	2 Loop	3	NA	NA	49	49	3
	3 Loop	2	NA	NA	130	130	2
US	2 Loop	2	170	590	98	98	0
	3 Loop	1	NA	NA	65	20	0
	4 Loop	7	NA	NA	221	169	16
TOTALS		106	–	–	6456	6005	287

FRENCH R/V CLOSURE HEAD PENETRATION CRACKING
EdF PLANTS - PENETRATIONS WITH CRACKING

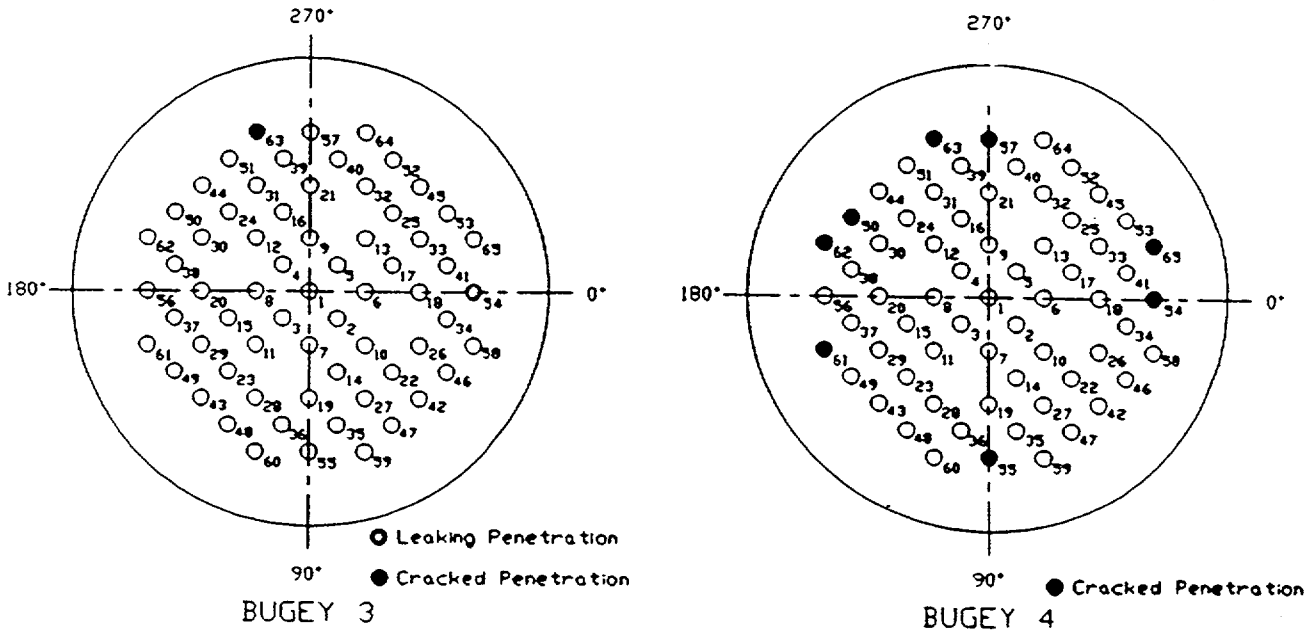

FIGURE 2-1

SECTION 3.0

OVERALL TECHNICAL APPROACH

The primary goal of this work is to provide technical justification for the continued safe operation of D. C. Cook Units One and Two in the event that cracking is discovered during inservice inspections of the Alloy 600 reactor vessel head penetrations.

3.1 PENETRATION STRESS ANALYSIS

Three dimensional elastic-plastic finite element stress analyses have been performed to determine the stresses in the head penetration region [6]. These analyses have considered the pressure and thermal transient loads associated with steady state operation, as well as the residual stresses which are produced by the fabrication process.

[

]^{a,c,e}

3.2 FLAW TOLERANCE APPROACH

A flaw tolerance approach has been developed to allow continued safe operation until an appropriate time for repair, or the end of plant life. The approach is based on the prediction of future growth of detected flaws, to ensure that such flaws would remain stable.

If an indication is discovered during inservice inspection, its size can be compared with the flaw size which is considered allowable for continued service. This "allowable" flaw size is determined from the

actual loadings (including mechanical, residual, and transient loads) on the head penetration for the plant of interest. Suitable margins to ensure the integrity of the reactor vessel as well as safety from unacceptable leakage rates, should also be considered. Acceptance criteria are discussed in Section 6.5.

The time for the observed crack to reach the allowable crack size determines the length of time the plant can remain online before repair, if required.

The results of the evaluation are presented in terms of simple charts, which show graphically the time required to reach the allowable length, which represents the additional service life before repair. This result is a function of the loadings on the particular head penetration, as well as the circumferential location of the crack in the penetration tube.

Schematic drawings of the head penetration flaw tolerance charts are presented as Figures 3-1 and 3-2. These two types of charts can be used to provide estimates of the time which remains before a leak would develop from an observed crack. For example, if a part-through flaw was discovered, the user would first refer to Figure 3-1, to determine the time (t_P) which would be remaining before the crack would penetrate the wall or reach the allowable depth (t_A) (eg a/t=.75). Once the crack penetrates the wall, the time (t_B) required to reach an allowable crack length would be determined from Figure 3-2. The total time remaining would then be the simple sum:

$$\text{Time remaining} = t_P + t_B$$

Another way to determine the allowable time of operation with a part-through flaw would be to use Figure 3-2 directly, in effect assuming the part-through flaw is a through-wall flaw. This approach would be more conservative than that above, and the time remaining would then be:

$$\text{Time remaining} = t_B$$

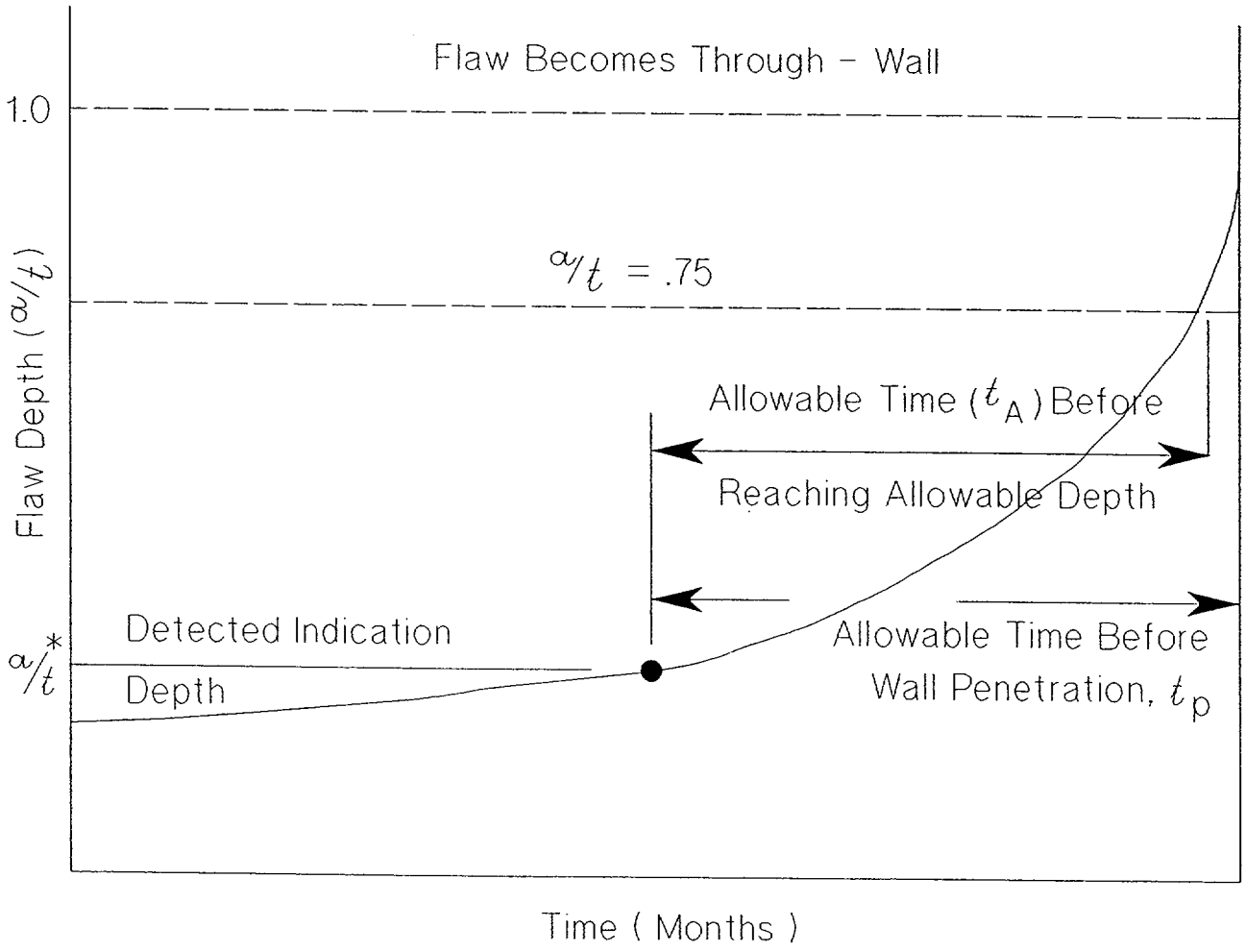

FIGURE 3-1

SCHEMATIC OF A HEAD PENETRATION FLAW GROWTH CHART FOR PART THROUGH FLAWS

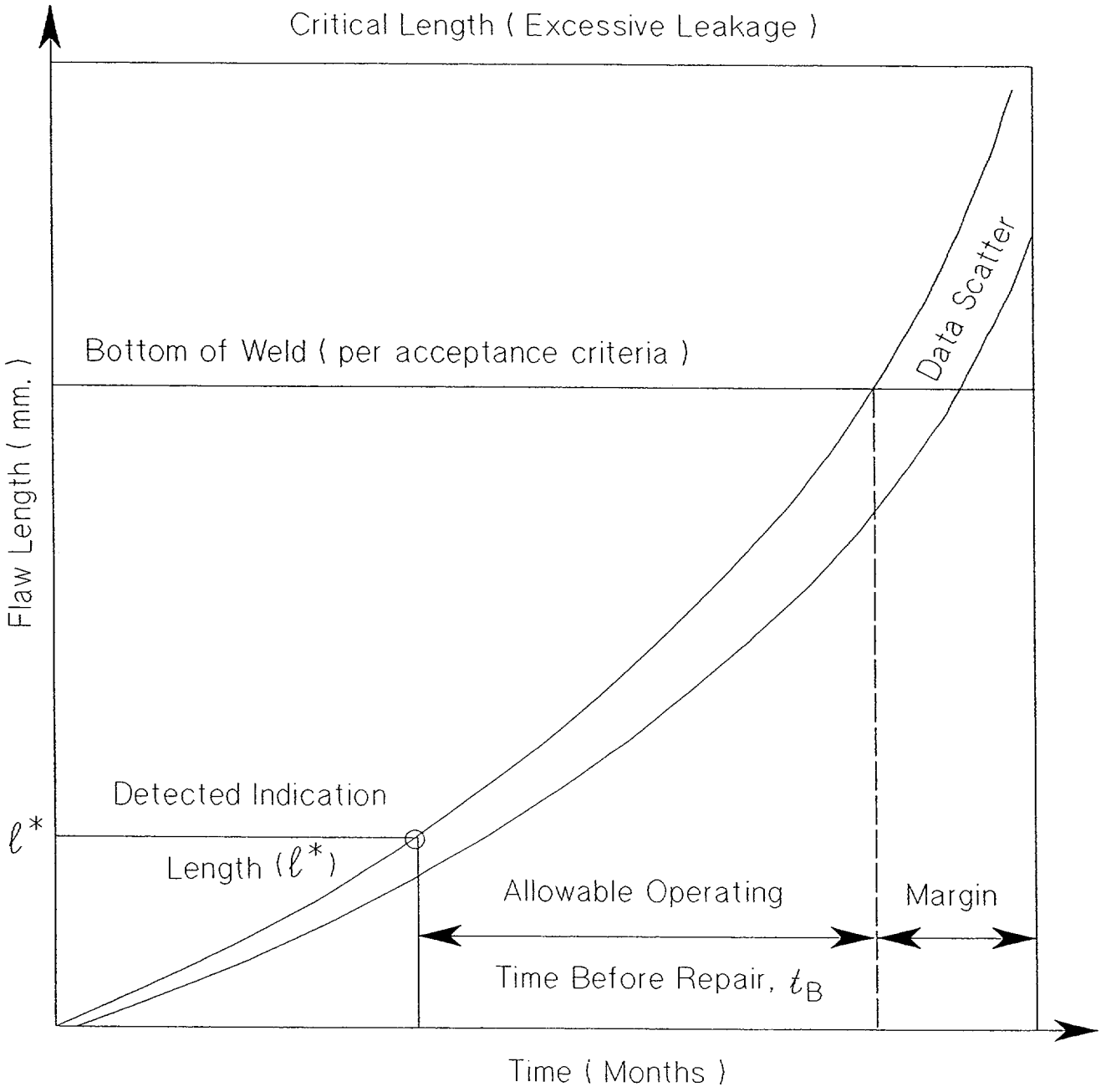

FIGURE 3-2

SCHEMATIC OF A HEAD PENETRATION FLAW TOLERANCE CHART

FOR THROUGH-WALL FLAWS

SECTION 4.0

MATERIAL PROPERTIES, FABRICATION HISTORY AND CRACK GROWTH PREDICTION

4.1 MATERIALS AND FABRICATION

The head adapters for D. C. Cook Units 1 and 2 were manufactured by Westinghouse from material produced by Huntington Alloys in the USA. The carbon content, mechanical properties and heat treatment of the Alloy 600 material used to fabricate the D. C. Cook vessels are provided in Tables 4-1 and 4-2. The material CMTRs were used to obtain the chemistry and mechanical properties for the vessel head penetrations. The CMTRs for the material do not indicate the heat treatment of the material. However, Westinghouse records indicate that the materials were annealed for one hour at a temperature of 1700 - 1800°F, followed by a water quench. Figures 4-1 and 4-2 illustrate the yield strengths and carbon content, based on percent of heats, of the head adapter penetrations in the D. C. Cook Units 1 and 2 vessels relative to a sample of the French head adapters which have experienced cracking. The general trend for the head adapter penetrations in the D. C. Cook vessels are a higher carbon content, higher mill annealing temperature and lower yield strength relative to those on the French vessels. These factors should all have a beneficial effect on the material resistance to PWSCC in the head penetrations.

4.2 CRACK GROWTH PREDICTION

The cracks in the penetration region have been determined to result from primary water stress corrosion cracking in the Alloy 600 base metal. There are a number of available measurements of static load crack growth rates in primary water environment, and in this section the available results will be compared and a representative growth rate established.

Direct measurements of SCC growth rates in Alloy 600 are relatively rare, and care should be used in interpreting the results because the materials may be excessively cold worked, or the loadings applied may be near or exceeding the limit load of the tube, meaning there will be an interaction between tearing and crack growth. In these cases the crack growth rates may not be representative of service conditions.

The effort to develop a reliable crack growth rate model for Alloy 600 began in the spring of 1992, when the Westinghouse Owners Group was developing a safety case to support continued operation of plants. At the time there was no available crack growth rate data for head penetration materials, and only a few publications existed on growth rates of Alloy 600 in any product form.

The best available publication was found to be that of Peter Scott of Framatome, who had developed a growth rate model for PWR steam generator materials [1]. His model was based on a study of results obtained by McIlree and Smialowska [2] who had tested short steam generator tubes which had been flattened into thin compact specimens. Upon study of his paper there were several ambiguities, and several phone conversations were held to clarify his conclusions. These discussions led to Scott's admission that reference 1 contains an error, in that no correction for cold work was applied to the McIllree/Smialowska data. The correct development is below.

An equation was fitted to the data of reference [2] for the results obtained in water chemistries that fell in within the standard specification. Results for chemistries outside the specification were not used. The following equation was fitted to the data:

$$\frac{da}{dt} = 2.8 \times 10^{-11} (K-9)^{1.16} \text{ m/sec}$$

where K is in MPa$\sqrt{m}$.

The next step described by Scott in his paper was to correct these results for the effects of cold work. Based on work by Cassagne and Gelpi [3], he concluded that dividing the above equation by a factor of 10 would be appropriate to account for the effects of cold work. This step was inadvertently omitted from Scott's paper, even though it is discussed. The crack growth law for 330°C then becomes:

$$\frac{da}{dt} = 2.8 \times 10^{-12} (K-9)^{1.16} \text{ m/sec}$$

This equation was verified by Scott in a phone call in July 1992.

Scott further corrected this law for the effects of temperature, but his correction was not used in the model employed here. Instead, an independent temperature correction was developed based on service experience, as will be discussed below.

[

]^{a,c,e}

[

]a,c,e

There is a general agreement that crack growth in Alloy 600 materials in the primary water environment can be modeled using a stress intensity factor relationship with differences in temperature accounted for by an activation energy (Arrhenius) model for thermally controlled processes. Figure 4-3 shows the provisional recommended CGR curve along with the laboratory data used to develop the curve.

[

]a,c,e

[

]a,c,e

[

]a,c,e

[

]a,c,e

(a,c,e)

TABLE 4-1
D. C. COOK UNIT 1 R/V HEAD ADAPTER MATERIAL INFORMATION

(a,c,e)

TABLE 4-2
D. C. COOK UNIT 2 R/V HEAD ADAPTER MATERIAL DATA

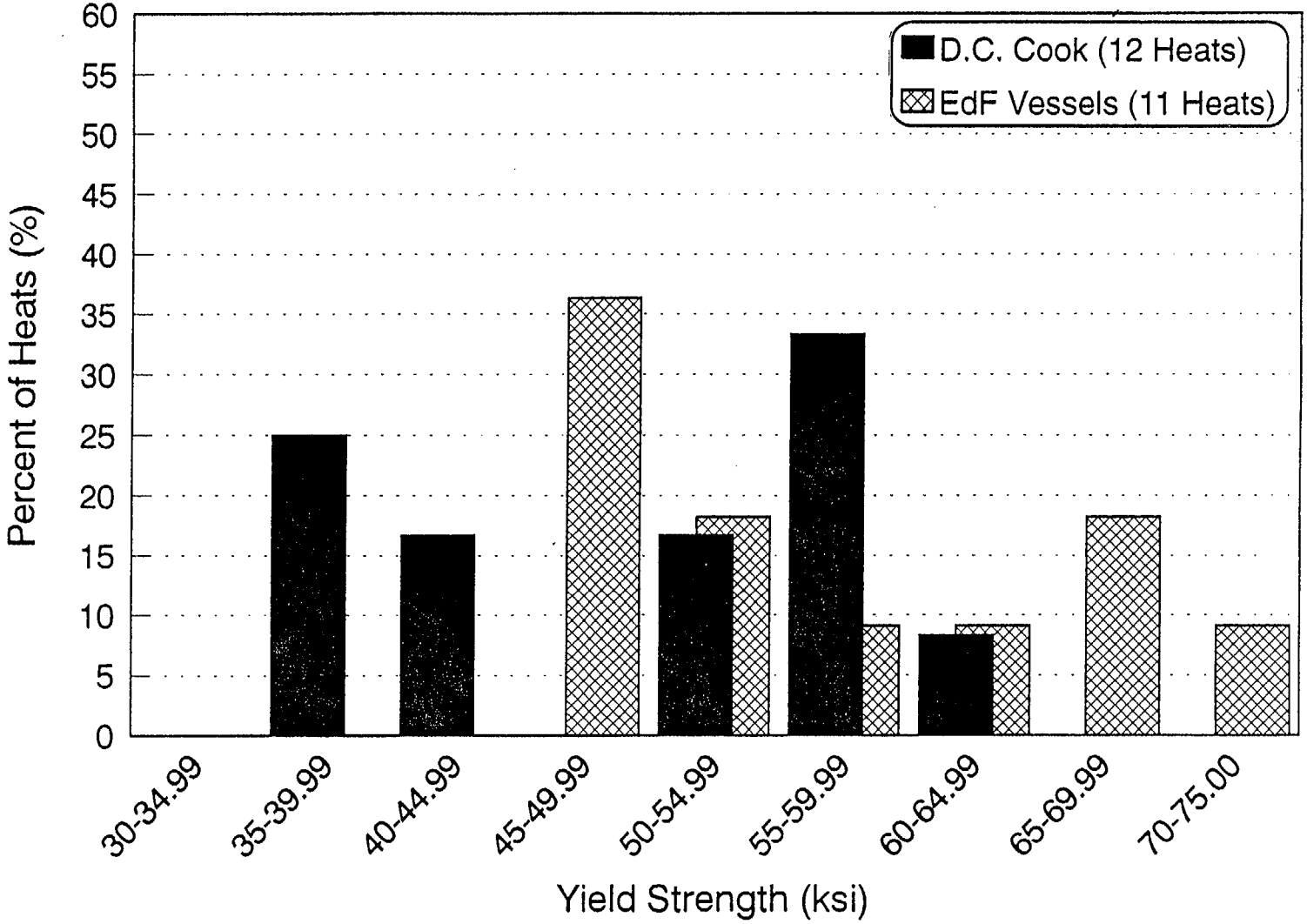

FIGURE 4-1
YIELD STRENGTH OF THE VARIOUS HEATS OF ALLOY 600 USED IN
FABRICATING THE D. C. COOK UNITS 1 AND 2 AND FRENCH HEAD ADAPTOR PENETRATIONS

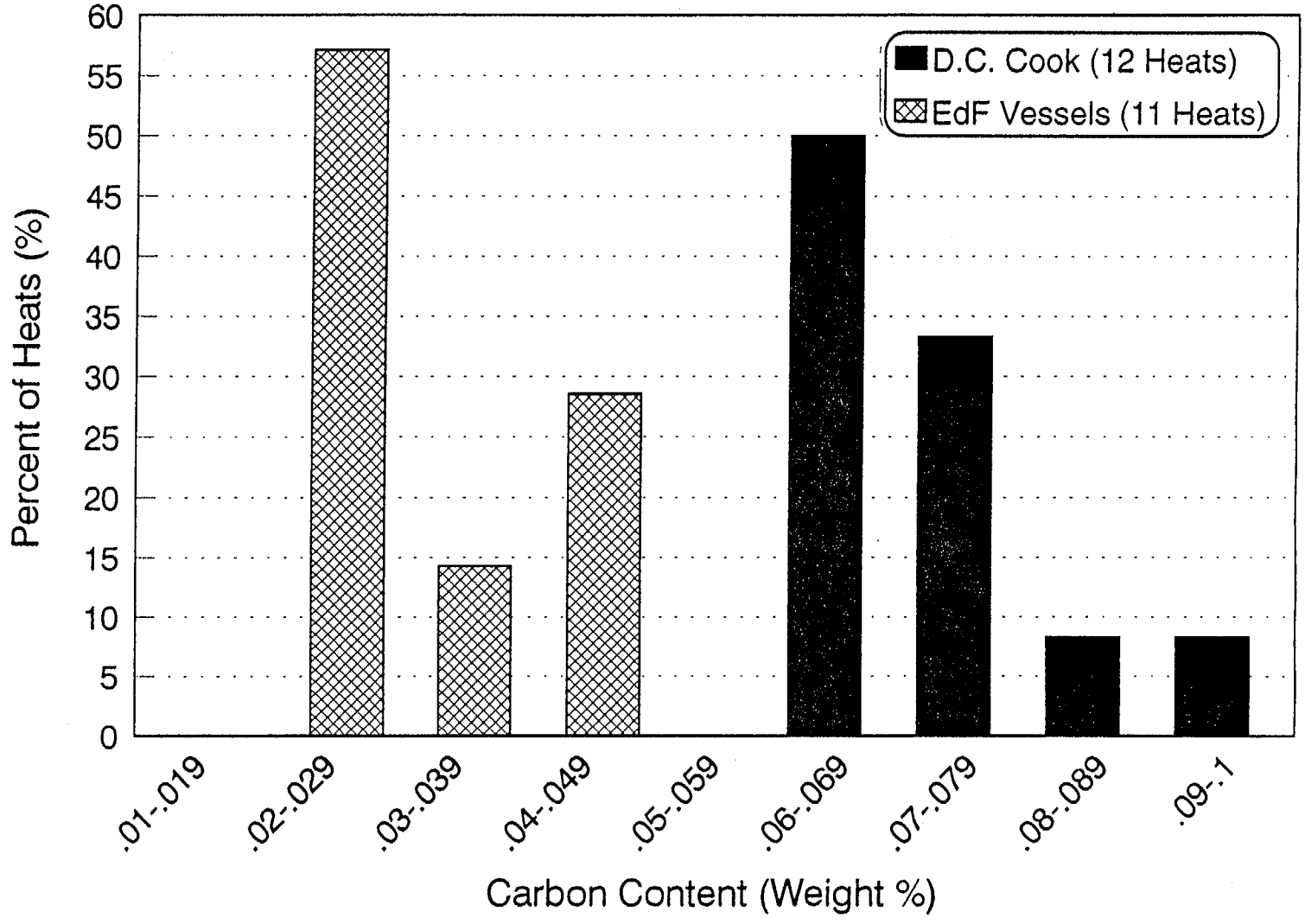

FIGURE 4-2
CARBON CONTENT OF THE VARIOUS HEATS OF ALLOY 600 USED IN
FABRICATING THE D. C. COOK UNITS 1 AND 2 AND FRENCH HEAD ADAPTOR PENETRATIONS

(a,c,e)

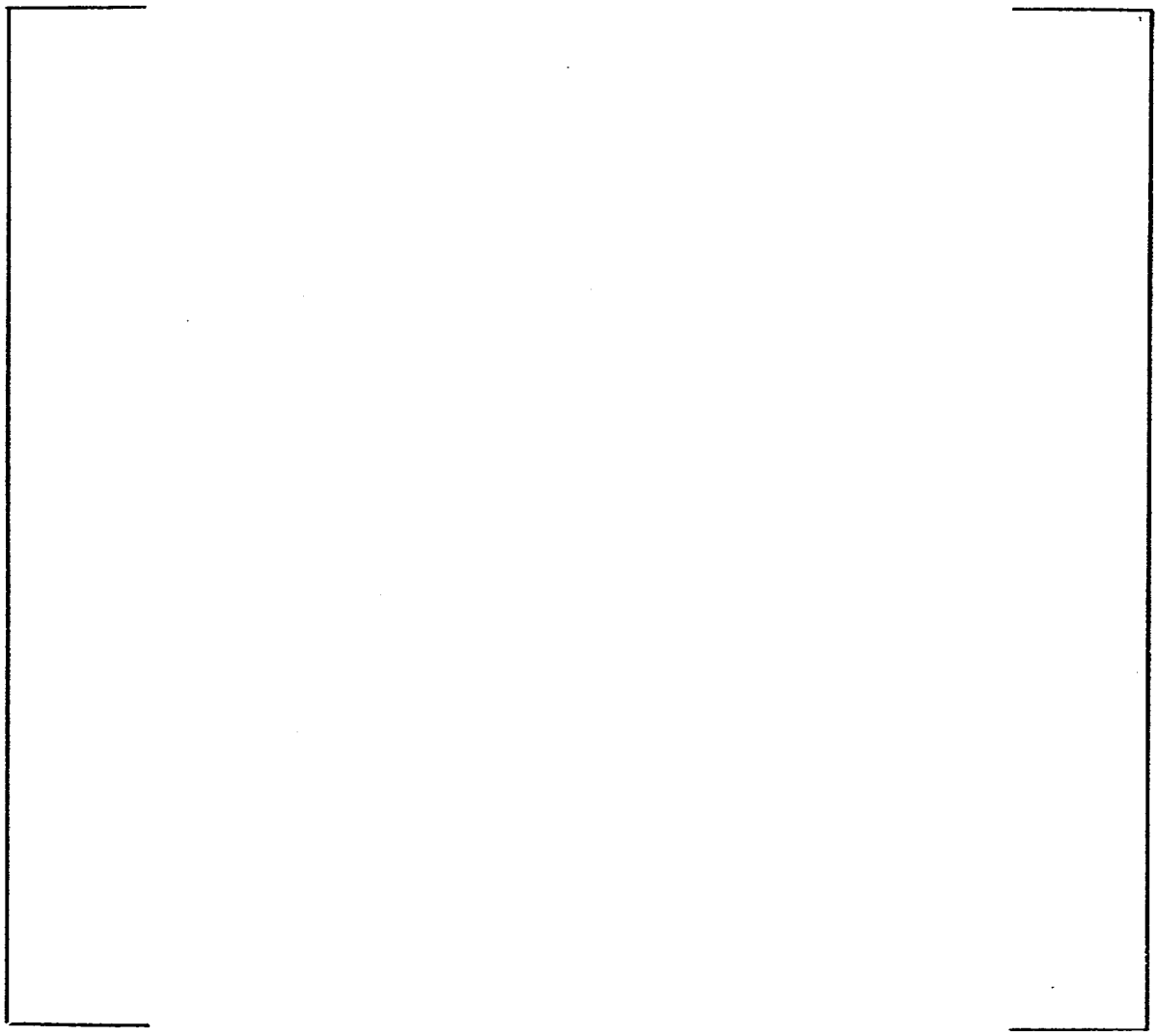

FIGURE 4-3

MODEL[4G] FOR SCC GROWTH RATES IN ALLOY 600 IN

PRIMARY WATER ENVIRONMENTS (330°C)

(a,c,e)

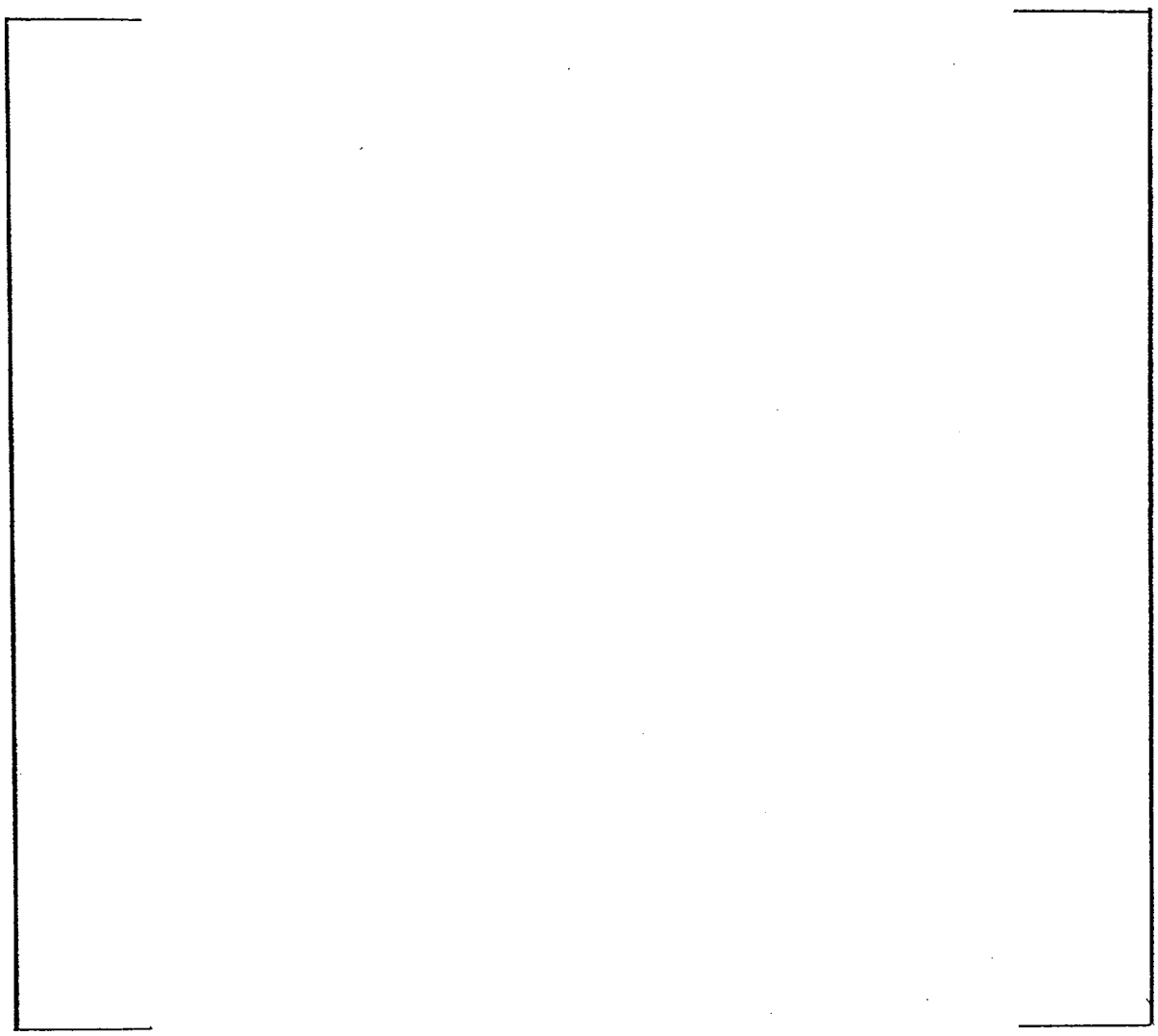

FIGURE 4-4

COMPARISON OF MRP RECOMMENDED CURVE USED IN THIS EVALUATION TO THE MODIFIED SCOTT CURVE

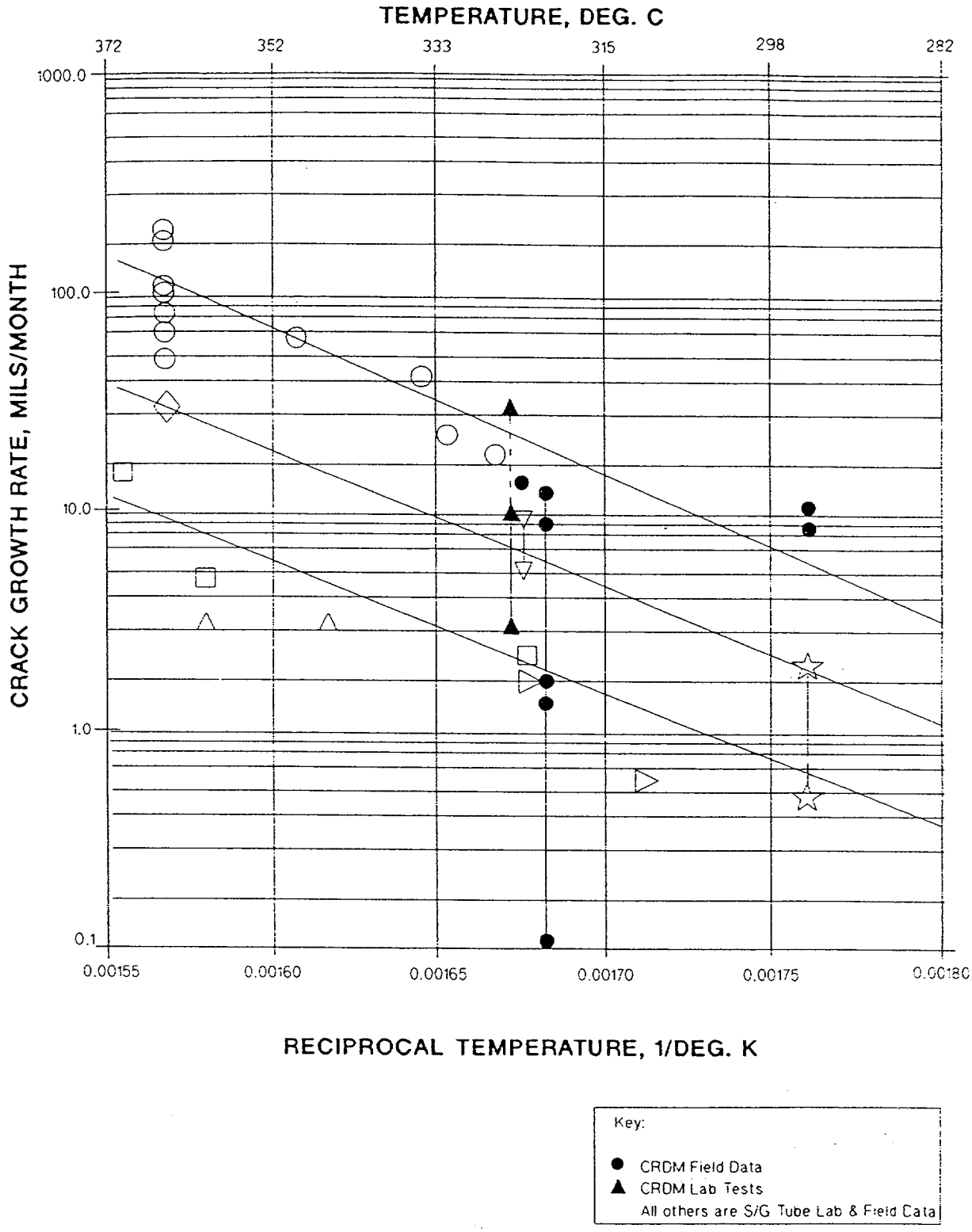

FIGURE 4-5

SUMMARY OF TEMPERATURE EFFECTS ON SCC GROWTH RATES FOR ALLOY 600 IN PRIMARY WATER, LABORATORY AND FIELD EXPERIENCE

SECTION 5.0
STRESS ANALYSIS

5.1 OBJECTIVES OF THE ANALYSIS

The objective of this analysis was to obtain accurate stresses in each CRDM housing and its immediate vicinity. To do so requires a three dimensional analysis which considers all the pertinent loadings on the penetration [6]. An investigation of deformations at the lower end of the housing was also performed using the same model. Three locations were considered: the outermost row, the next outermost row, and the center location.

The analyses were used to provide information for the flaw tolerance evaluation which follows in Section 6. Also, the results of the stress analysis were compared to the findings from service experience, to help assess the causes of the cracking which has been observed. The geometry of D.C. Cook Units 1 and 2 in the head penetration and head regions is identical, so one stress analysis covers both units.

5.2 MODEL

A three dimensional finite element model comprised of isoparametric brick and wedge elements with midside nodes on each face was used to obtain the stresses and deflections. A view of the unstressed model is shown in Figure 5-1. Taking advantage of symmetry through the vessel and penetration centerlines only half of the penetration geometry plus the surrounding vessel were modeled for the outermost and next outermost penetrations. In the center penetration case, it was necessary to model only one-quarter of the penetration as opposed to one-half of the penetration. The difference between the hillside penetrations and the center penetration was that there was no differential height across the weld for the center penetration.

In the models, the lower portion of the Control Rod Drive Mechanism (CRDM) Adapter tube (i.e., penetration tube), the adjacent section of the vessel closure head, and the joining weld were modeled. The vessel to penetration tube weld was simulated with two layers of elements. The penetration tube, weld metal and cladding were modeled as Alloy 600 and the vessel head shell as carbon steel.

5.3 STRESS ANALYSIS RESULTS - OUTERMOST PENETRATION

Figure 5-2 shows the outward displacement of the entire model for the steady state condition. For the steady state, the tube OD is pressing on the vessel (i.e. couple each tube node, except for the vertical direction, to its neighbor in the vessel). Figure 5-3 presents the hoop stresses for the steady state condition.

[

]a,c,e

5.4 STRESS ANALYSIS RESULTS-NEXT OUTERMOST PENETRATION

[

]a,c,e

5.5 STRESS ANALYSIS RESULTS-CENTER PENETRATION

[

]a,c,e

[

]a,c,e

5.6 STRESS ANALYSIS RESULTS: HEAD VENT

The head vent is a smaller penetration than the CRDM head penetrations, but is also constructed of Alloy 600 material, with a partial penetration weld at the inside of the reactor vessel head. The head vent is located 7.8 inches from the centerline of the head dome, and its dimensions are shown in Figure 5-7.

The head vent was evaluated using a three dimensional finite element model, as shown in Figure 5-8.
[

]a,c,e

[

]a,c,e

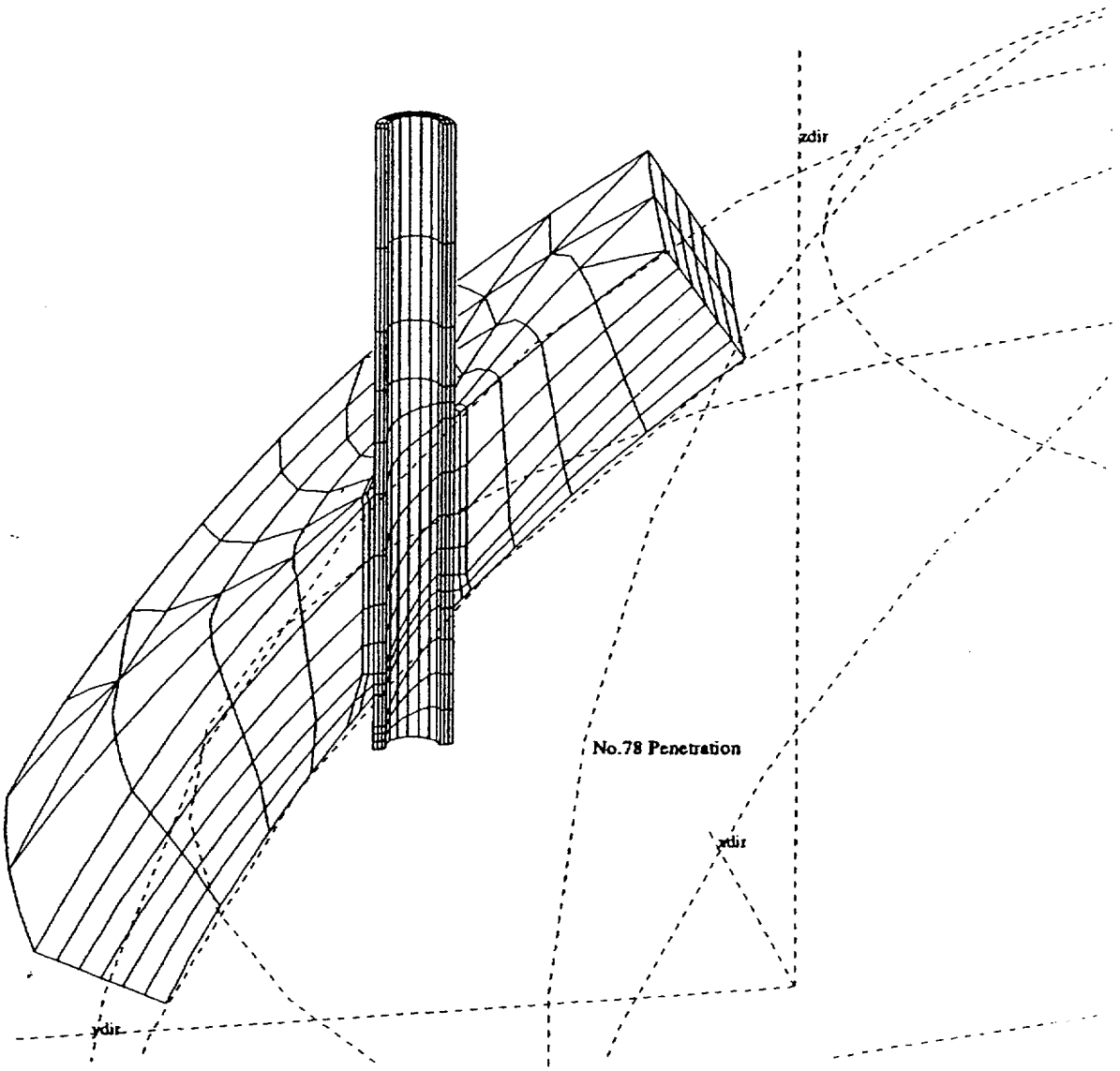

FIGURE 5-1

THREE-DIMENSIONAL MODEL OF THE OUTERMOST PENETRATION

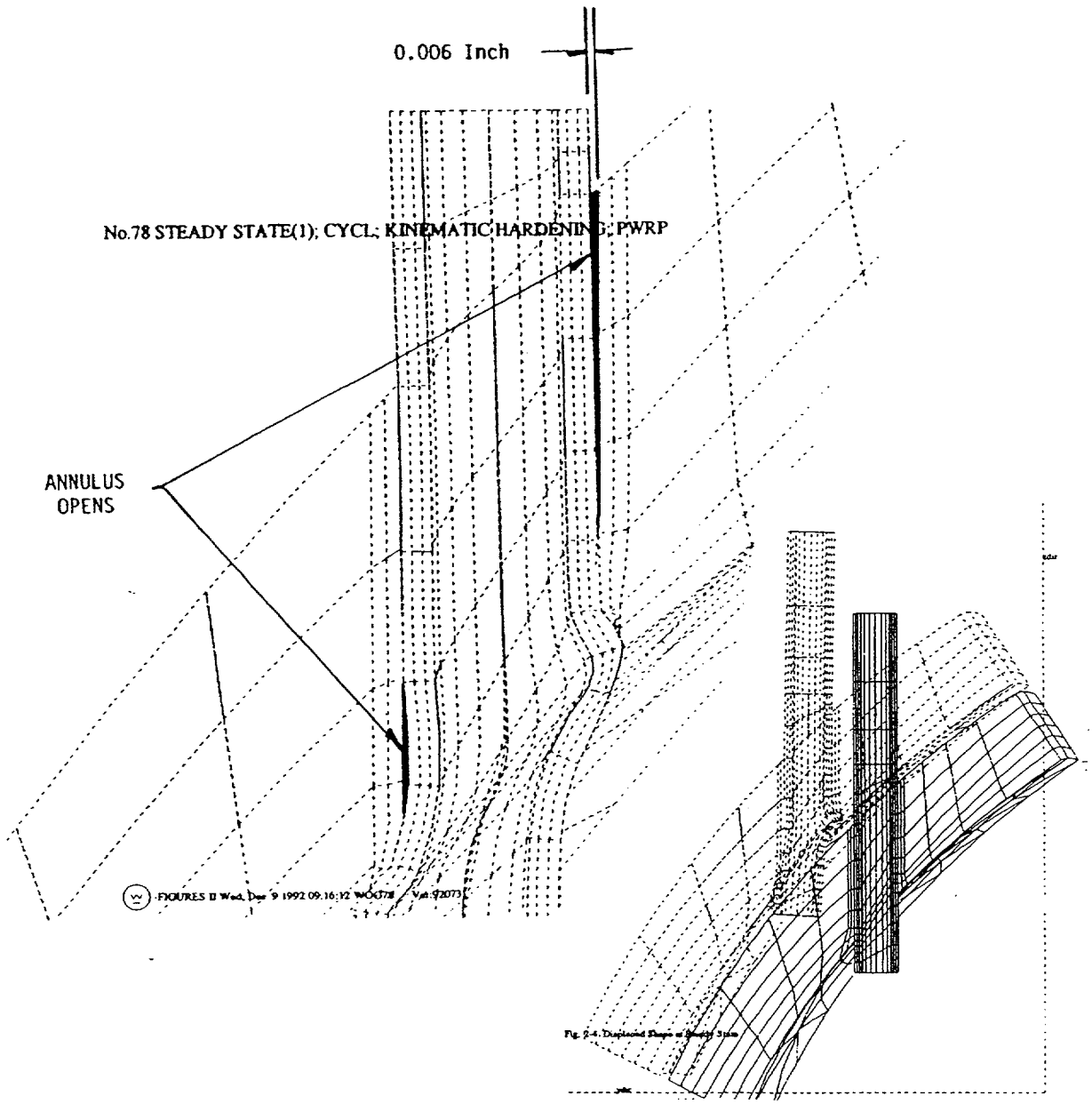

FIGURE 5-2

STEADY STATE DISPLACEMENT OF R/V CLOSURE HEAD AND OUTERMOST PENETRATION

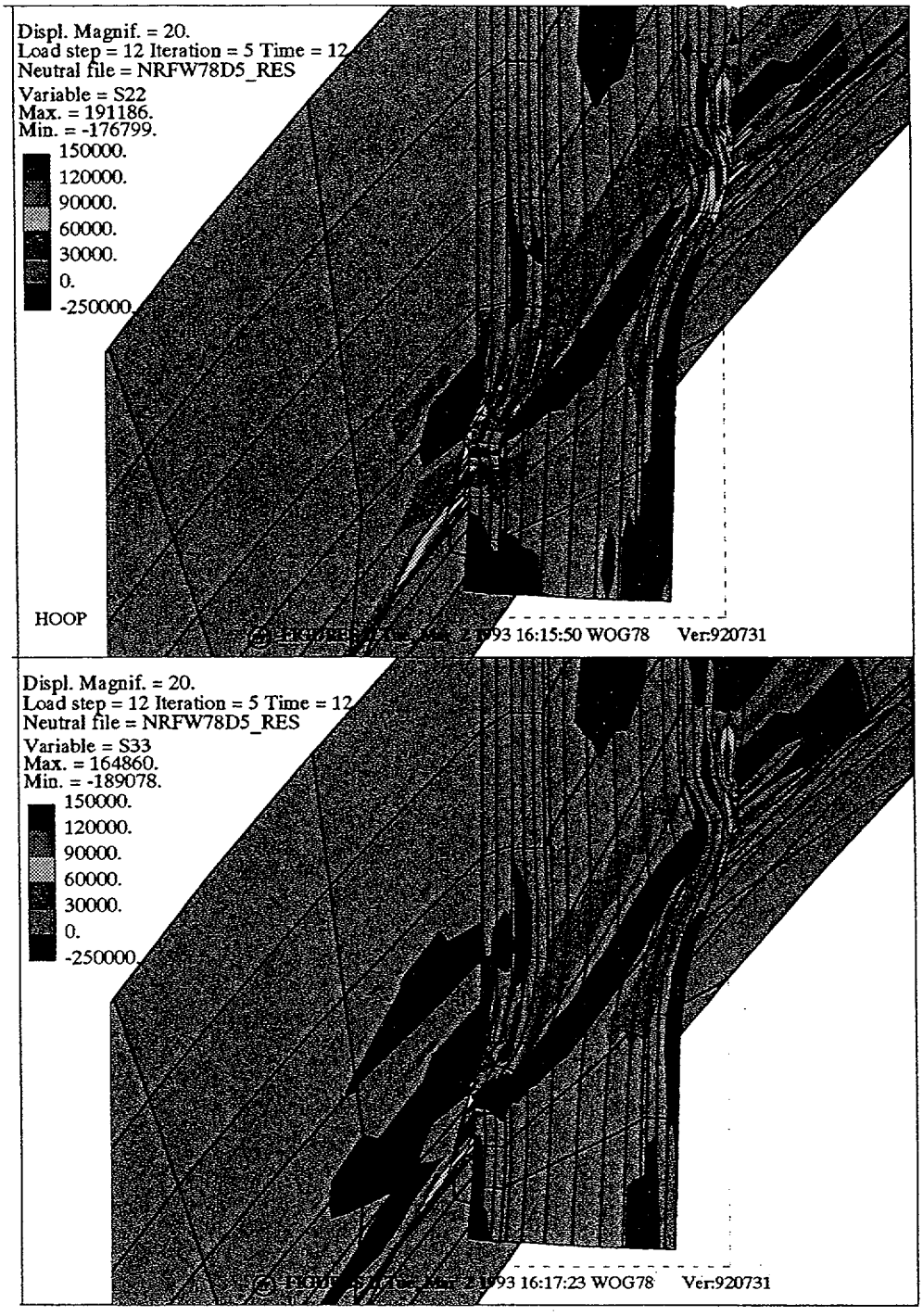

FIGURE 5-3

STRESS DISTRIBUTION AT STEADY STATE CONDITIONS: OUTERMOST PENETRATION

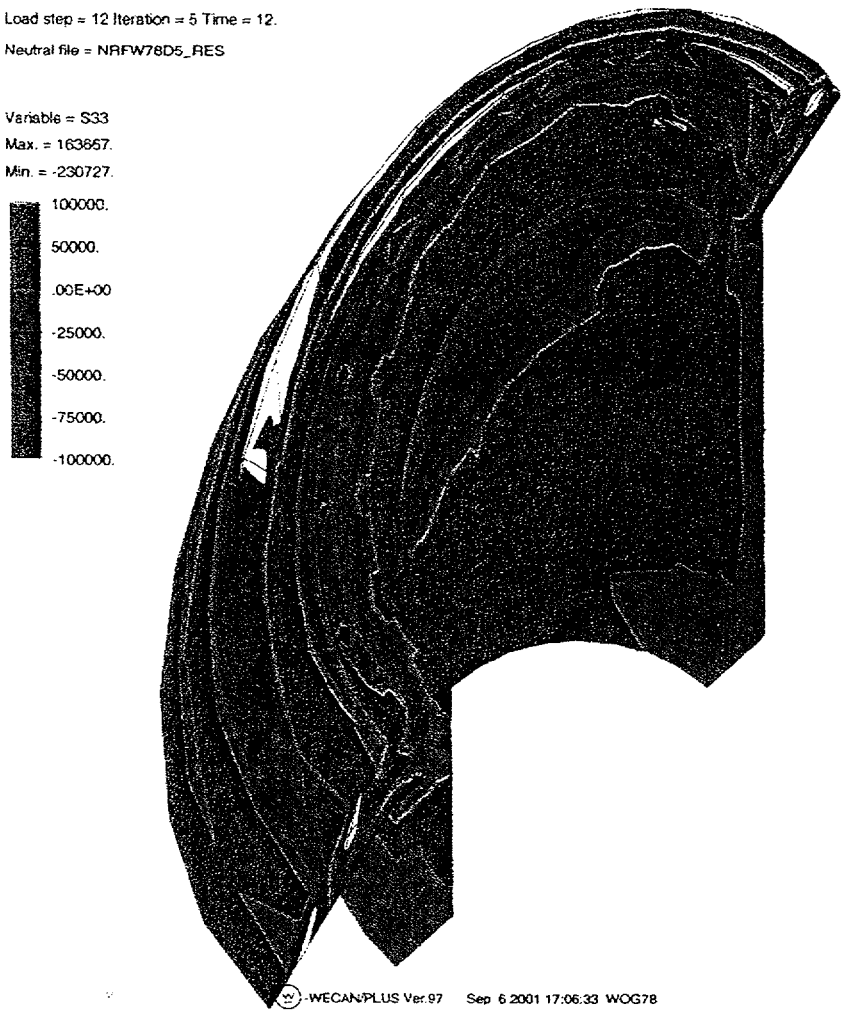

FIGURE 5-4

STRESS DISTRIBUTION AT STEADY STATE FOR THE OUTERMOST PENETRATION, ALONG A PLANE ORIENTED PARALLEL TO, AND JUST ABOVE, THE ATTACHMENT WELD.

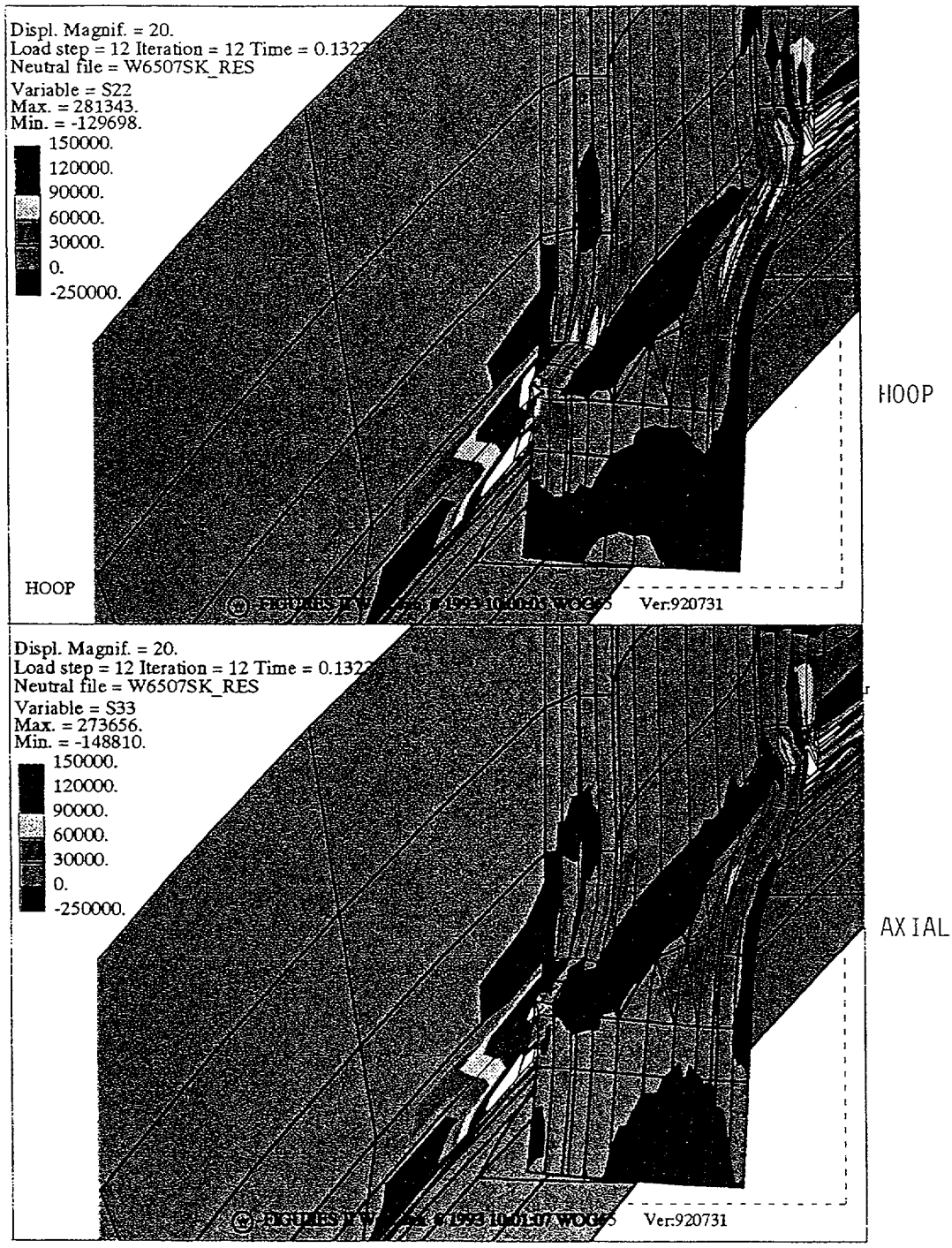

FIGURE 5-5

STRESS DISTRIBUTION AT STEADY STATE CONDITION

FOR THE NEXT OUTERMOST PENETRATION

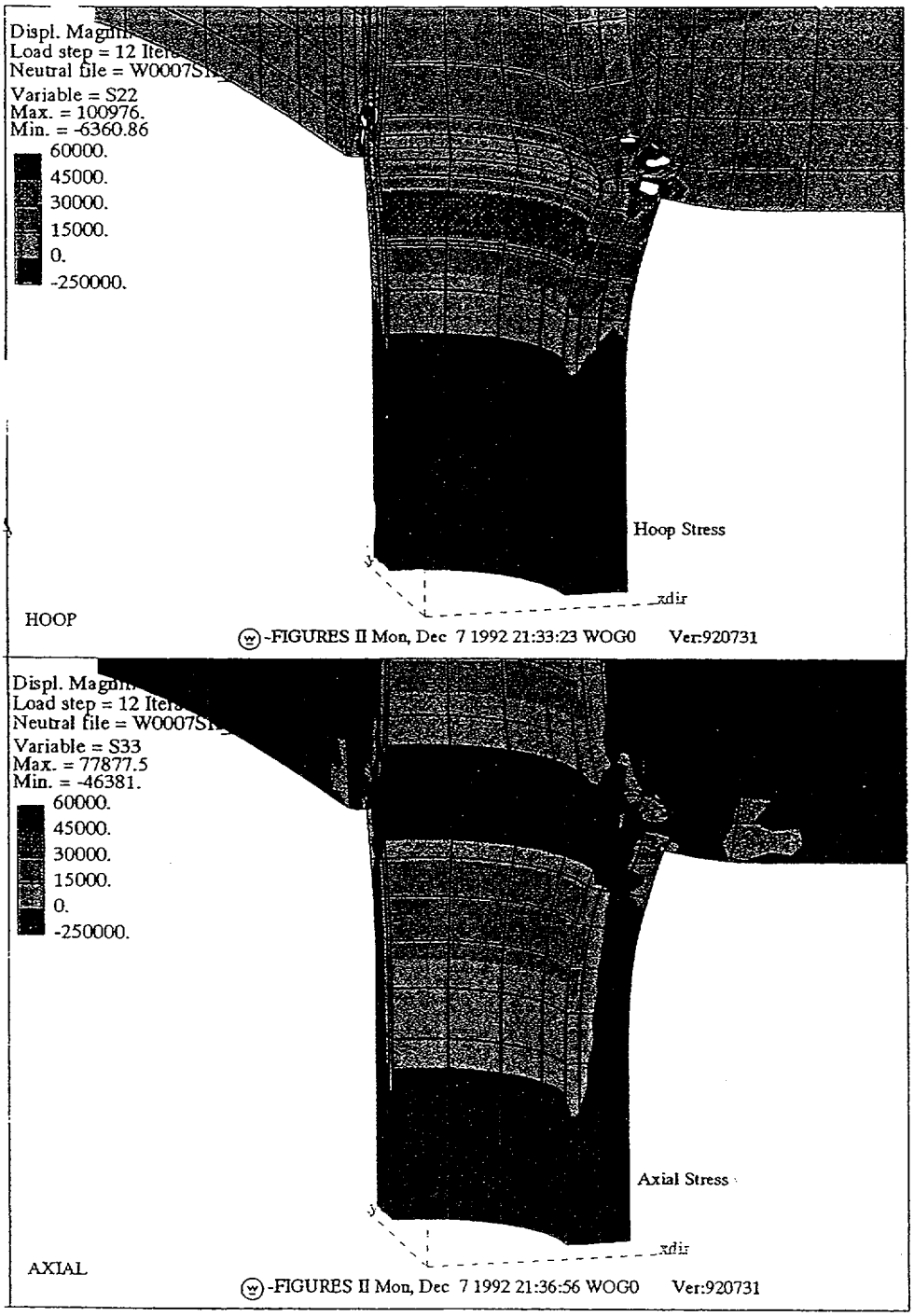

HOOP

AXIAL

FIGURE 5-6

STRESS DISTRIBUTION AT STEADY STATE CONDITION FOR THE CENTER PENETRATION

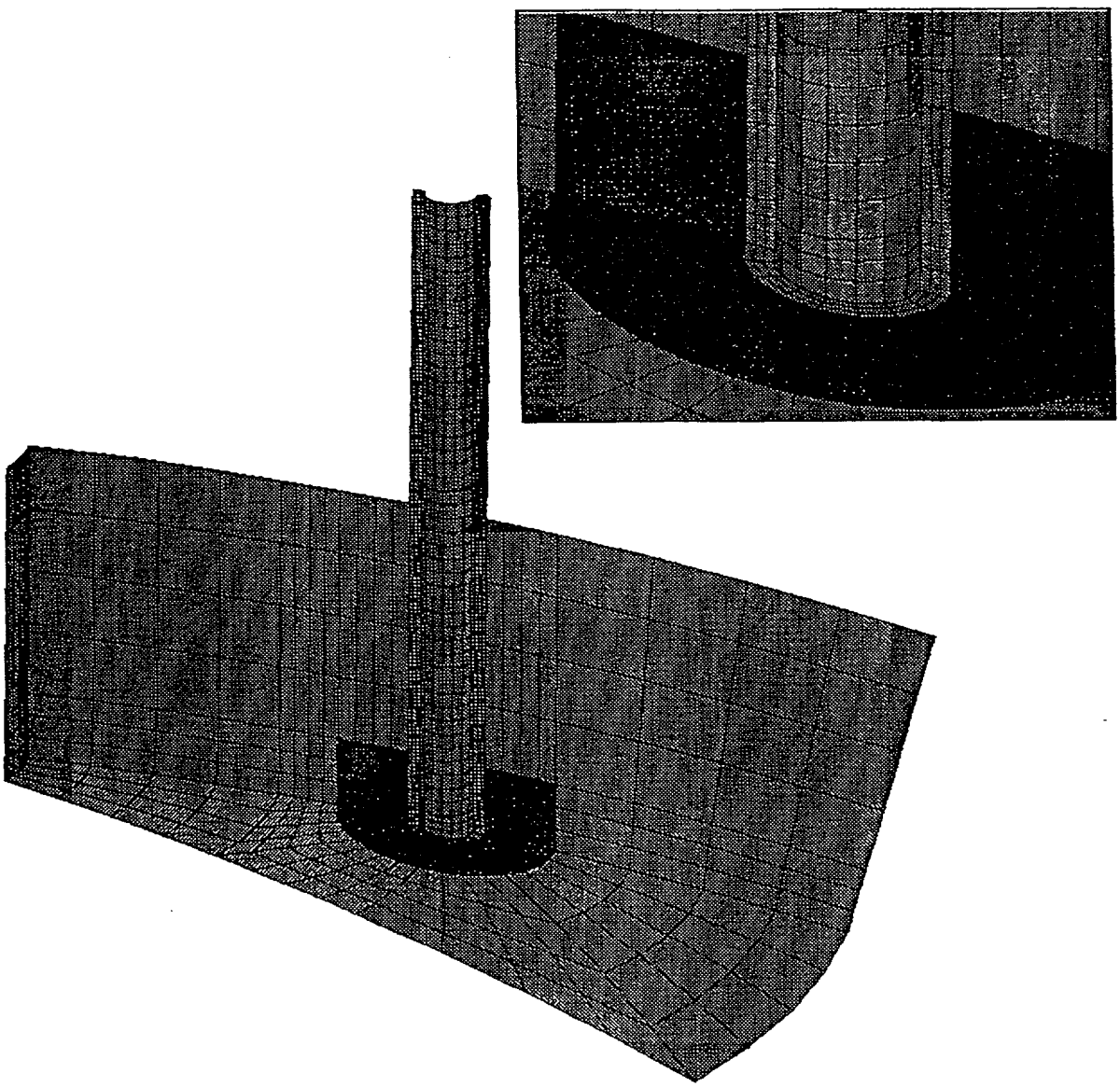

FIGURE 5-7

VENT PIPE DIMENSIONS (INCHES)

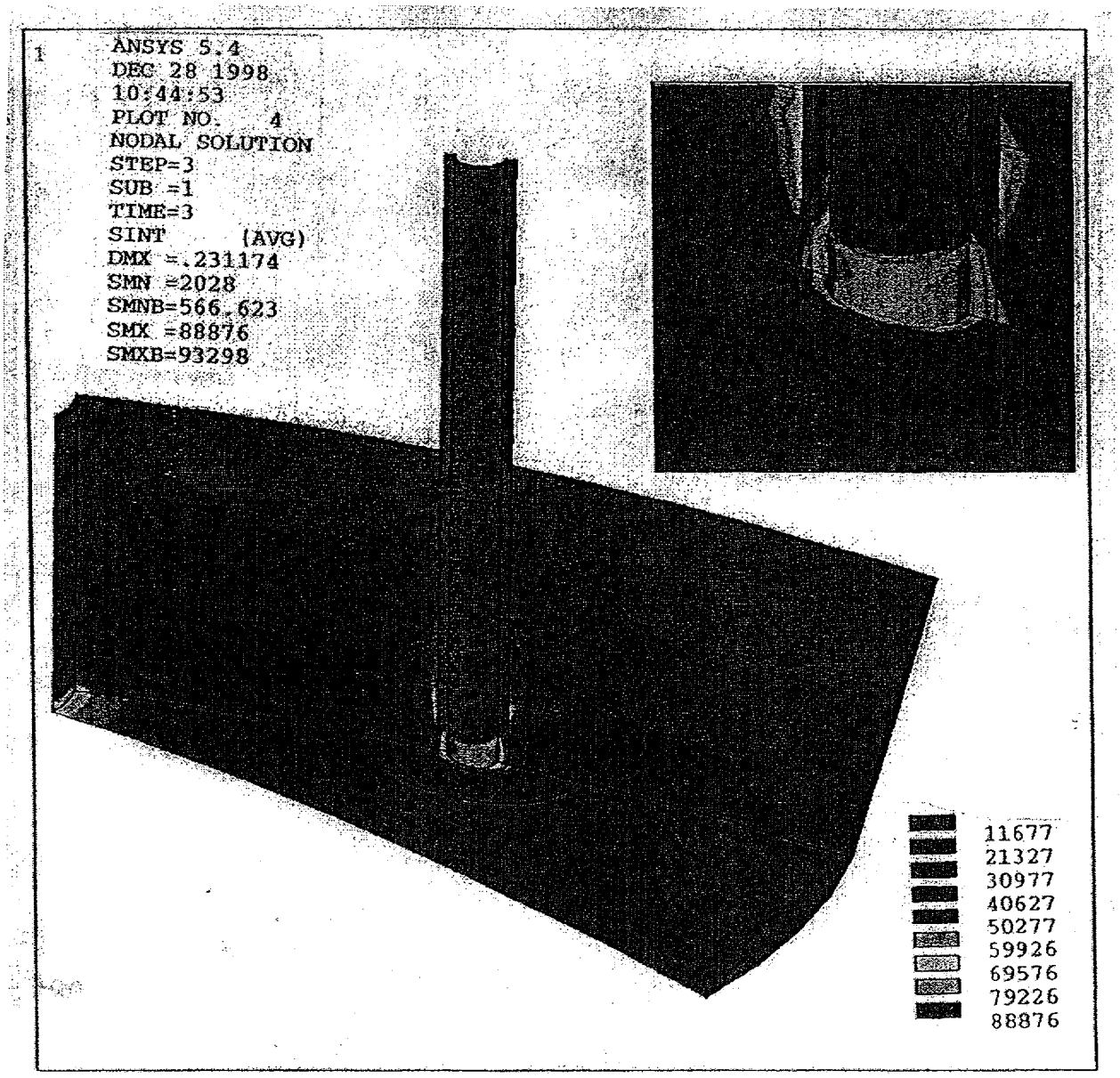

FIGURE 5-8

VENT PIPE FINITE ELEMENT MODEL

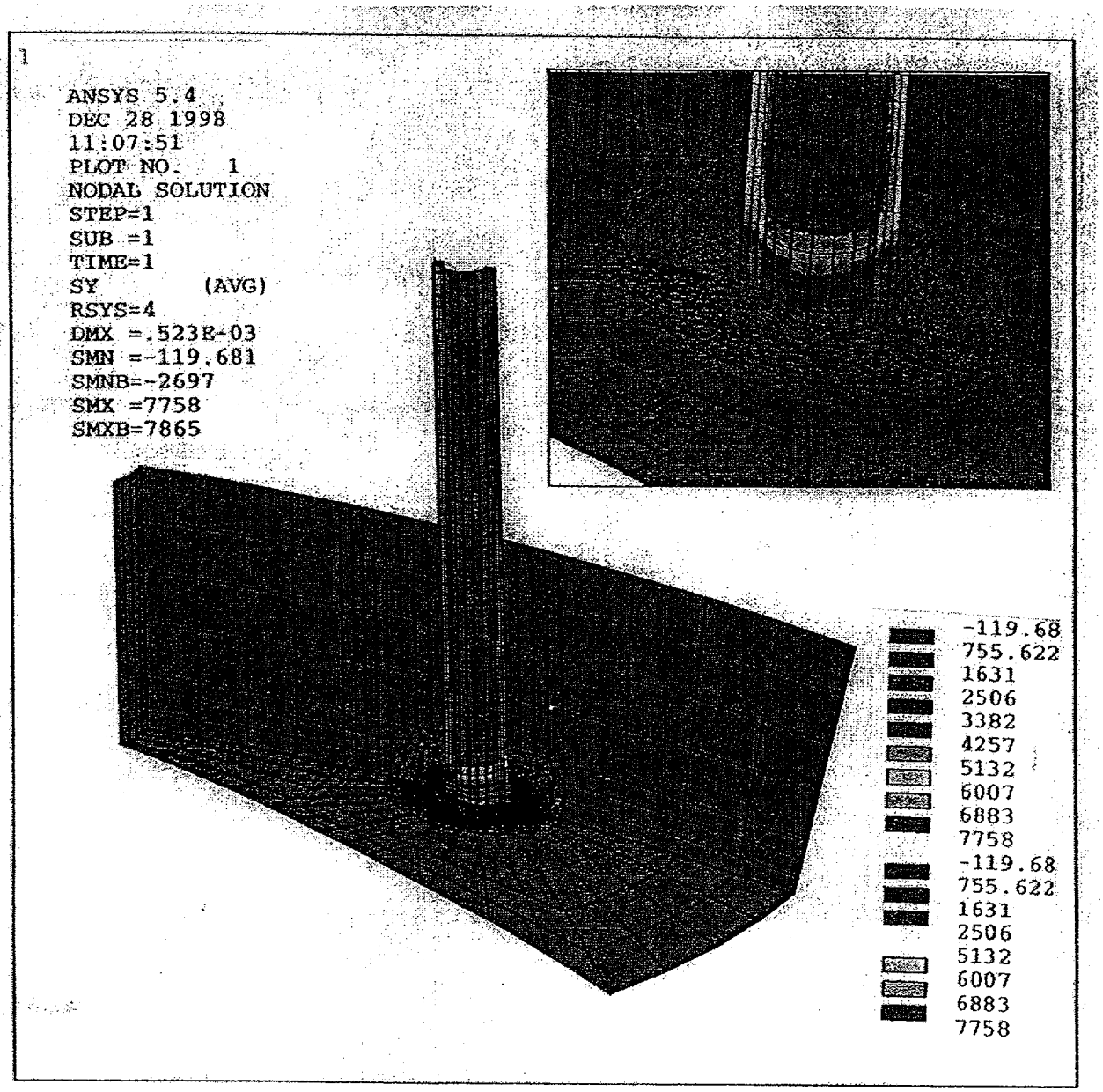

FIGURE 5-9

HOOP STRESS IN THE HEAD VENT AS A RESULT OF DESIGN PRESSURE OF 2500 PSI

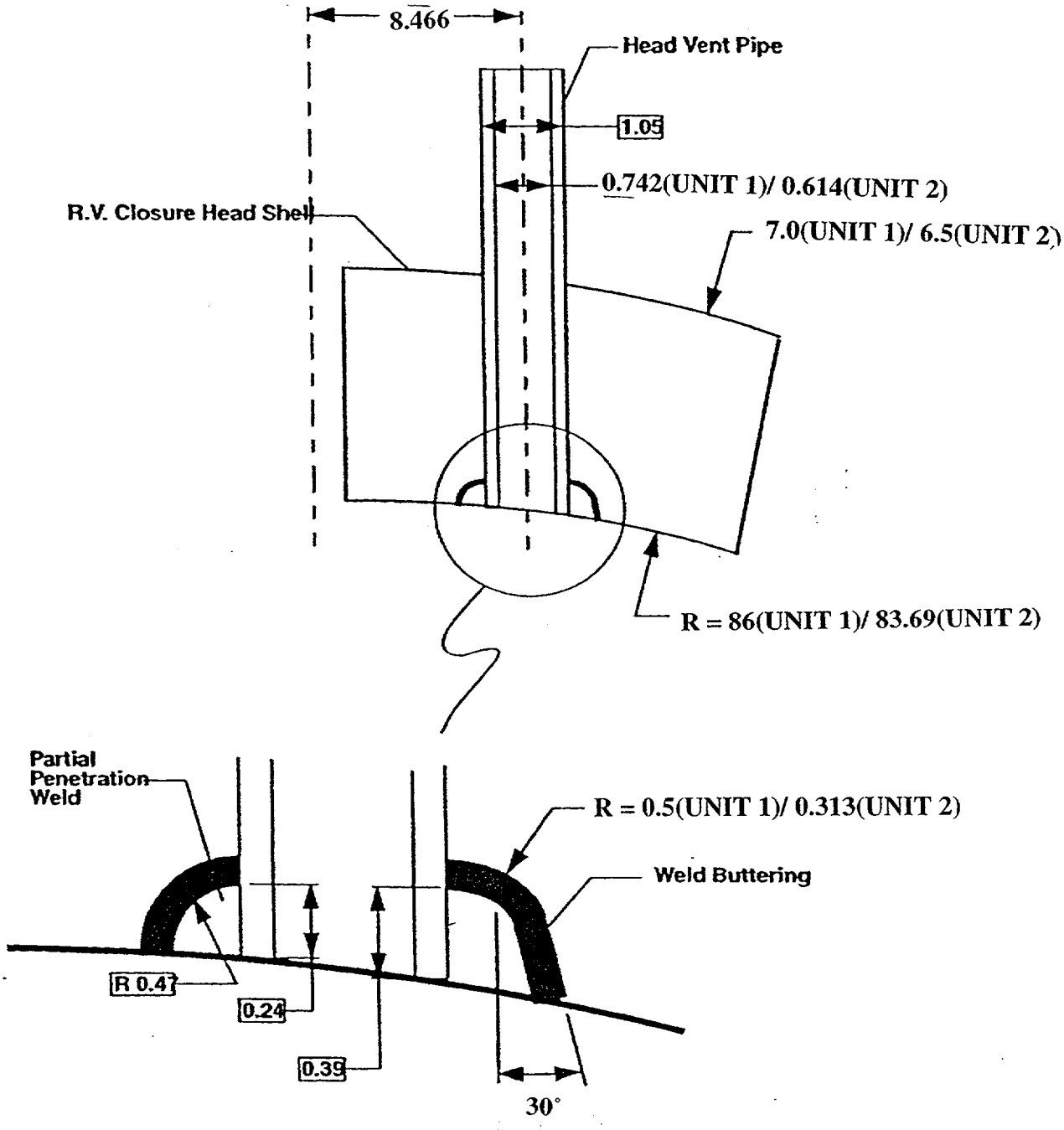

FIGURE 5-10

STRESS INTENSITY RESULTS IN THE HEAD VENT FOR THE GOVERNING UPSET CONDITION

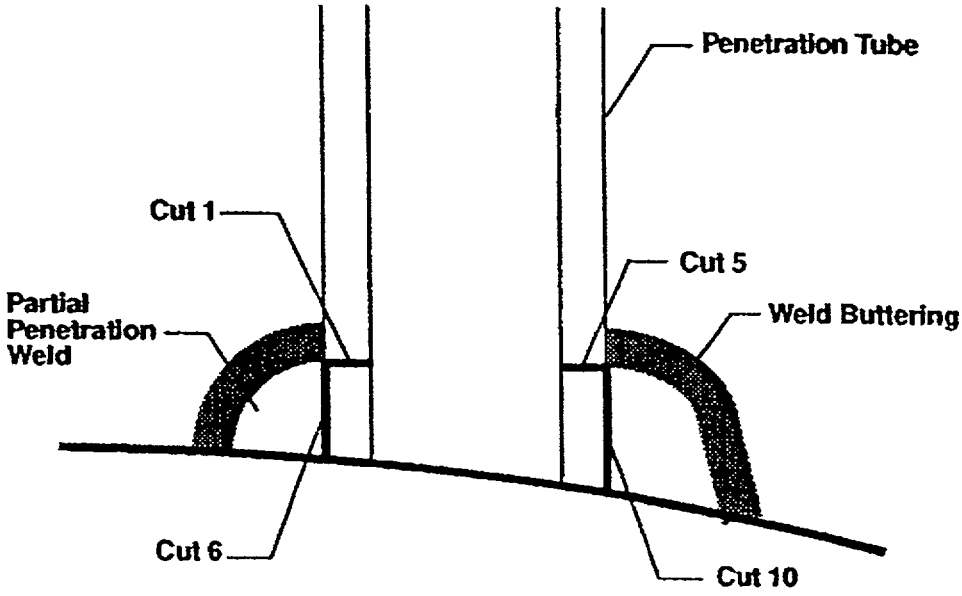

FIGURE 5-11

VARIOUS CUTS TAKEN FOR ANALYSIS OF THE HEAD VENT

NOTE: CUT 1 WAS THE GOVERNING LOCATION

SECTION 6.0

FLAW EVALUATION CHARTS

6.1 INTRODUCTION

The flaw evaluation charts were developed from the stress analysis of each of the penetration locations, as discussed in Section 5. The crack growth law developed for D. C. Cook in Section 4.2 was used for each case, and two flaw tolerance charts were developed for each penetration location. The first chart characterizes the growth of a part through flaw, and the second chart characterizes the growth of a through-wall flaw in the length direction. The allowable remaining life of the penetration may then be directly determined, using the combined results of the two charts. All times resulting from these calculations are effective full power years.

6.2 OVERALL APPROACH

The results of the three-dimensional stress analysis of the penetration locations were used directly in the flaw tolerance evaluation. The maximum stress is the hoop stress, and the flaws which have been found inservice are all longitudinally oriented, so the hoop stress component was used.

The crack growth evaluation for the part-through flaws was based on the stress distribution through the penetration wall at the location which corresponds to the highest stress along the inner surface of the penetration. The highest stressed location was found to be in the immediate vicinity of the weld for both the center and outermost penetrations.

The stress profile was represented by a cubic polynomial:

$$\sigma(x) = A_0 + A_1 \frac{x}{t} + A_2 \left(\frac{x}{t}\right)^2 + A_3 \left(\frac{x}{t}\right)^3$$

where	x		is the coordinate distance into the wall
	t	=	wall thickness
	σ	=	stress perpendicular to the plane of the crack
	A_i	=	coefficients of the cubic fit

For the surface flaw with a length six times its depth, the stress intensity factor expression of McGowan and Raymund [5A] was used. The stress intensity factor $K_I(\varphi)$ can be calculated anywhere along the crack front. The point of maximum crack depth is represented by $\varphi = 0$. The following expression is used for calculating $K_I(\varphi)$, where φ is the angular location around the crack.

$$K_I(\varphi) = \left[\frac{\pi a}{Q}\right]^{0.5}(\cos^2\varphi + \frac{a^2}{C^2}\sin^2\varphi)^{1/4}(A_O H_O + \frac{2}{\pi}\frac{a}{t}A_1 H_1$$

$$+ \frac{1}{2}\frac{a^2}{t^2}A_2 H_2 + \frac{4}{3\pi}\frac{a^3}{t^3}A_3 H_3)$$

The magnification factors $H_O(\varphi)$, $H_1(\varphi)$, $H_2(\varphi)$ and $H_3(\varphi)$ are obtained by the procedure outlined in reference [5A]. The parameter C is the flaw half-length.

[

]^{a,c,e}

6.3 RESULTS: AXIAL FLAWS

CRDM Surface Flaws

The results of the calculated growth through the wall for inside surface axial flaws postulated in the penetrations are summarized in Figures 6-1a and 6-1b for Unit 1, and Figures 6-2a and 6-2b for Unit 2. Figures 6-1 and 6-2 apply to surface crack locations anywhere in the weld region of any of the penetrations, since the stress results were taken at the highest stressed location, which is in the outermost penetration. The "a" figure in each case is a prediction of crack growth at and below the attachment weld region, while the "b" figure covers crack growth above the weld. Figures 6-1c and 6-2c apply to crack growth for outside surface axial flaws, regardless of location, for the two units. Note that the predicted extension through the penetration thickness requires many years at the operating temperature for either D. C. Cook Unit 1 or 2, regardless of the location.

Head Vent

The only flaw evaluation chart necessary for the head vent region is for flaws at and above the weld, since there is no portion of the head vent which projects below the weld. Figure 6-1d and 6-2d provide the projected growth of a part through flaw in the head vent just above the attachment weld (cut 1 in Figure 5-11). The growth through the wall is relatively rapid, because the thickness of the head vent is small.

CRDM Through-Wall Flaws

Figures 6-3 and 6-4 present the predicted crack growth for a through-wall flaw postulated to exist below the weld region in the outermost row of penetrations. These results are for the lower hillside and centerside locations respectively. Note that on each of these figures there are two curves of crack growth vs time. The two curves are generally parallel, show the projected growth for the two different Units. The growth for Unit 1 is slower, because it operates at a lower temperature. Although there are different levels of ovality (and therefore residual stress) in the different penetrations, it is clear that in the vicinity of the weld and below it, the total stresses approach the yield stress of the material, which was set at 378.6 MPa (55 ksi) for this calculation. Figures 6-5 and 6-6 provide similar results for the next outermost row of penetrations.

Figure 6-7 provides projections of growth above the weld region for the center penetration. The upper edge of the weld has been assumed to be at the 2.0 inch location in this figure, and the growth above this location is presented as a function of time in years.

Note that for some of the penetrations crack extension actually stops, as the stress intensity factor decreases with the lower stresses, to a value below the threshold cracking susceptibility value of 9 MPa $\sqrt{m}$

6.4 CIRCUMFERENTIAL CRACK PROPAGATION

Since circumferentially oriented flaws have been found at three plants (Bugey3, Oconee 2, and Oconee 3), it is important to consider the possibility of crack extension in the circumferential direction. The first case was discovered as part of the destructive examination of the tube with the most extensive longitudinal cracking at Bugey 3, and the crack was found to have extended to a depth of 2.25 mm in a wall thickness of 16 mm. The flaw was found at the outside surface of the penetration (number 54) at the lower hillside location, just above the weld.

The circumferential flaws in Oconee Unit 3 were discovered during the process of repairing a number of axial flaws, while the circumferential flaw in Oconee Unit 2 was discovered by UT. Experience gained from these findings has enabled the development of UT procedures capable of detecting circumferential flaws reliably.

It is important to realize that a flaw would have to propagate through the penetration or the attachment weld, and result in a leak, before the outer surface of the penetration would be exposed to the water. Cracking could then begin for an outside surface flaw. (This is believed to have been the case at all three plants in which circumferential flaws were found). This time period was conservatively ignored in the calculations to be discussed.

To investigate this issue completely, a series of crack growth calculations were carried out for a postulated surface circumferential flaw located just above the head penetration weld, in a plane parallel to the weld itself. This is the only flaw plane which could result in a complete separation of the penetration, since all others would result in propagation below the weld, and therefore no chance of complete separation because the remaining weld would hold the penetration in place.

[

]a,c,e

[

]a,c,e

Therefore we see that the time required for propagation of a circumferential flaw to a point where the integrity of the penetration would be affected would be at least 38 years. Because of the conservatisms in the calculations, as discussed above, it is likely to be even longer.

6.5 FLAW ACCEPTANCE CRITERIA

Now that projected crack growth curves have been developed, the question which remains to be addressed is what size flaw would be acceptable for further service.

Acceptance criteria have been developed for indications found during inspection of reactor vessel upper head penetrations. These criteria were developed as part of an industry program coordinated by NUMARC (now NEI). Such criteria are normally found in Section XI of the ASME Code, but Section XI does not require inservice inspection of these regions and therefore acceptance criteria are not

available. In developing the enclosed acceptance criteria, the approach used was very similar to that used by Section XI, in that an industry consensus was reached using input from both operating utility technical staff and each of the three PWR vendors. The criteria developed are applicable to all PWR plant designs.

Since the discovery of the leaks at Oconee and ANO-1, the acceptance criteria have been revised slightly, to cover flaws on the outside diameter of the penetration below the attachment weld, and flaws in the attachment weld. These revised criteria are now in draft form, but they are expected to be acceptable to the NRC, and will be used in these evaluations. The draft portions of the acceptance criteria will be noted below.

The criteria which are presented herein are limits on flaw sizes which are acceptable. The criteria are to be applied to inspection results. It should be noted that determination of the future service during which the criteria are satisfied is plant-specific and dependent on flaw geometry and loading conditions.

It has been previously demonstrated by each of the owners groups that the penetrations are very tolerant of flaws and there is only a small likelihood of flaw extension to large sizes. Therefore, it was concluded that complete fracture of the penetration is highly unlikely and, therefore, protection against leakage during service is the priority.

The approach used here is more conservative than that used in Section XI applications where the acceptable flaw size is calculated by putting a margin on the critical flaw size. In this case, the critical flaw size is far too large to allow a practical application of this approach so protection against leakage is the key element.

The acceptance criteria apply to all flaw types regardless of orientation and shape. The same approach is used by Section XI, where flaws are characterized according to established rules and then compared with acceptance criteria.

Flaw Characterization

Flaws detected must be characterized by length and preferably depth. If only the length is determined, assume the depth is half the length based on experience with the shape of flaws reported. The proximity rules of Section XI for considering flaws as separate, may be used directly (Section XI, Figure IWA 3400-1). This figure is reproduced here as Figure 6-10.

When a flaw is found, its projections in both the axial and circumferential directions must be determined. Note that the axial direction is always the same for each penetration, but the circumferential direction will be different depending on the angle of intersection of the penetration with the head. The "circumferential" direction of interest here is along the top of the attachment weld, as illustrated in Figure 6-11. It is this angle which will change for each penetration and which is also the plane which could cause separation of the penetration tube from the head. The location of the flaw relative to both the top and bottom of the partial penetration attachment weld must be determined since a potential leak path exists when a flaw progresses through the wall and up the penetration past this weld. A schematic of a typical weld geometry is shown in Figure 6-12.

Flaw Acceptance Criteria

The maximum allowable depth (a_f) for flaws on the inside surface of the penetration, at or above the weld is 75 percent of the penetration wall thickness regardless of the flaw orientation. The term a_f is defined as the maximum size to which the detected flaw is calculated to grow in a specified time period. This 75 percent limitation was selected to be consistent with the maximum acceptable flaw depth in Section X1 and to provide an additional margin against through wall penetration. There is no concern about separation of the head penetration from the head, unless the flaw is above the attachment weld and oriented circumferentially. Calculations have been completed to show that all penetration geometries can support a continuous circumferential flaw with a depth of 75 percent of the wall.

Axial inside surface flaws found below the weld are acceptable regardless of depth as long as their upper extremity does not reach the bottom of the weld during the period of service until the next inspection. Axial flaws which extend above the weld are limited to 75 percent of the wall.

Axial flaws on the OD of the penetration below the attachment weld are acceptable regardless of depth, as long as they do not extend into the attachment weld during the period of service until next inspection. Axial OD flaws above the attachment weld must be evaluated on a case by case basis, and must be discussed with the regulatory authority.

Circumferential flaws located below the weld are acceptable regardless of their depth, provided the length is less than 75 percent of the circumference for the period of service until the next inspection. Flaws in this area have no structural significance but loose parts must be avoided. To this end,

intersecting axial and circumferential flaws shall be removed or repaired. Circumferential flaws at and above the weld must be discussed with the regulatory authority on a case by case basis.

Flaws located in the attachment welds themselves are not acceptable regardless of their depth. This is because the crack propagation rate is several times faster than that of the Alloy 600 tube material, and also because depth sizing capability does not yet exist for indications in the weld.

These criteria are summarized in Table 6-1. Flaws which exceed these criteria must be repaired unless analytically justified for further service. These criteria have been reviewed and approved by the NRC, as documented in references 7 and 8, with the exception of the draft criteria discussed above, for OD flaws and flaws in the attachment weld.

It is expected that the use of these criteria and crack growth curves will provide conservative predictions of the allowable time of service. Similar criteria have been proposed in Sweden and France, and are under discussion in other countries.

6.6 EXAMPLE CALCULATIONS

The crack growth prediction curves in Figures 6-1 through 6-9 can be used with the acceptance criteria of Section 6.5 to determine the available service time for either unit. In this section, a few examples will be presented to illustrate the use of these figures. Although this handbook allows calculations to be done for either unit, the examples presented here have used Unit 2. The example cases are listed in Table 6-2.

Example 1. For an axially oriented surface flaw, the crack growth curves of Figure 6-2 are appropriate. Since the flaw is located below the weld, Figure 6-2a is appropriate, and has been reproduced as Figure 6-13. Figures 6-2a and 6-2b here both use the same crack growth curve, but illustrate two different scenarios. Figure 6-2a shows the result if the flaw is close to the weld, or is projected to grow to the bottom of the weld during service. In this case the flaw initial depth is 25 percent of the wall thickness, so project a line horizontally at $a/t = 0.25$, intersecting the crack growth curve. The service life is then determined as the time for this flaw to grow to the limit of 75 percent of the wall thickness, or approximately 5.6 years (labelled Service Life 1).

The other case, illustrated in figure 6-2b, is that the flaw remains below the bottom of the weld. In this case, the criteria allow the flaw to extend through the wall, which results in a longer service life,

approximately 7.5 years (labelled Service Life 2). If the flaw were sufficiently far below the weld, we could take advantage of the additional time for a through wall flaw to grow up to the weld. This case will be illustrated in example 6.

Example 2. In this case the flaw is identical in size to example 1, but located at the weld, and at a location 180° away from the flaw in example 1. The curve to use is in Figure 6-2b. The circumferential location is not important for surface flaws, only for through-wall flaws. The determination of service life is illustrated in Figure 6-14, where we see the result is approximately 5.6 years.

Example 3. The flaw is at the weld, and twice as deep as the flaw considered in example 2. It is oriented at 0°. The curve from Figure 6-2a is again used to determine the service life. The flaw depth is 50 percent of the wall thickness, so project horizontally at this value to intersect the crack growth curve. The allowable service life is then determined as the time for the flaw to reach a depth of 75 percent of the wall. As shown in Figure 6-15, this time is approximately 2.3 years.

Example 4. This case is for a circumferential flaw which has been discovered above the weld. The appropriate figure for this type flaw is Figure 6-8, which has been reproduced as Figure 6-16, where the flaw size has been plotted. The additional service life is obtained by plotting the flaw depth ($a/t = 0.25$) on the vertical axis and projecting horizontally to the crack growth curve. The service life is the time for the flaw to reach 75 percent of the vessel wall, which is approximately 11 years, as seen in Figure 6-16.

Example 5. This case considers a shallow surface flaw at the weld, which again requires use of Figure 6-2a, reproduced here as Figure 6-17. The flaw is 2 mm deep, or 12.5 percent of the wall thickness. Note that this value falls on the crack growth curve in Figure 6-17. In this case the flaw would be predicted to follow the curve during future service, because the crack growth curve has been based on the smallest flaw size which would be predicted to grow. Therefore, the true service life would be over 8 years.

Example 6. This case is an axial surface flaw well below the weld region. From Figure 6-2a we obtain the appropriate curve for the crack growth prediction through the wall, and this is reproduced as the upper figure of Figure 6-18. This figure gives a service life estimate of approximately 6.2 years to through wall penetration. Additional life can still be added by considering the growth of the flaw up the tube to the bottom of the weld. This is illustrated in the bottom figure of Figure 6-18.

The bottom figure is taken from Figure 6-3. When the surface flaw grows through the wall, it will have increased in size by a factor of three, so its length will be 30 mm. If the flaw is centered at one inch below the weld, its new length after growth through the thickness is 15 mm (0.6 inches) above and 15 mm below its center point. This makes its upper extent at 2.6 inches. The additional service life for propagation to the bottom of the weld is approximately three years, making a total service life of approximately 9.2 years before the flaw would be predicted to violate the acceptance criteria.

It is clear from these examples that the most important figures for use in evaluating flaws in head penetrations are the surface flaw Figures 6-1 and 6-2 for axial flaws and 6-8 for circumferential flaws. The figures which project the growth of through-wall flaws are valuable, but may be of limited practical use with the acceptance criteria. There is an important safety aspect to the through-wall flaw charts, however, in that they demonstrate that flaw propagation above the weld will be very limited.

TABLE 6-1

SUMMARY OF R.V. HEAD PENETRATION ACCEPTANCE CRITERIA

Location	Axial		Circ	
	a_f	ℓ	a_f	ℓ
Below Weld (ID)	t	no limit	t	.75 circ.
At and Above Weld (ID)	0.75 t	no limit	*	*
Below Weld (OD)	t	no limit	t	.75 circ.
Above Weld (OD)	*	*	*	*

Note: Flaws of any size in the attachment weld are not acceptable.

* Requires case-by-case evaluation and discussion with regulatory authority.

a_f = Flaw Depth as defined in IWB 3600

ℓ = Flaw Length

t = Wall Thickness

TABLE 6-2

EXAMPLE PROBLEM INPUTS

Example No.	Orientation	Vertical Location	Radial* Location	Penetration Row	Length	Depth (t)
1	Axial	Below Weld	0°	Outer	10 mm.	4 mm.
2	Axial	At Weld	180°	Outer	10 mm.	4 mm.
3	Axial	At Weld	0°	Outer	10 mm.	8 mm.
4	Circumferential	Above Weld	180°	Outer	8 mm.	4 mm.
5	Axial	At Weld	0°	Outer	10 mm.	2 mm.
6	Axial	1" Below Weld	0°	Outer	10	5.3 mm.

*Note: Centerside = 0°
Lower Hillside = 180°

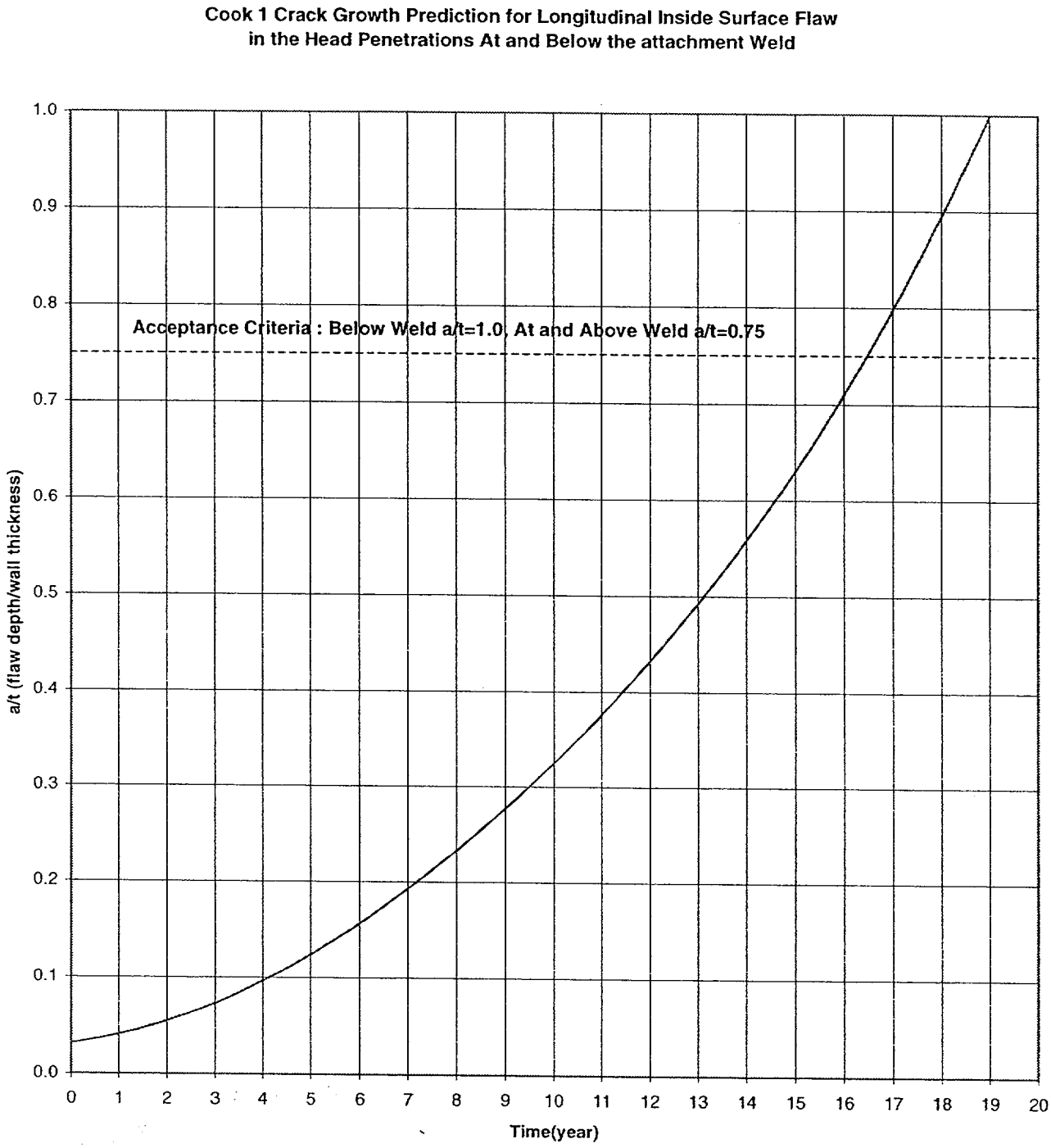

FIGURE 6-1a

CRACK GROWTH PREDICTIONS FOR LONGITUDINAL INSIDE SURFACE FLAWS IN THE HEAD PENETRATIONS IN THE D. C. COOK UNIT 1 AT AND BELOW THE ATTACHMENT WELD

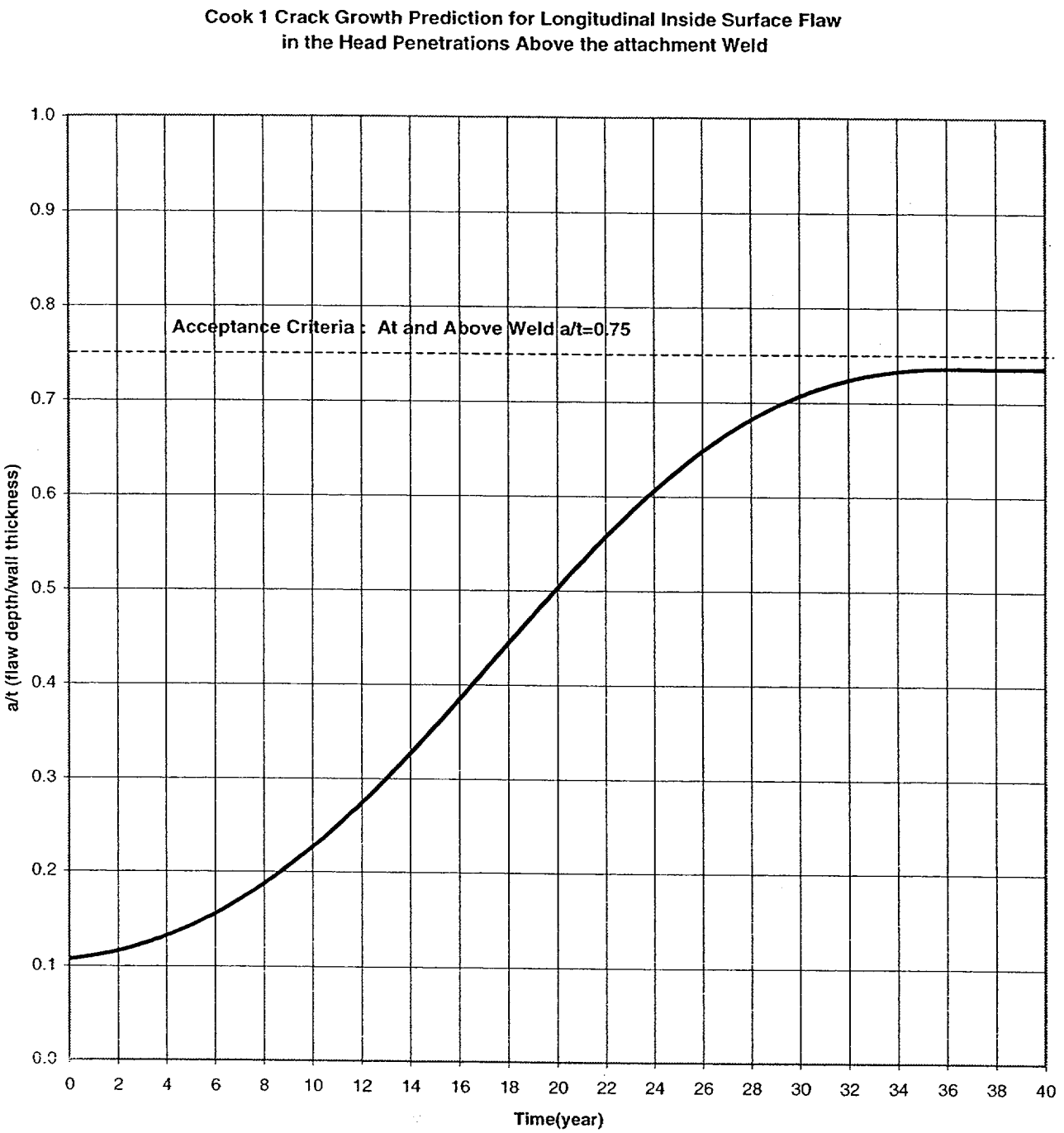

FIGURE 6-1b

CRACK GROWTH PREDICTIONS FOR LONGITUDINAL INSIDE SURFACE FLAWS IN THE HEAD PENETRATIONS AT THE D. C. COOK UNIT 1 ABOVE THE ATTACHMENT WELD

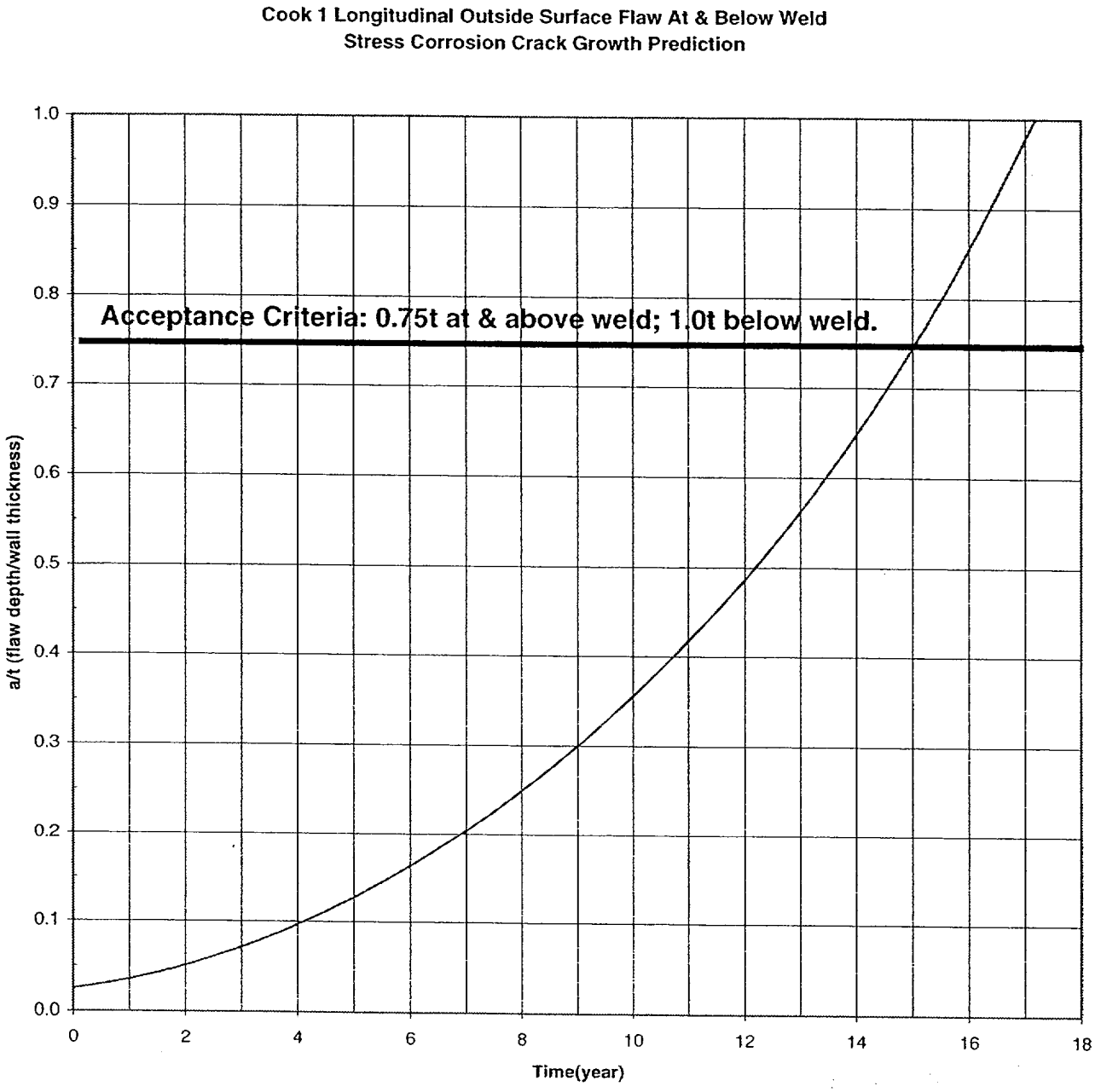

FIGURE 6-1c

CRACK GROWTH PREDICTIONS FOR LONGITUDINAL OUTSIDE SURFACE FLAWS IN THE HEAD PENETRATIONS AT THE D. C. COOK UNIT 1

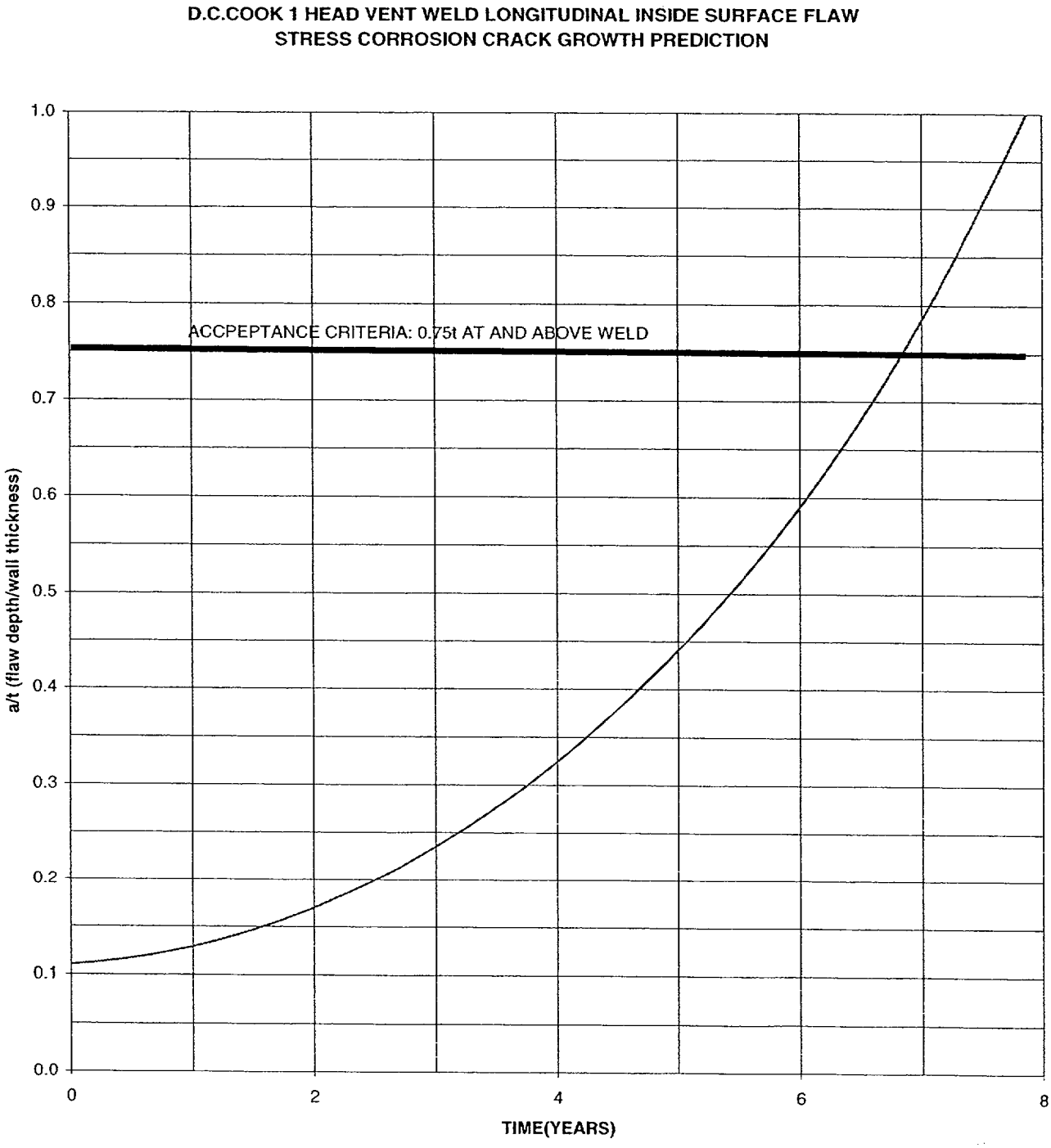

FIGURE 6-1d

CRACK GROWTH PREDICTION FOR LONGITUDINAL SURFACE FLAWS IN THE HEAD VENT NEAR THE ATTACHMENT WELD

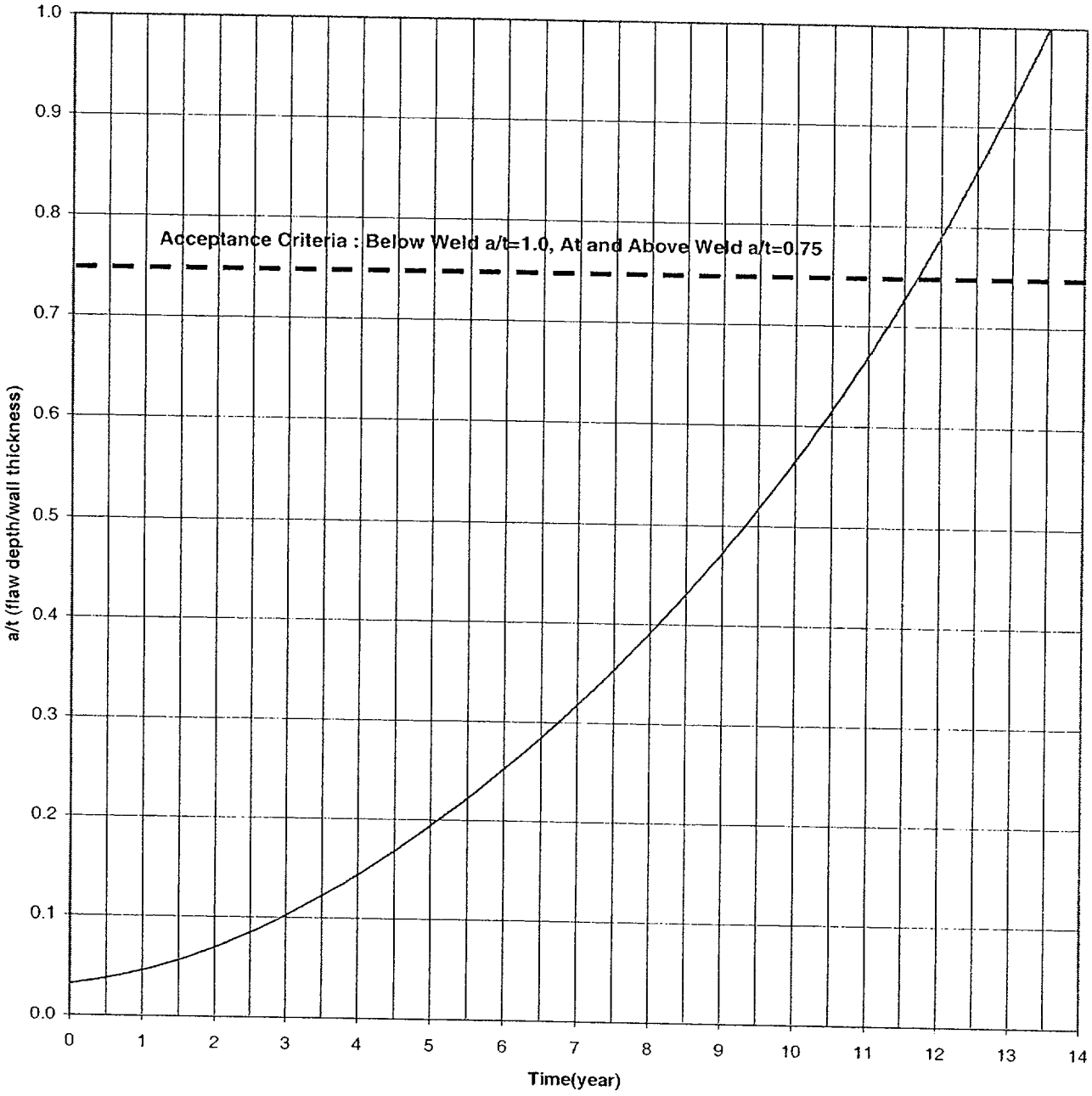

FIGURE 6-2a

CRACK GROWTH PREDICTIONS FOR LONGITUDINAL INSIDE SURFACE FLAWS IN THE HEAD PENETRATIONS AT THE D. C. COOK UNIT 2 AT AND BELOW THE ATTACHMENT WELD

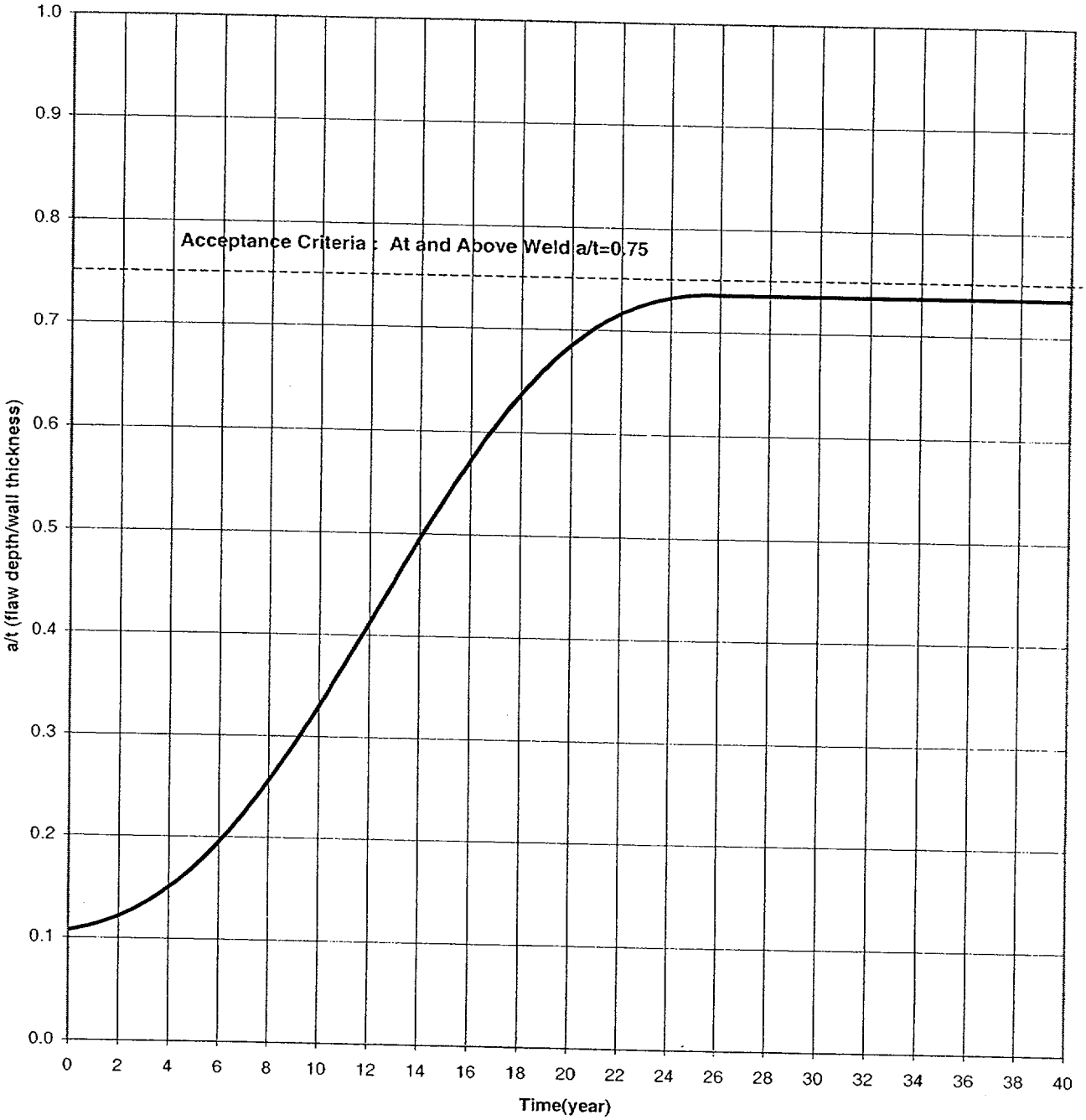

FIGURE 6-2b

CRACK GROWTH PREDICTIONS FOR LONGITUDINAL INSIDE SURFACE FLAWS IN THE HEAD PENETRATIONS AT THE D. C. COOK UNIT 2 ABOVE THE ATTACHMENT WELD

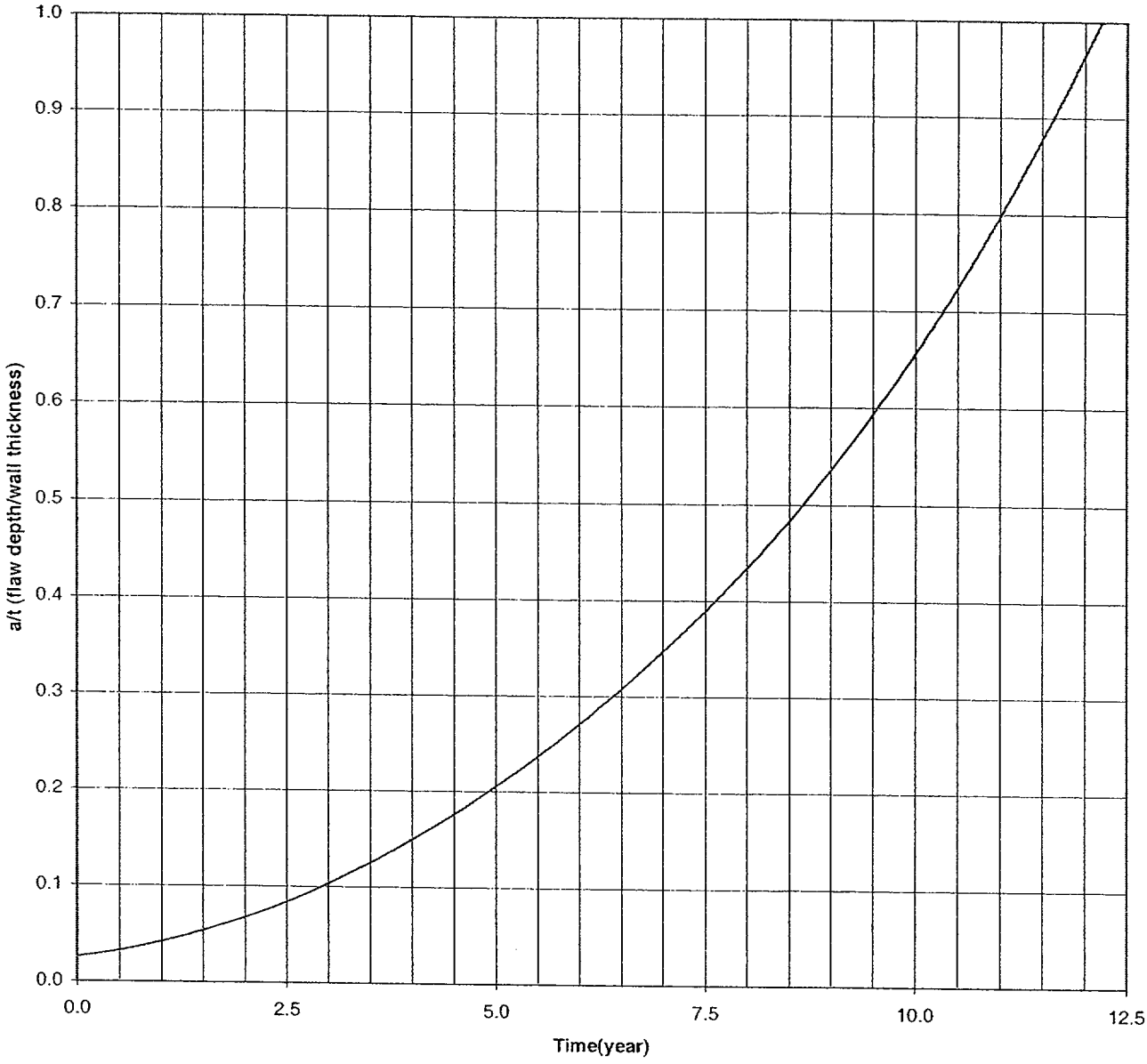

FIGURE 6-2c

CRACK GROWTH PREDICTIONS FOR LONGITUDINAL OUTSIDE SURFACE FLAWS IN THE HEAD PENETRATIONS AT THE D. C. COOK UNIT 2

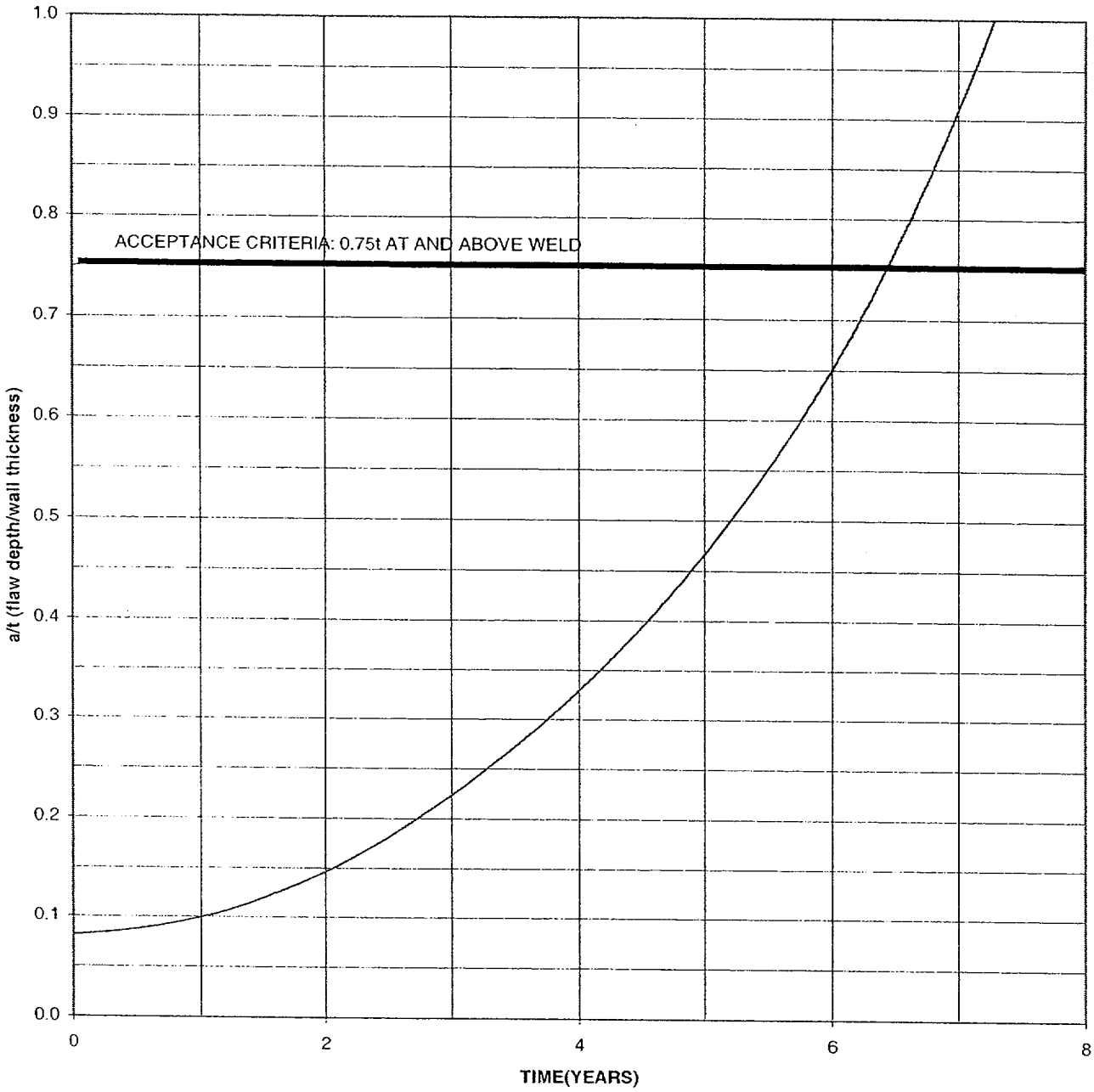

FIGURE 6-2d

CRACK GROWTH PREDICTION FOR LONGITUDINAL SURFACE FLAWS IN THE HEAD VENT NEAR THE ATTACHMENT WELD

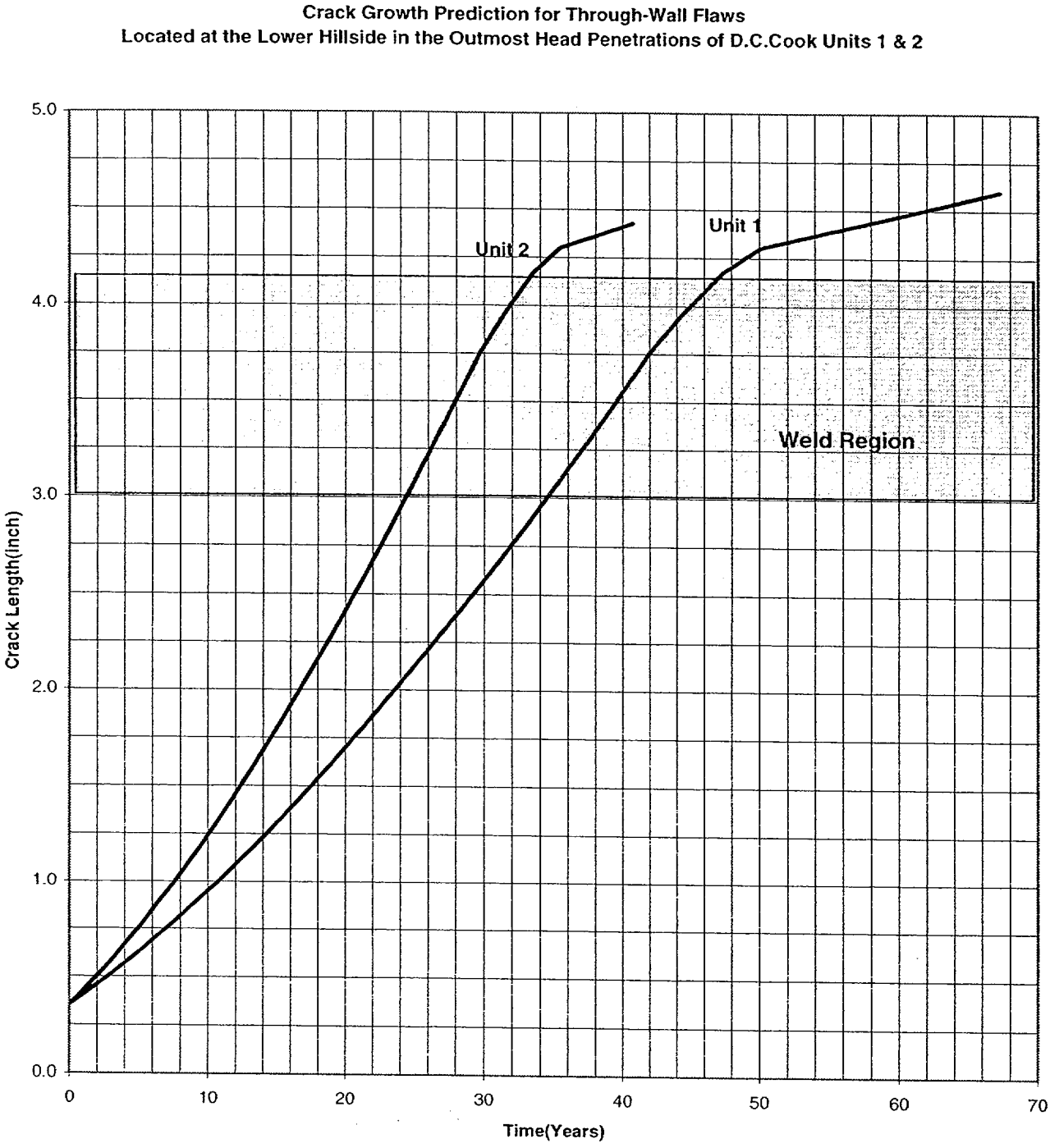

FIGURE 6-3

CRACK GROWTH PREDICTIONS FOR THROUGH-WALL FLAWS LOCATED AT THE LOWER HILLSIDE IN THE OUTERMOST HEAD PENETRATIONS OF D. C. COOK UNITS 1 AND 2

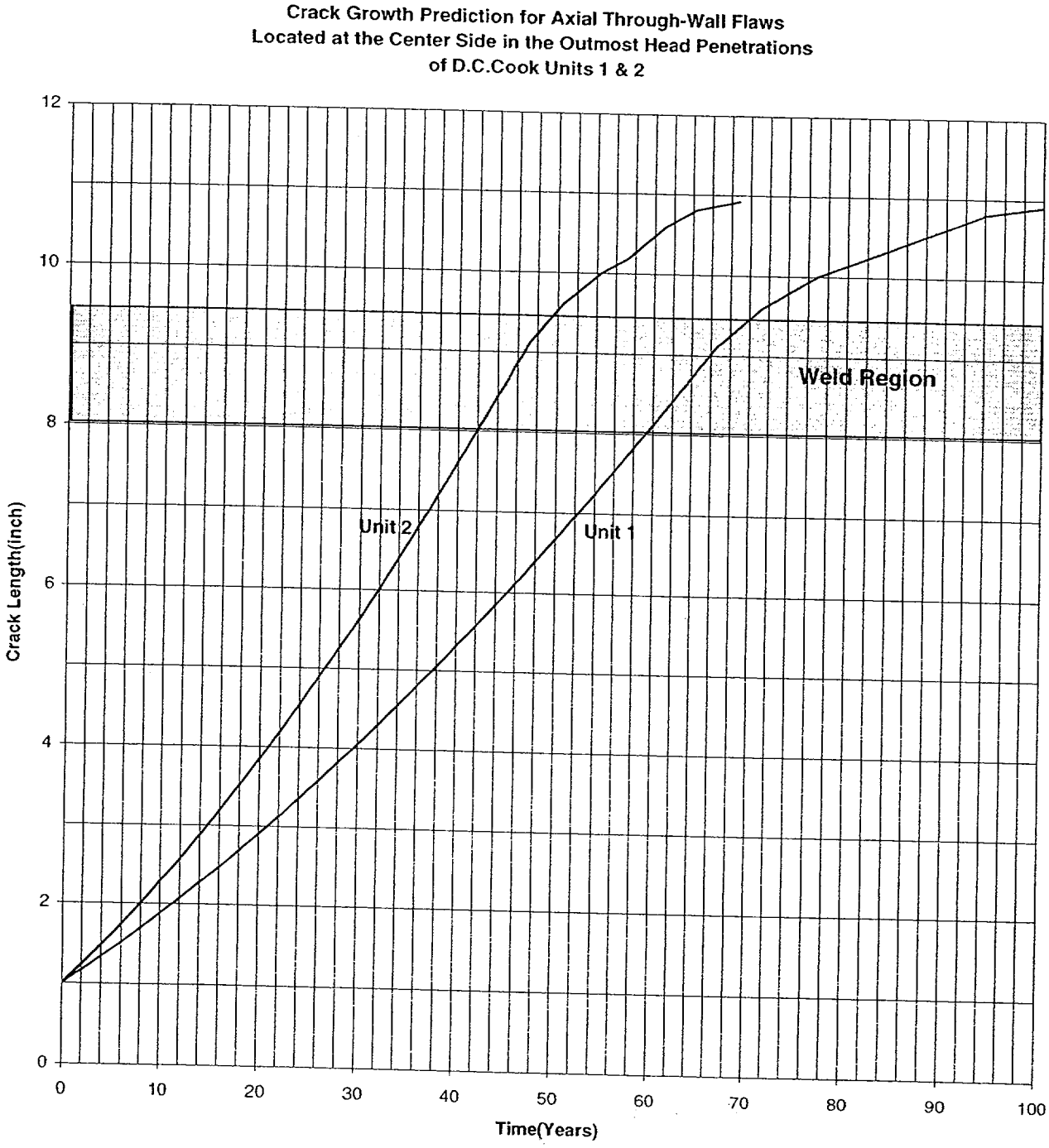

FIGURE 6-4

CRACK GROWTH PREDICTIONS FOR THROUGH-WALL FLAWS LOCATED AT THE CENTER SIDE OF THE OUTERMOST HEAD PENETRATIONS OF D. C. COOK UNITS 1 AND 2

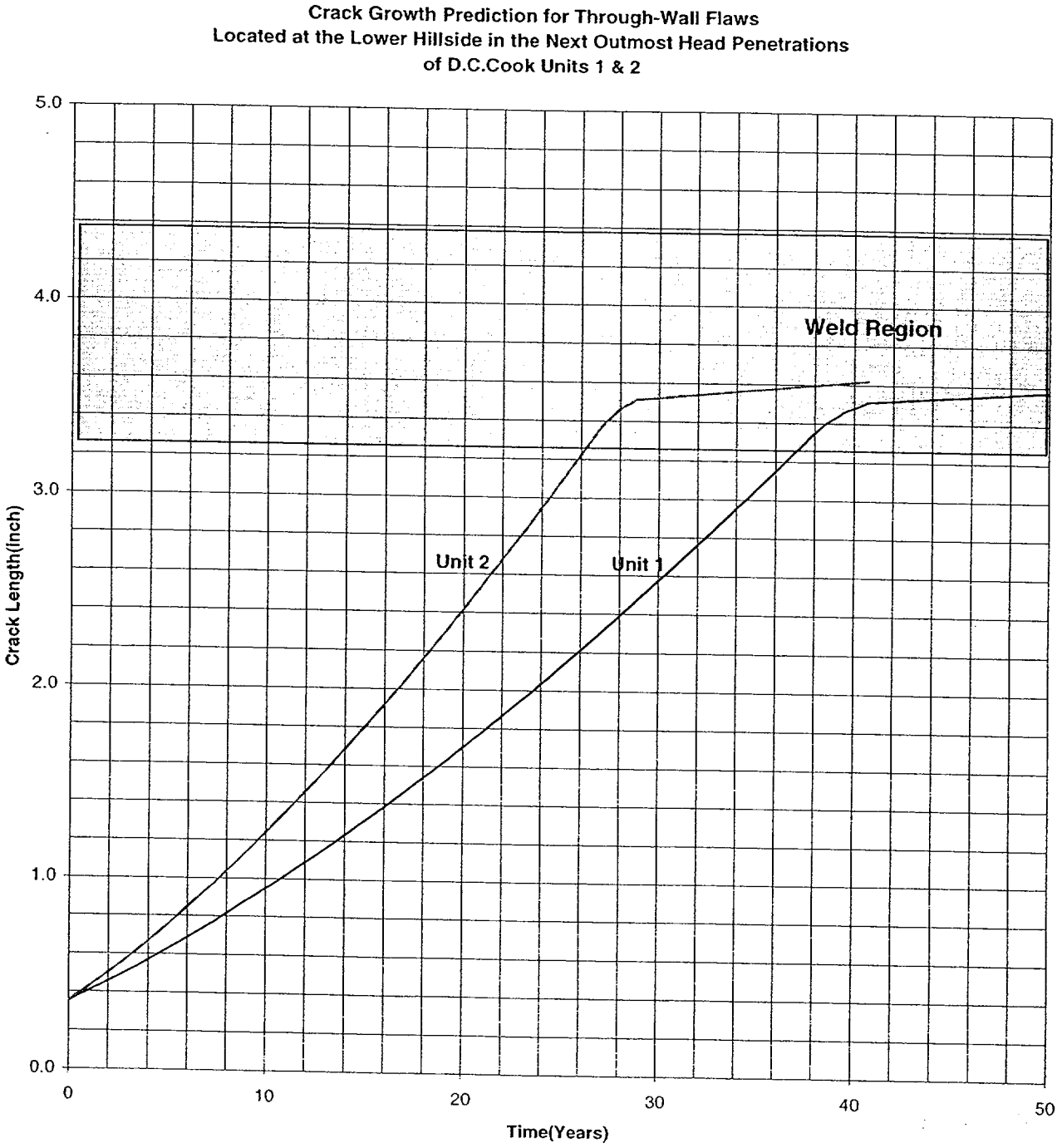

FIGURE 6-5

CRACK GROWTH PREDICTIONS FOR THROUGH-WALL FLAWS LOCATED AT THE LOWER HILLSIDE IN THE NEXT OUTERMOST HEAD PENETRATIONS OF D. C. COOK UNITS 1 AND 2

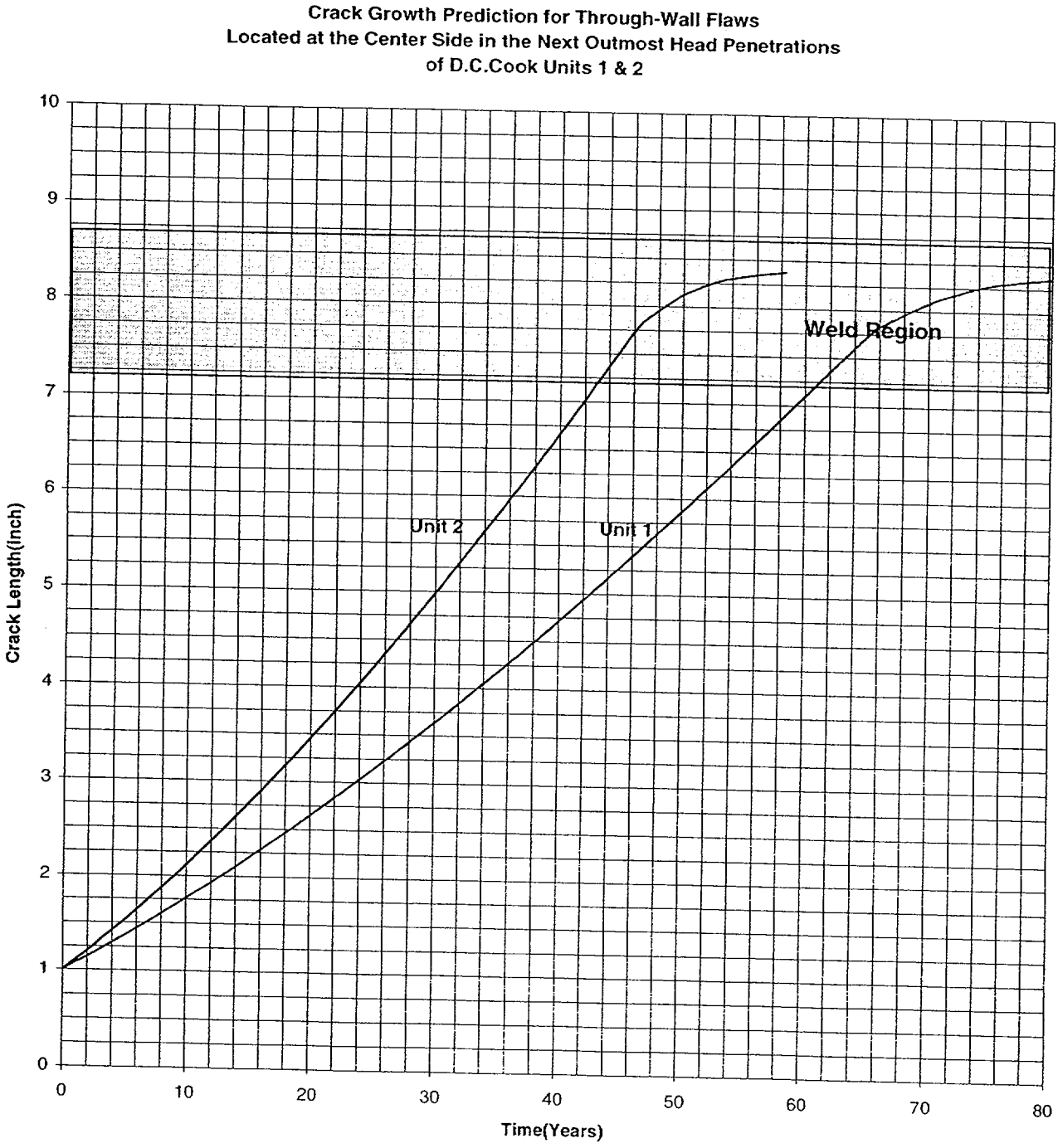

FIGURE 6-6

CRACK GROWTH PREDICTIONS FOR THROUGH-WALL FLAWS LOCATED AT THE CENTER SIDE OF THE NEXT OUTERMOST HEAD PENETRATIONS OF D. C. COOK UNITS 1 AND 2

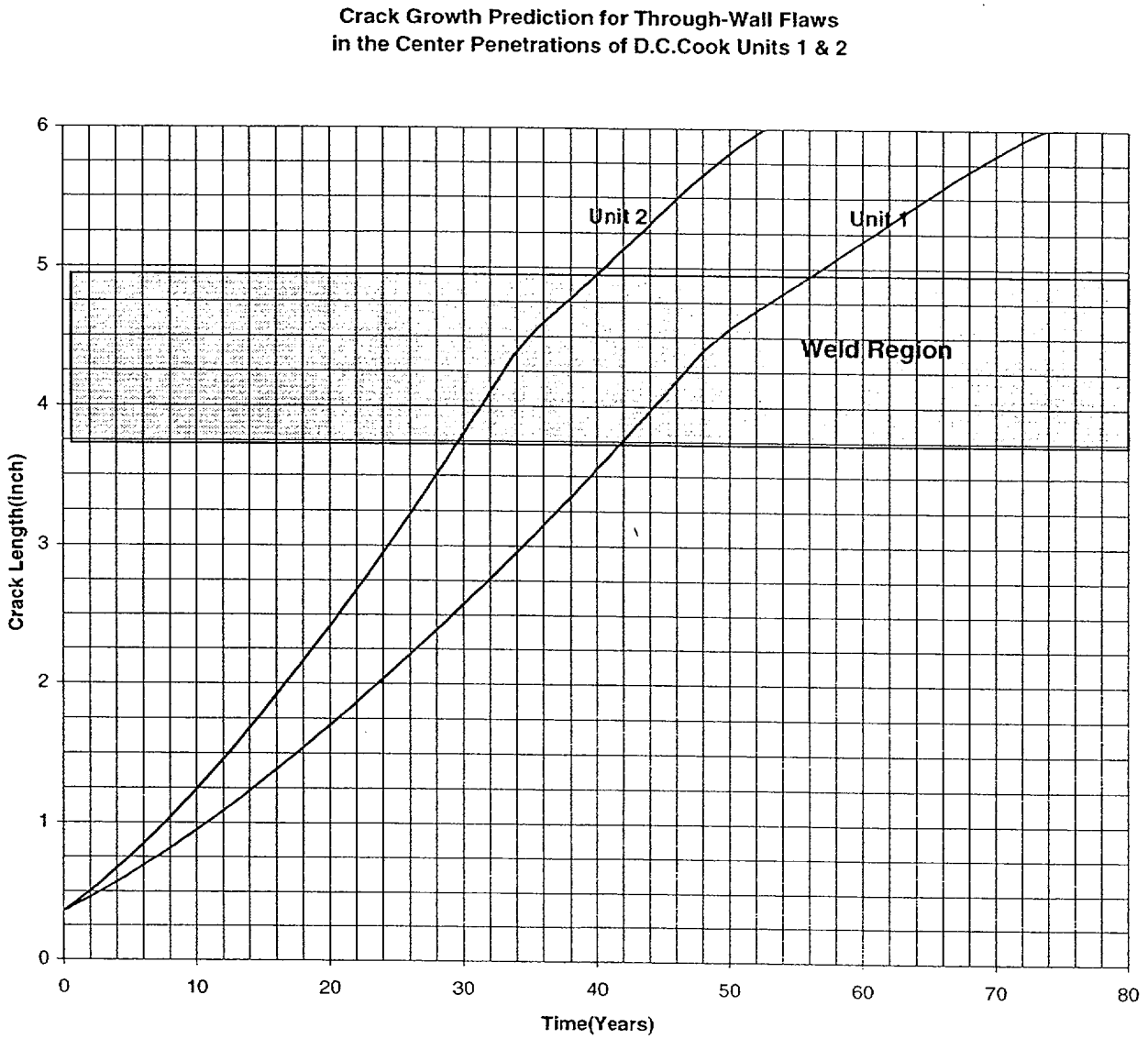

FIGURE 6-7

CRACK GROWTH PREDICTIONS FOR GROWTH OF THROUGH-WALL FLAWS

IN THE CENTER PENETRATION AT D. C. COOK UNITS 1 AND 2

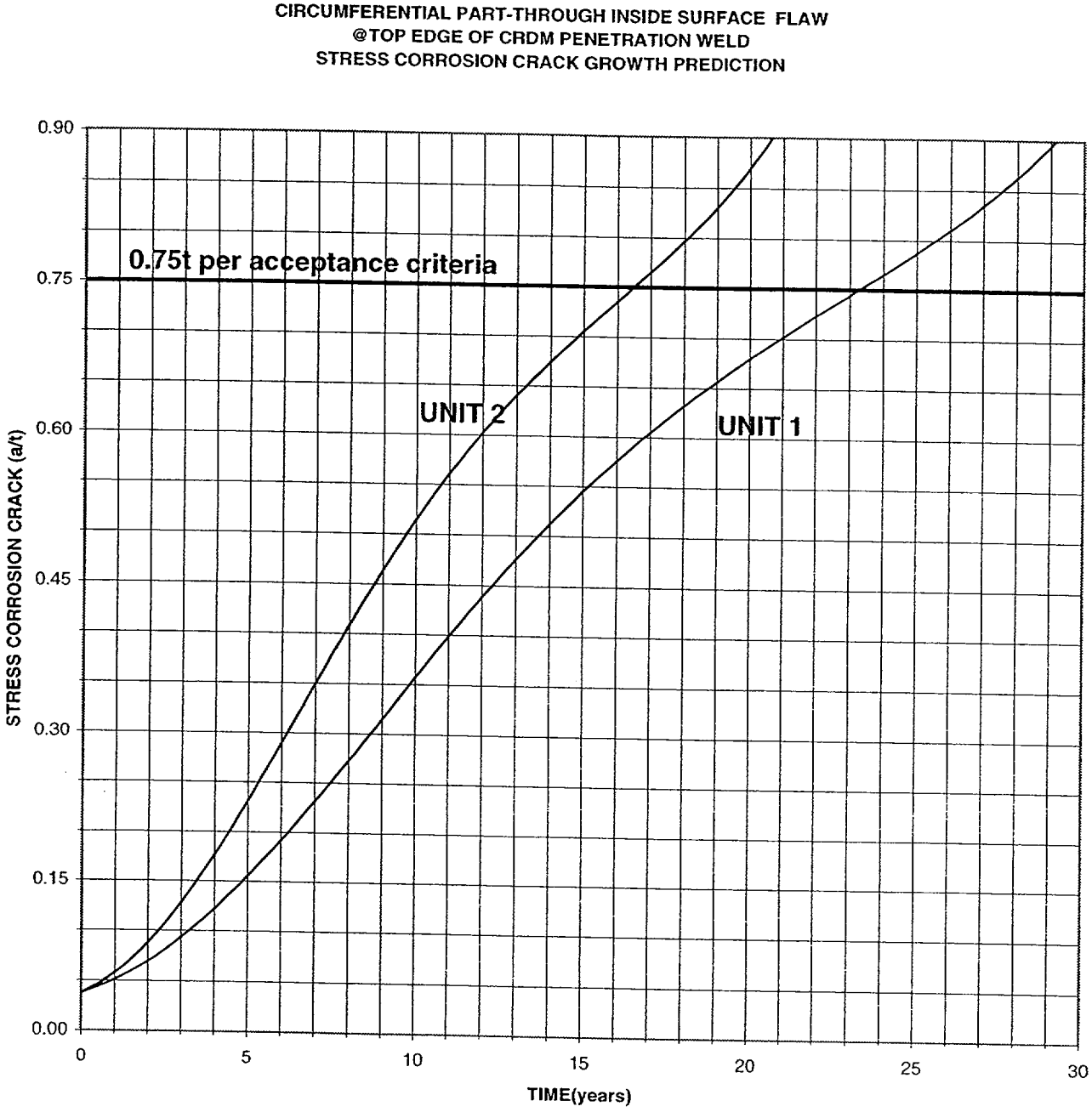

FIGURE 6-8

CRACK GROWTH PREDICTIONS FOR CIRCUMFERENTIAL SURFACE FLAWS

NEAR THE TOP OF THE ATTACHMENT WELD

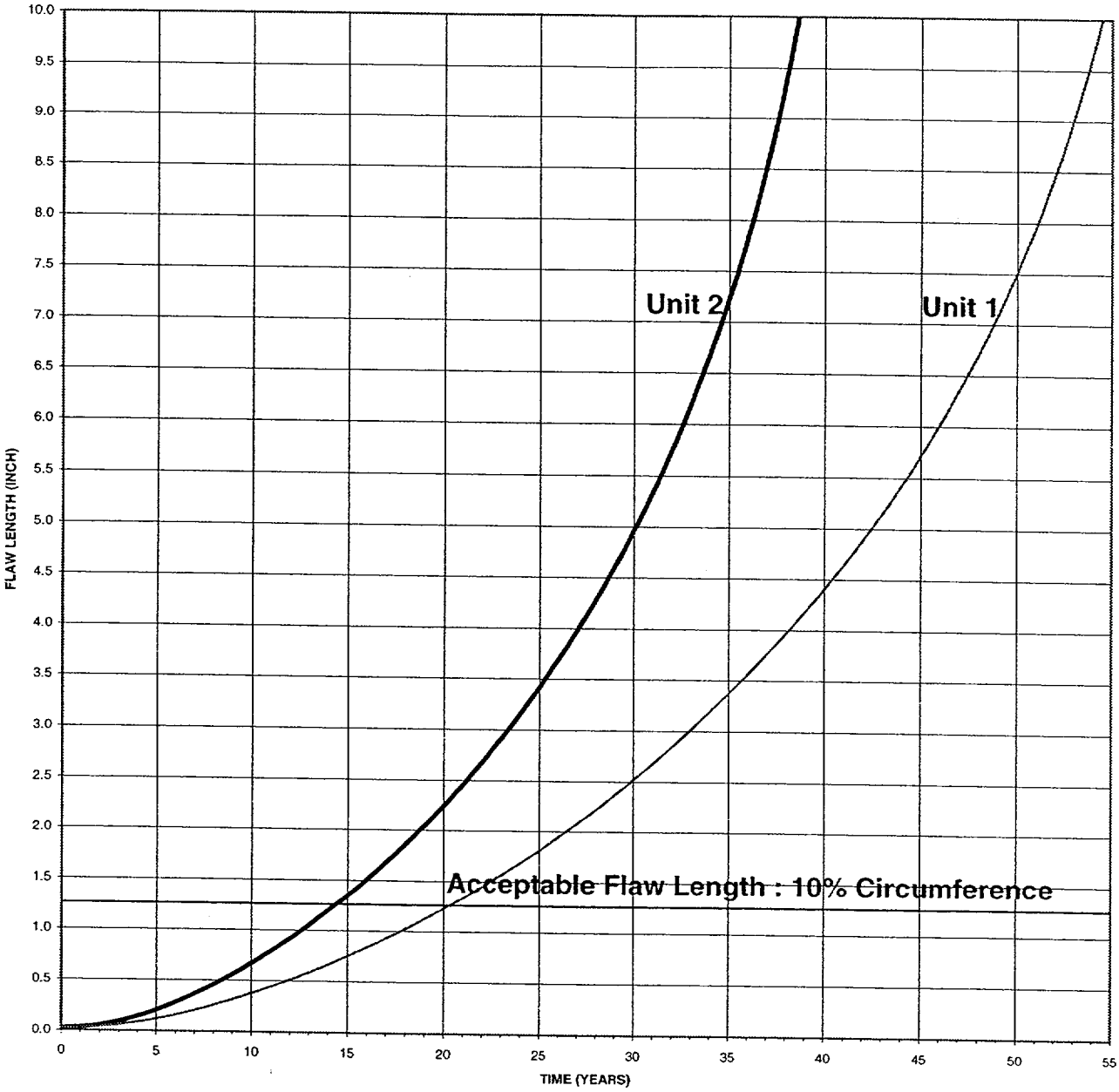

FIGURE 6-9

CRACK GROWTH PREDICTIONS FOR CIRCUMFERENTIAL THROUGH-WALL CRACKS NEAR THE TOP OF THE ATTACHMENT WELD

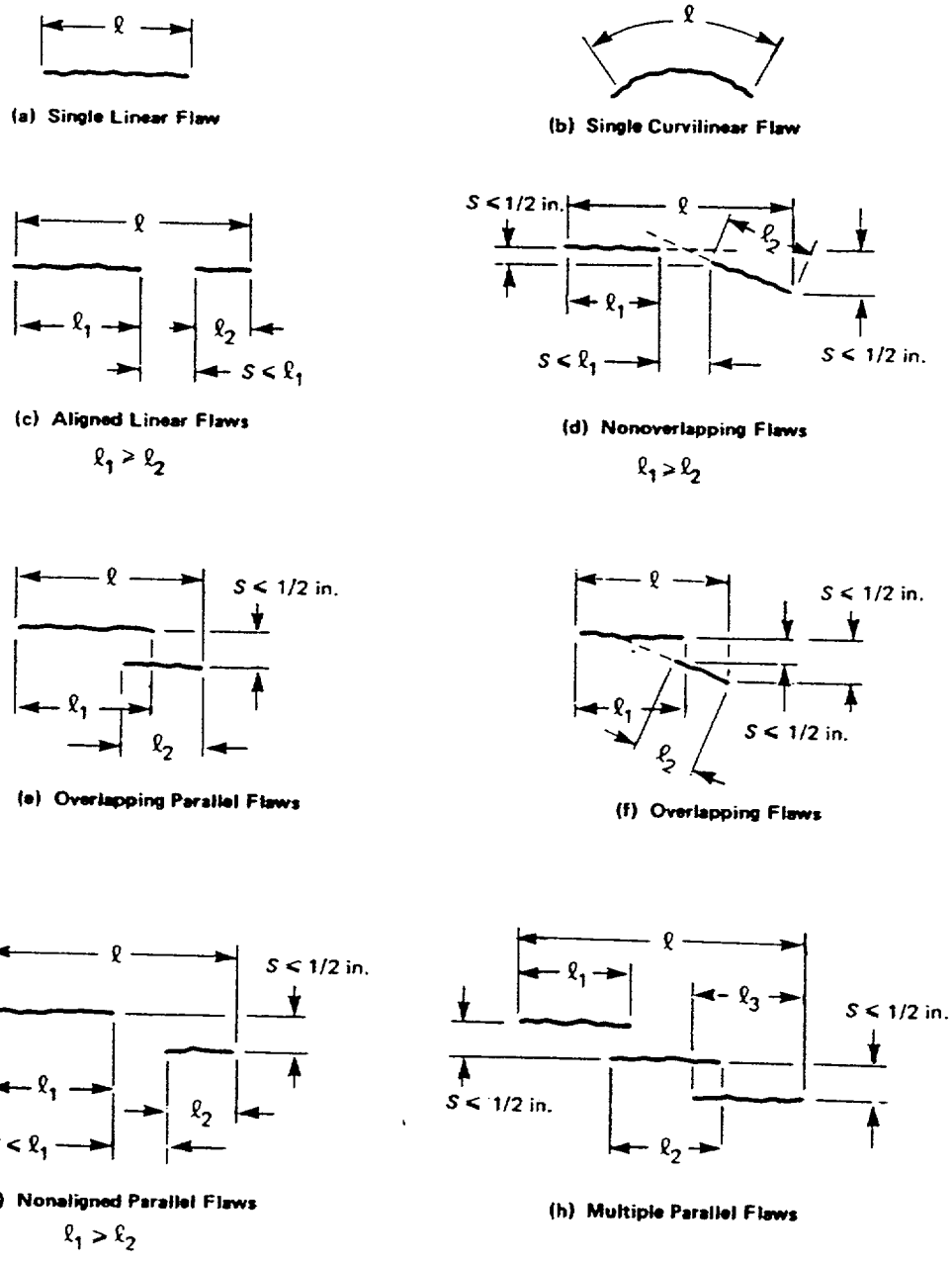

FIGURE 6-10

SECTION XI FLAW PROXIMITY RULES (FIGURE IWA-3400-1)

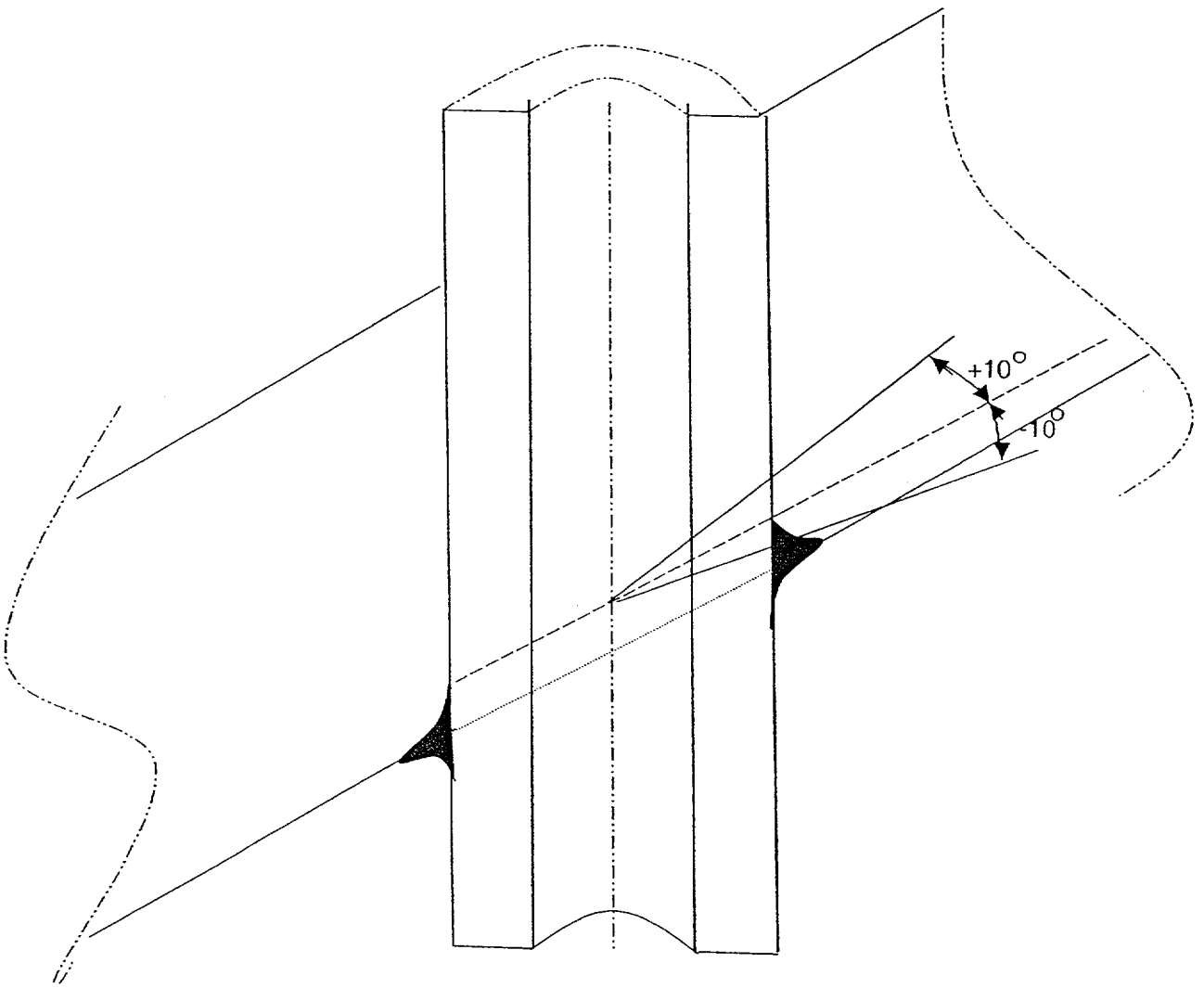

FIGURE 6-11

DEFINITION OF "CIRCUMFERENTIAL"

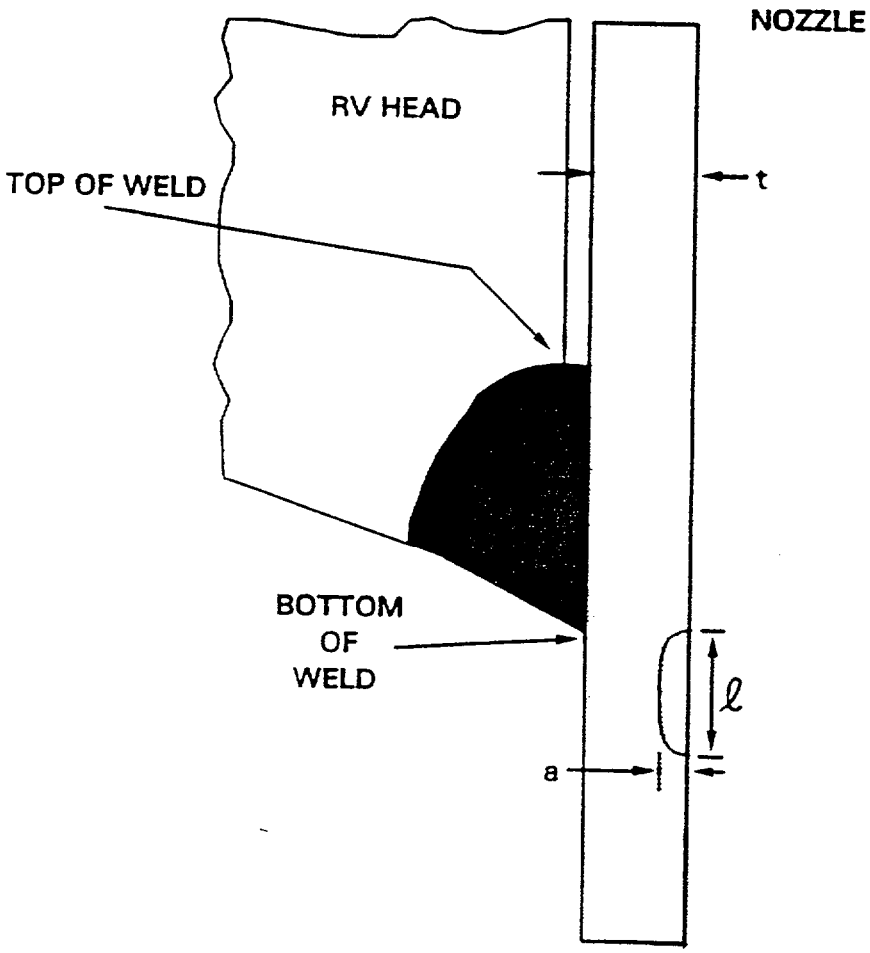

FIGURE 6-12

SCHEMATIC OF HEAD PENETRATION GEOMETRY

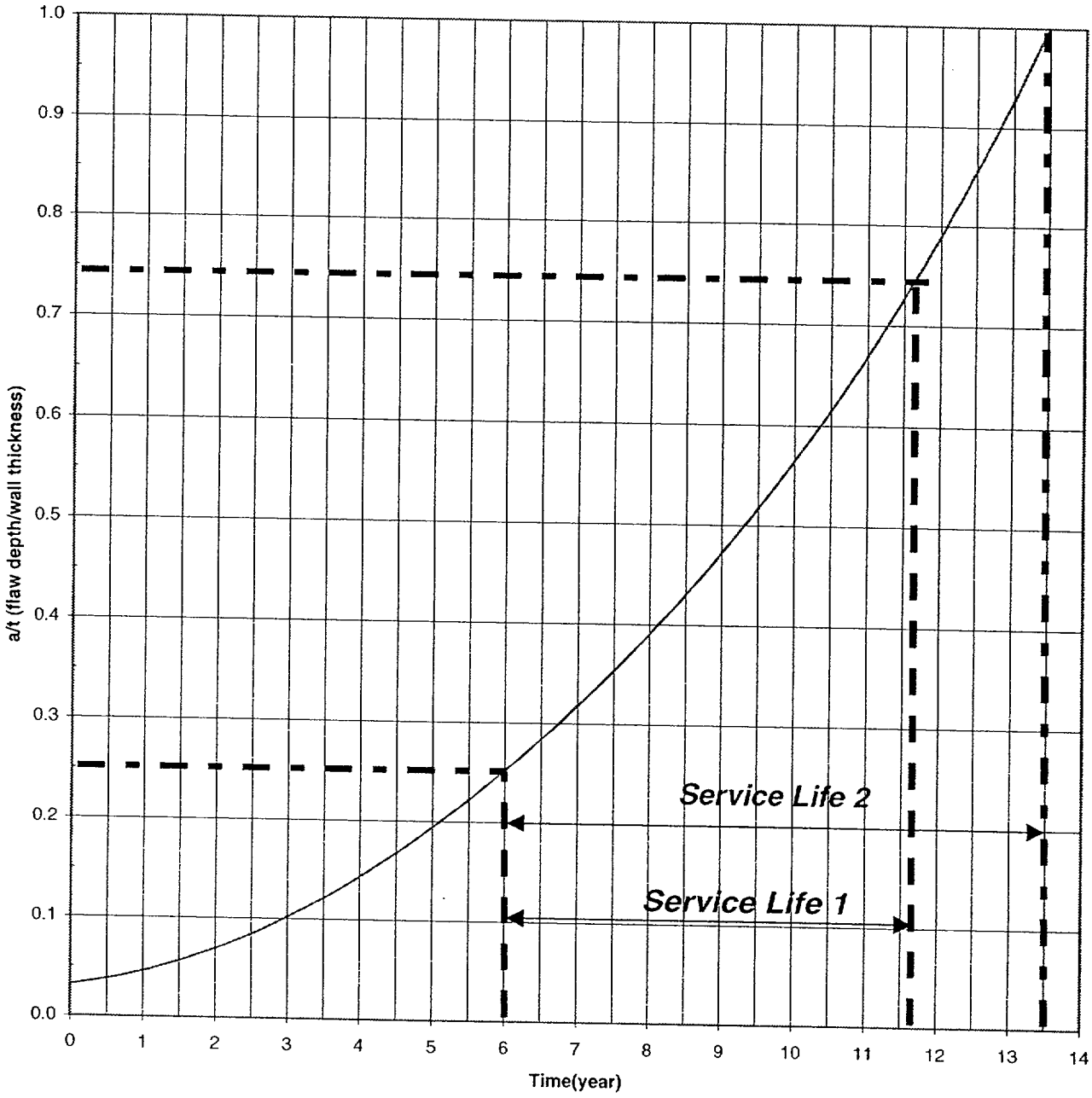

FIGURE 6-13

EXAMPLE PROBLEM 1

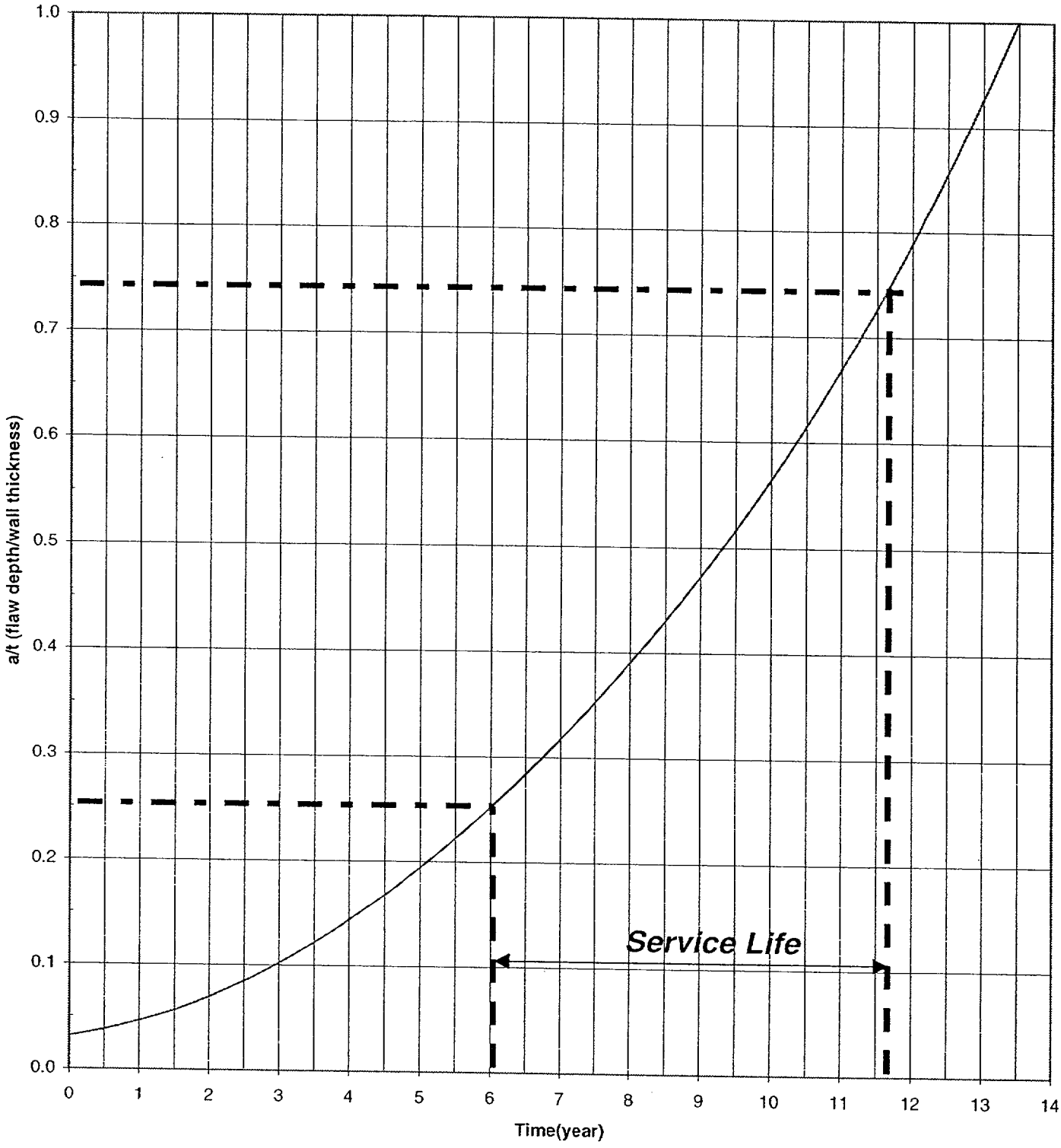

FIGURE 6-14

EXAMPLE PROBLEM 2

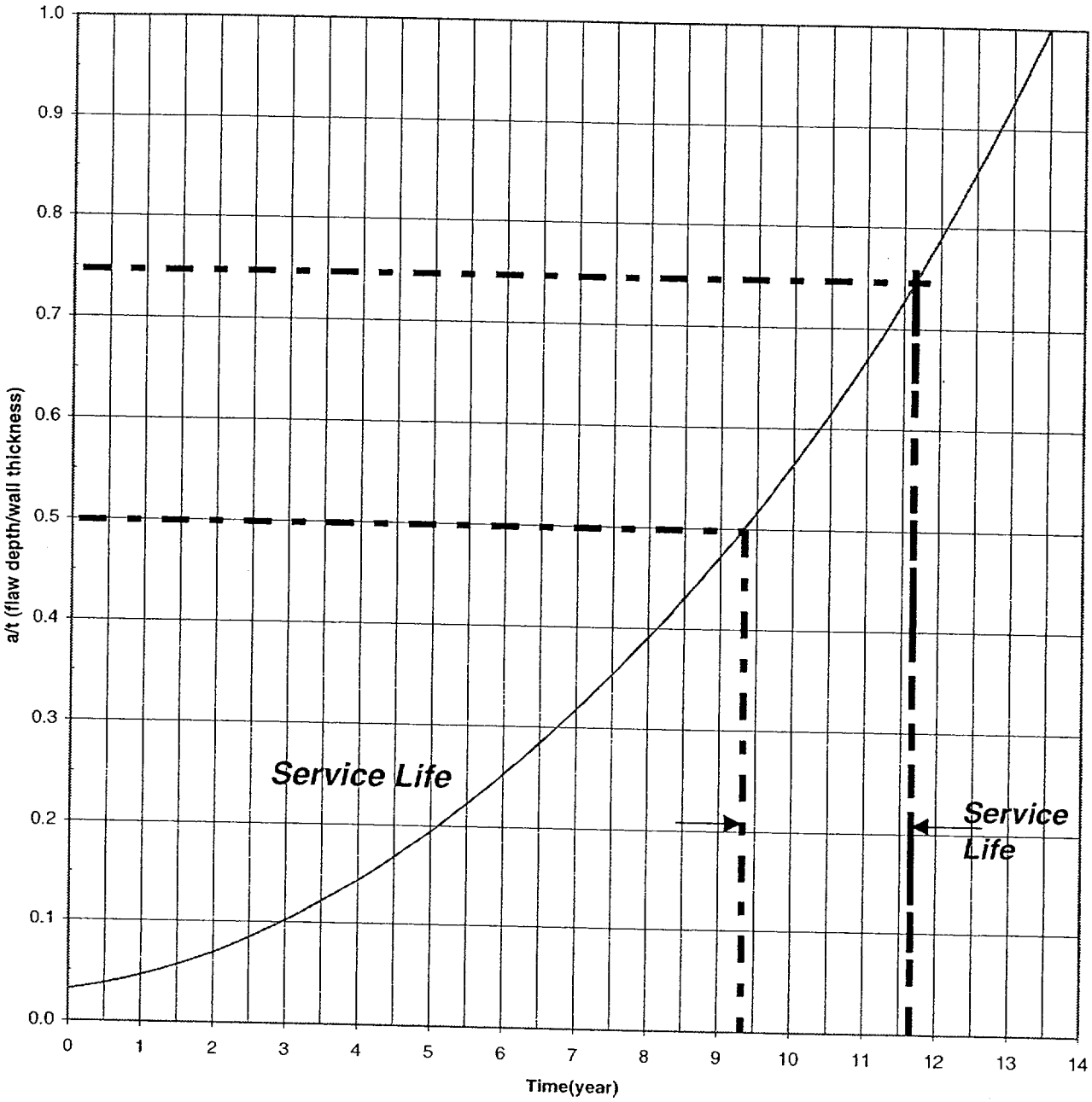

FIGURE 6-15

EXAMPLE PROBLEM 3

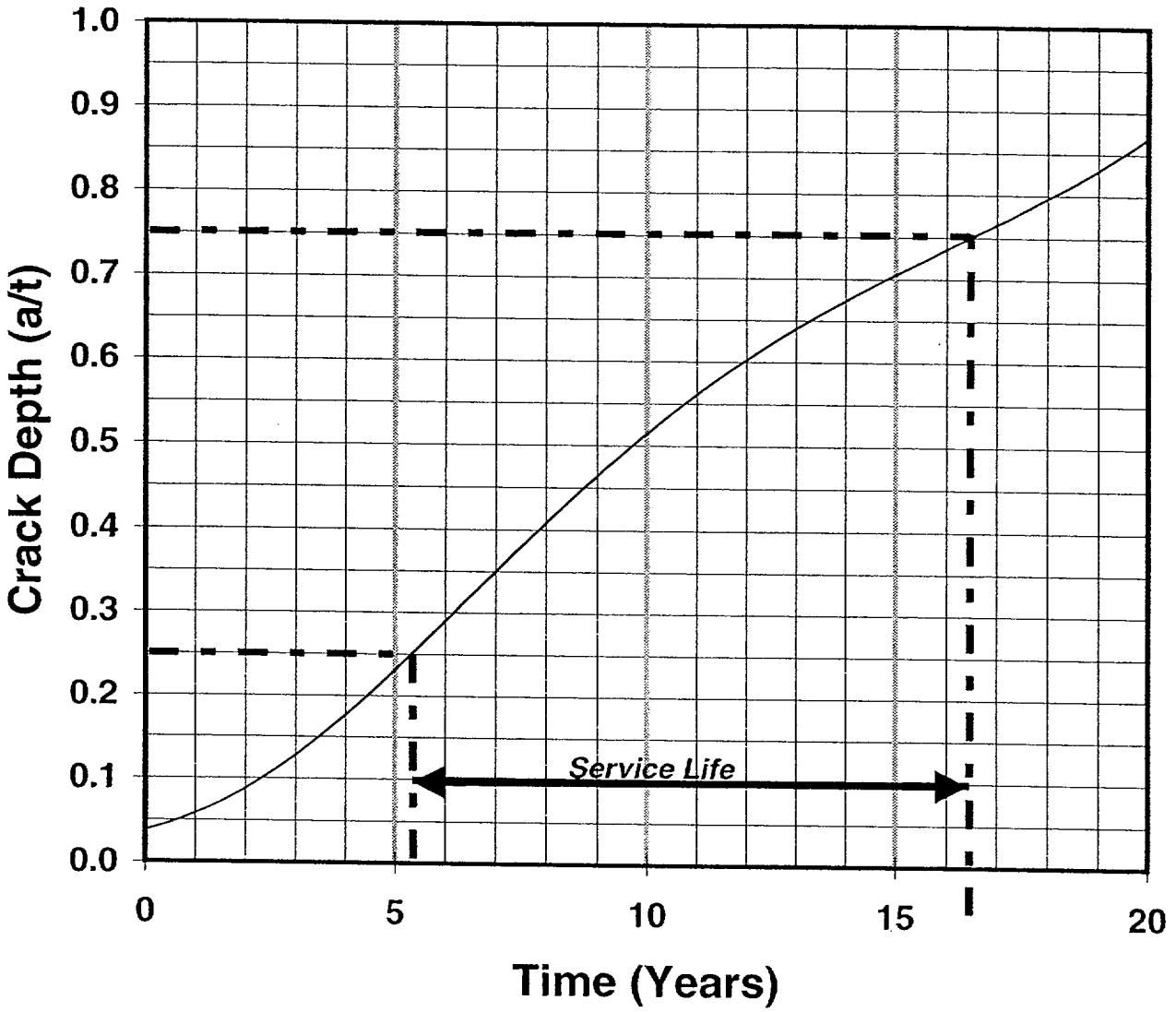

FIGURE 6-16

EXAMPLE PROBLEM 4

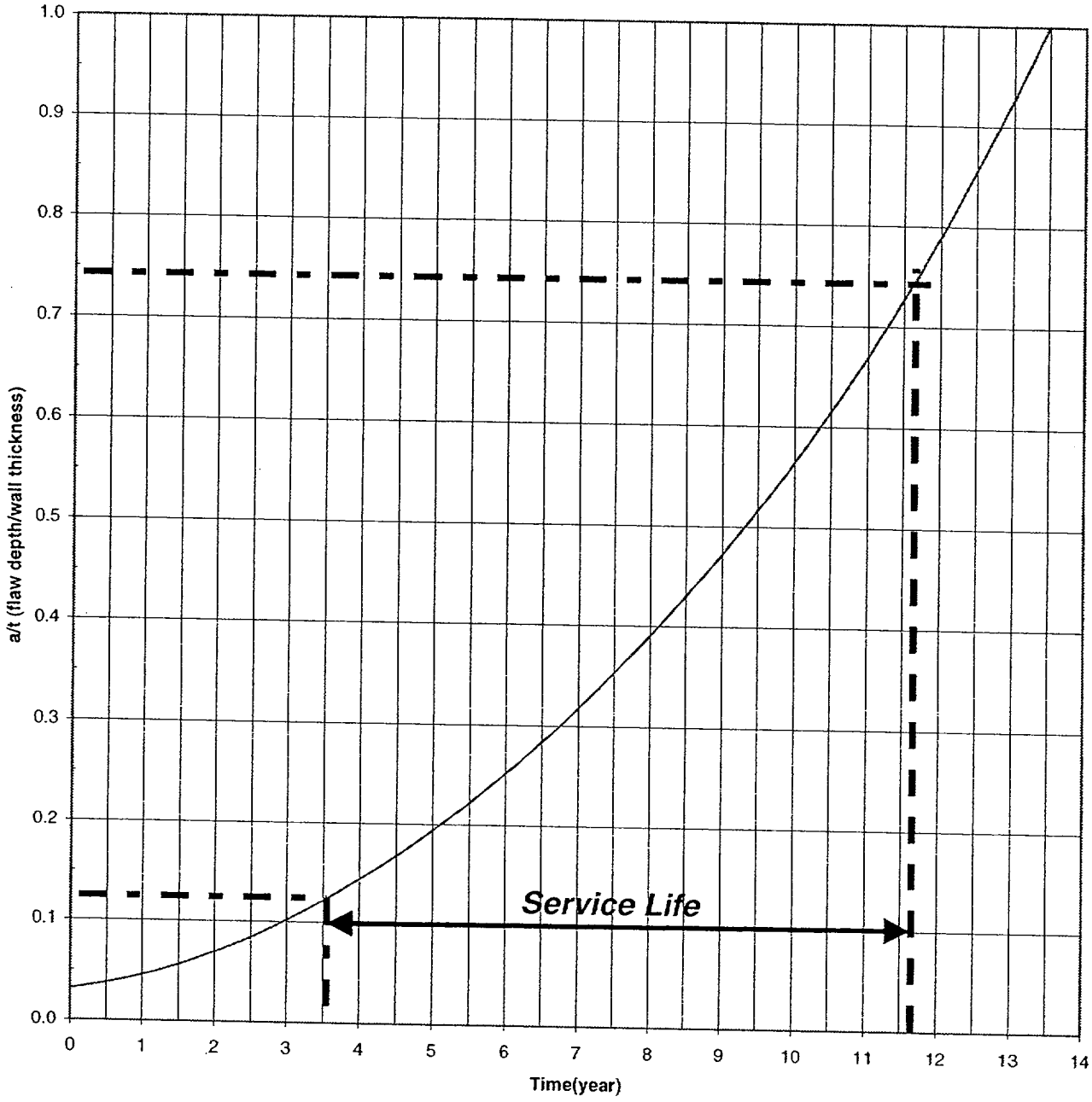

FIGURE 6-17

EXAMPLE PROBLEM 5

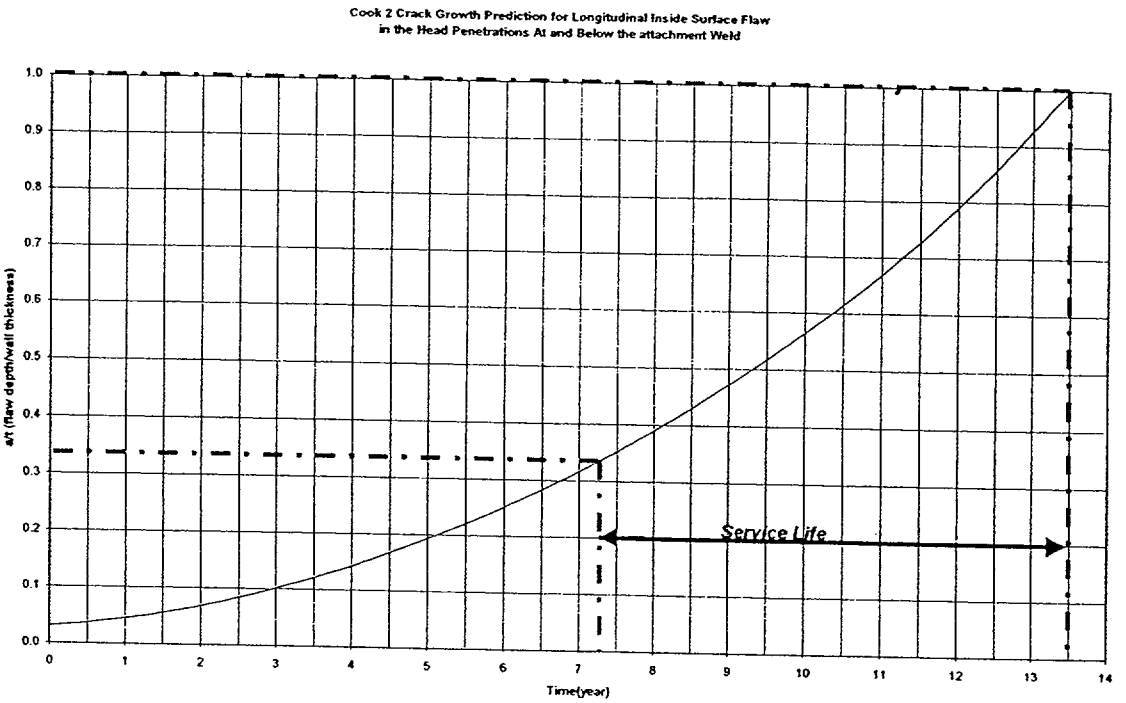

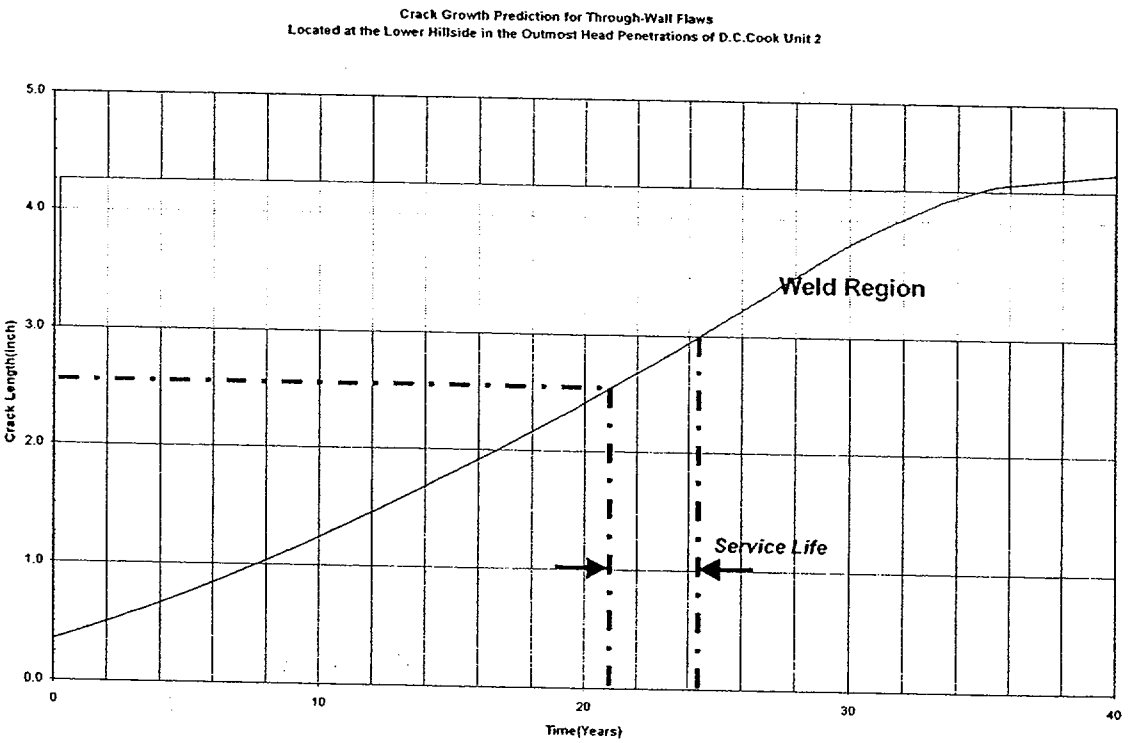

FIGURE 6-18

EXAMPLE PROBLEM 6

SECTION 7.0
SUMMARY AND CONCLUSIONS

An extensive evaluation has been carried out to characterize the loadings and stresses which exist in the head penetrations at D. C. Cook Units 1 and 2. Three-dimensional finite element models were constructed, and all pertinent loadings on the penetrations were analyzed [6]. These loadings included internal pressure and thermal expansion effects typical of steady state operation. In addition, residual stresses due to the welding of the penetrations to the vessel head were considered.

Results of the analyses reported here are consistent with the axial orientation and location of flaws which have been found in service in a number of plants, in that the largest stress component is the hoop stress, and the maximum stresses were found to exist in the circumferential locations nearest and farthest away from the center of the vessel. The most important loading conditions were found to be those which exist on the penetration for the majority of the time, which are the steady state loading and the residual stresses.

These stresses are important because the cracking which has been observed to date in operating plants has been determined to result from primary water stress corrosion cracking (PWSCC). These stresses were used in fracture calculations to predict the future growth of flaws postulated to exist in the head penetrations. A crack growth law was developed specifically for the operating temperature of the head at D. C. Cook Units 1 and 2, based on information from the literature as well as a compilation of crack growth results for operating plants.

The crack growth predictions contained in Section 6 show that the future growth of cracks which might be found in the penetrations will be very slow, and that a number of effective full power years will be required for any significant extensions.

Safety Assessment

It is appropriate to examine the safety consequences of an indication which might be found. The indication, even if it were to propagate through the penetration wall, would have only minor consequences, since the pressure boundary would not be broken, unless it were to propagate above the weld.

Further propagation of the indication would not change its orientation, since the hoop stresses in the penetration are much larger than the axial stresses. Therefore, it is extremely unlikely that the head penetration would be severed as a result of any indications.

If the indication were to propagate to a position above the weld, a leak could result, but the magnitude of such a leak would be very small, because the crack could not open significantly due to the tight fit between the penetration and the vessel head. Such a leak would have no immediate impact on the structural integrity of the system, but could lead to wastage in the ferritic steel of the vessel head, as the borated primary water concentrates due to evaporation.

Any indication is unlikely to propagate very far up the penetration above the weld, because the hoop stresses decrease in this direction, and this will cause it to slow down, and to stop before it reaches the outside surface of the head. This result supports the conclusion that it is extremely unlikely that leakage of any magnitude will occur.

The high likelihood that the indication will not propagate up the tube beyond the vessel head ensures that no catastrophic failure of the head penetration will occur, since the indication will be enveloped in the head itself, which precludes the opening of the crack and limits leakage.

SECTION 8
REFERENCES

1. Scott, P. M., "An Analysis of Primary Water Stress Corrosion Cracking in PWR Steam Generators," in Proceedings, Specialists Meeting on Operating Experience With Steam Generators, Brussels Belgium, Sept. 1991, pages 5, 6.

2. McIlree, A. R., Rebak, R. B., Smialowska, S., "Relationship of Stress Intensity to Crack Growth Rate of Alloy 600 in Primary Water," Proceedings International Symposium Fontevraud II, Vol, 1, p. 258-267, September 10-14, 1990.

3. Cassagne, T., Gelpi, A., "Measurements of Crack Propagation Rates on Alloy 600 Tubes in PWR Primary Water," in Proceedings of the 5th International Symposium on Environmental Degradation of Materials in Nuclear Power Systems-Water Reactors," August 25-29, 1991, Monterey, California.

4A. *Crack Growth and Microstructural Characterization of Alloy 600 PWR Vessel Head Pentration Materials,* EPRI, Palo Alto, CA. 1997. TR-109136.

4B. Vaillant, F. and C. Amzallag. "Crack Growth Rates of Alloy 600 in Primary Water," Presentation to the EPRI-MRP Crack Growth Rate (CGR) Review Team, Lake Tahoe, NV, August 10, 2001.

4C. Vaillant, F. and S. Le Hong. *Crack Growth Rate Measurements in Primary Water of Pressure Vessel Penetrations in Alloy 600 and Weld Metal 182,* EDF, April 1997. HT-44/96/024/A.

4C. Framatome laboratory data provided by C. Amzallag (EDF) to MRP Crack Growth Rate Review Team, October 4, 2001 (Proprietary to EDF).

4E. Cassagne, T., D. Caron, J. Daret, and Y. Lefevre. "Stress Corrosion Crack Growth Rate Measurements in Alloys 600 and 182 in Primary Water Loops Under Constant Load," *Ninth International Symposium on Environmental Degradation of Materials in Nuclear Power Systems-Water Reactors* (Newport Beach, CA, August 1-5, 1999), Edited by F. P. Ford, S. M. Bruemmer, and G. S. Was, The Minerals, Metals & Materials Society (TMS), Warrendale, PA, 1999.

4F. Studsvik laboratory data provided by Anders Jenssen (Studsvik) to MRP Crack Growth Rate Review Team, October 3, 2001 (Proprietary to Studsvik).

4G. [

]a,c,e

5A. McGowan, J. J. and Raymund, M., "Stress Intensity Factor Solutions for Internal Longitudinal Semi-elliptic Surface Flaw in a Cylinder Under Arbitrary Loading," ASTM STP 677, 1979, pp. 365-380.

5B. Newman, J. C. and Raju, I. S., "Stress Intensity Factor Influence Coefficients for Internal and External Surface Cracks in Cylindrical Vessels," in Aspects of Fracture Mechanics in Pressure Vessels and Piping, PVP Vol. 58, ASME, 1982, pp. 37-48.

6. [

]a,c,e

7. USNRC Letter, W. T. Russell to W. Raisin, NUMARC, "Safety Evaluation for Potential Reactor Vessel Head Adapter Tube Cracking," November 19, 1993.

8. USNRC Letter, A. G. Hansen to R. E. Link, "Acceptance Criteria for Control Rod Drive Mechanism Penetrations at Point Beach Nuclear Plant, Unit 1," March 9, 1994.

9. Letter from V. Vanderburg to B. Mickatavage, American Electric Power, "Best Estimate Hot Leg Temperature for D.C. Cook Unit 2," July 21, 1994.

10. Letter from V. Vanderburg to W. Bamford, American Electric Power, "Best Estimate Hot Leg Temperature for D. C. Cook Unit 1," October 14, 1994.

11. Donald C. Cook Nuclear Plant Units 1 and 2, NRC Bulletin 2001-01 Response (TAC Numbers MB2624 and MB2625), September 4, 2001.

APPENDIX A

ALLOWABLE AREAS OF LACK OF FUSION: WELD FUSION ZONES

There are two fusion zones of interest for the head penetration attachment welds, the penetration itself (Alloy 600) and the reactor vessel head material (A533B ferritic steel). The operating temperature of the upper head region of the D. C. Cook Unit 1 is 303°C (578°F) Unit 2 is 316°C (601°F), so both materials will be very ductile. The toughness of both materials is quite high, so any flaw propagation along either of the fusion zones will be totally ductile.

Two calculations were completed for the fusion zones, one for the critical flaw size, and the second for the allowable flaw size, which includes the margins required in the ASME code. The simpler case is the Alloy 600 fusion zone, where the potential failure will be a pure shearing of the penetration as the pressurized penetration tube is forced outward from the vessel head, as shown in Figure A-1.

The failure criterion will be that the average shear stress along the fusion line exceeds the limit shear stress. For the critical flaw size, the limiting shear stress is the shear flow stress, which is equal to half the tensile flow stress, according to the Tresca criterion. The tensile flow stress is the average of the yield stress and ultimate tensile stress of the material. The criterion for Alloy 600 at 318°C (604°F) is:

$$\text{Average shear stress} < \text{shear flow stress} = 26.85 \text{ ksi}$$

This value was taken from the ASME Code, Section III, Appendix I, at 600°F.

For each penetration, the axial force which produces this shear stress results from the internal pressure. Since each penetration has the same outer diameter, the axial force is the same. The average shear stress increases as the load carrying area decreases (the area of lack of fusion increases). When this increasing lack of fusion area increases the stress to the point at which it equals the flow stress, failure occurs. This point may be termed the critical flaw size. This criterion is actually somewhat conservative. Alternatively, use of the Von Mises failure criterion would have set the shear flow stress equal to 60 percent of the axial flow stress, and would therefore have resulted in larger critical flaw sizes.

The allowable flaw size, as opposed to the critical flaw size discussed above, was calculated using the allowable limit of Section III of the ASME Code, paragraph NB 3227.2. The criterion for allowable shear stress then becomes:

$$\text{Average shear stress} < 0.6\ S_m = 13.98 \text{ ksi}$$

where S_m = the ASME Code limiting design stress from Section III, Appendix I.

The above approach was used to calculate the allowable flaw size and critical flaw size for the outermost and center penetrations. The results show that a very large area of lack of fusion can be tolerated by the head penetrations, regardless of their orientation. These results can be illustrated for the outermost presentation.

The total surface contact area for the fusion zone on the outermost head penetration is 17.4 in^2. The calculations above result in a required area to avoid failure of only 1.45 in^2, and using the ASME Code criteria, the area required is 2.79 in^2. These calculations show that as much as 83.9 percent of the weld may be unfused, and the code acceptance criteria can still be met.

To envision the extent of lack of fusion which is allowable, Figure A-2 was prepared. In this figure, the weld fusion region for the outermost penetration has been shown in an unwrapped, or developed view. The figure shows the extent of lack of fusion which is allowed, in terms of limiting lengths for a range of circumferential lack of fusion. This figure shows that the allowable vertical length of lack of fusion for a full circumferential unfused region is 84 percent of the weld length. Conversely, for a region of lack of fusion which extends the full vertical length of the weld, the circumferential extent is limited to 302 degrees. The extent of lack of fusion which would cause failure is labelled "critical" on this figure, and is even larger. The dimensions shown on this figure are based on an assumed rectangular area of lack of fusion.

The full extent of this allowable lack of fusion is shown in Figure A-3, where the axes have been expanded to show the full extent of the tube-weld fusion line. This figure shows that a very large area of lack of fusion is allowable for the outer most penetration. Similar results were found for the center penetration, where the weld fusion area is somewhat smaller at 16.1 in^2.

A similar calculation was also carried out for the fusion zone between the weld and the head, and the result is shown in Figure A-4. The allowable area of unfused weld for this location is 84.8 percent of the total area. This approach to the fusion zone with the carbon steel head is only approximate, but may provide a realistic estimate of the allowable. Note that even a complete lack of fusion in this region would not result in rod ejection, because the weld to the tube would prevent the tube from moving up through the vessel head.

The allowable lack of fusion for the weld fusion zone to the head may be somewhat in doubt, because of the different geometry, where one cannot ensure that the failure would be due to pure shear. To investigate this concern, additional finite element models were constructed with various degrees of lack of fusion discretely modeled, ranging from 30 to 65 percent. The stress intensities around the circumference of the penetration were calculated, to provide for the effects of all stresses, as opposed to the shear stress only, as used above. When the average stress intensity reaches the flow stress (53.7 ksi), failure is expected to occur. The code allowable stress intensity is 1.5 Sm, or 35 ksi, using the lower of the Alloy 600 and ferritic allowables at 316°C (600°F).

The results of this series of analyses are shown in Figure A-5, where it is clear that large areas of lack of fusion are allowable. As the area of lack of fusion increases, the stresses redistribute themselves, and the stress intensity does not increase in proportion to the area lost. These results seem to confirm that the shear stress is the only important stress governing the critical flaw size for the head fusion zone as well.

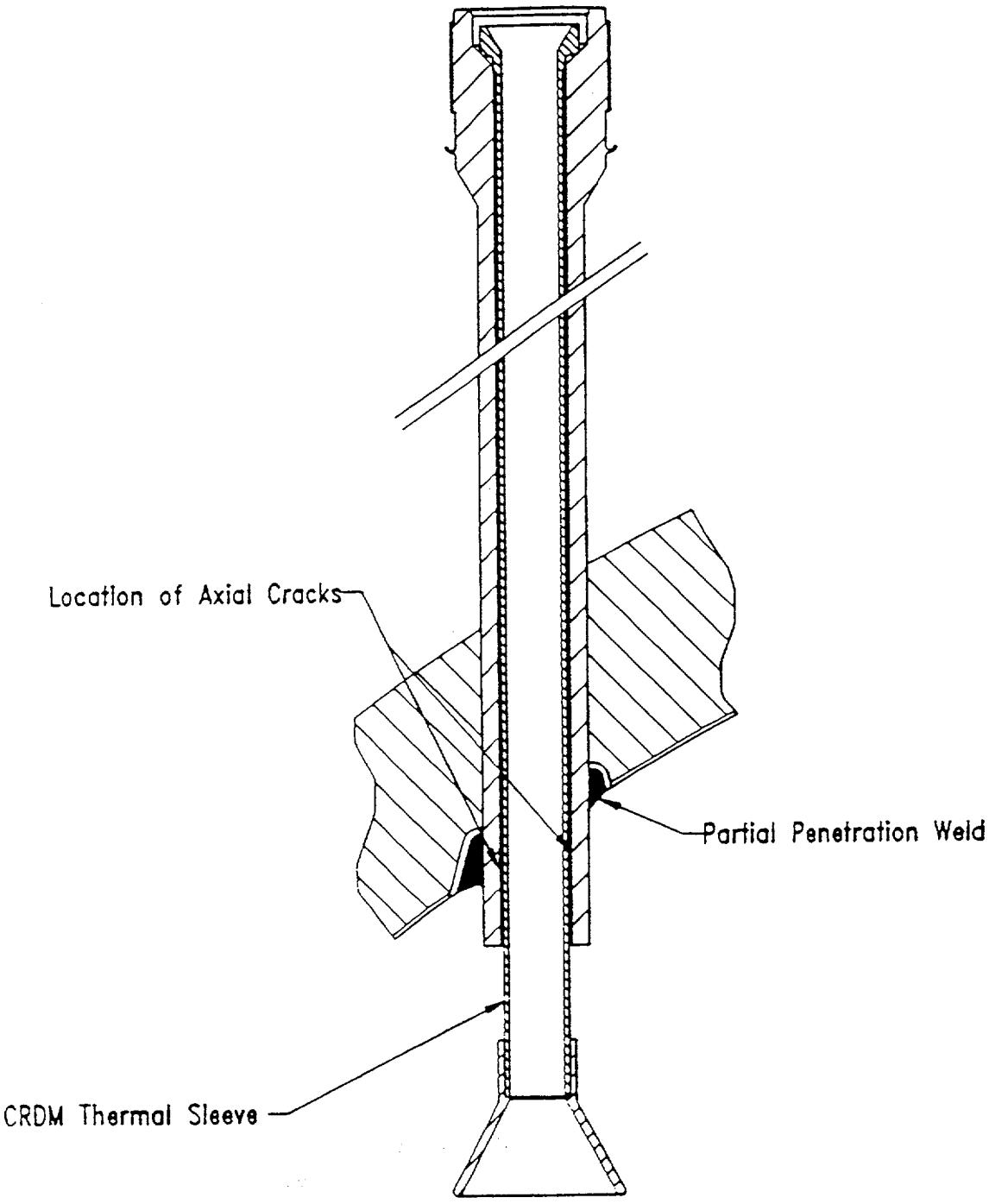

Figure A-1 Typical Head Penetration

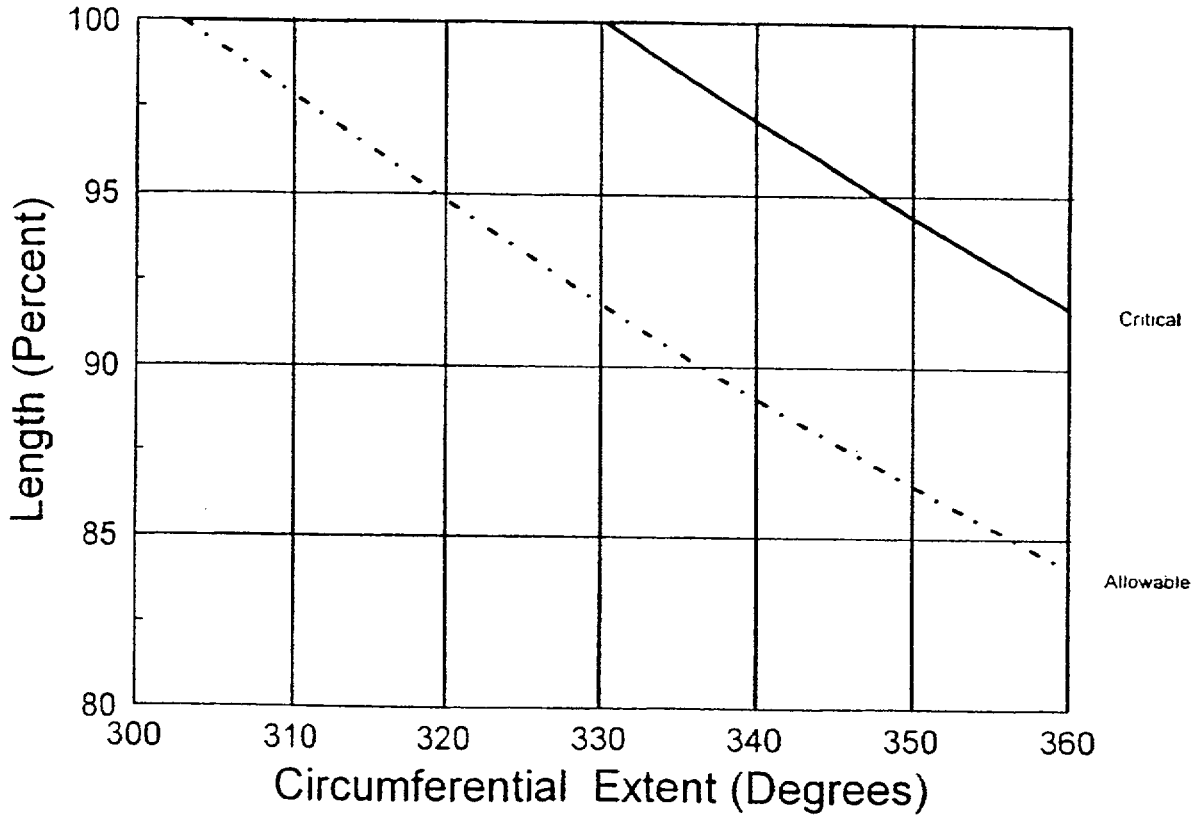

Figure A-2 Allowable Regions of Lack of Fusion for the Outermost Penetration Tube to Weld Fusion Zone: Detailed View.

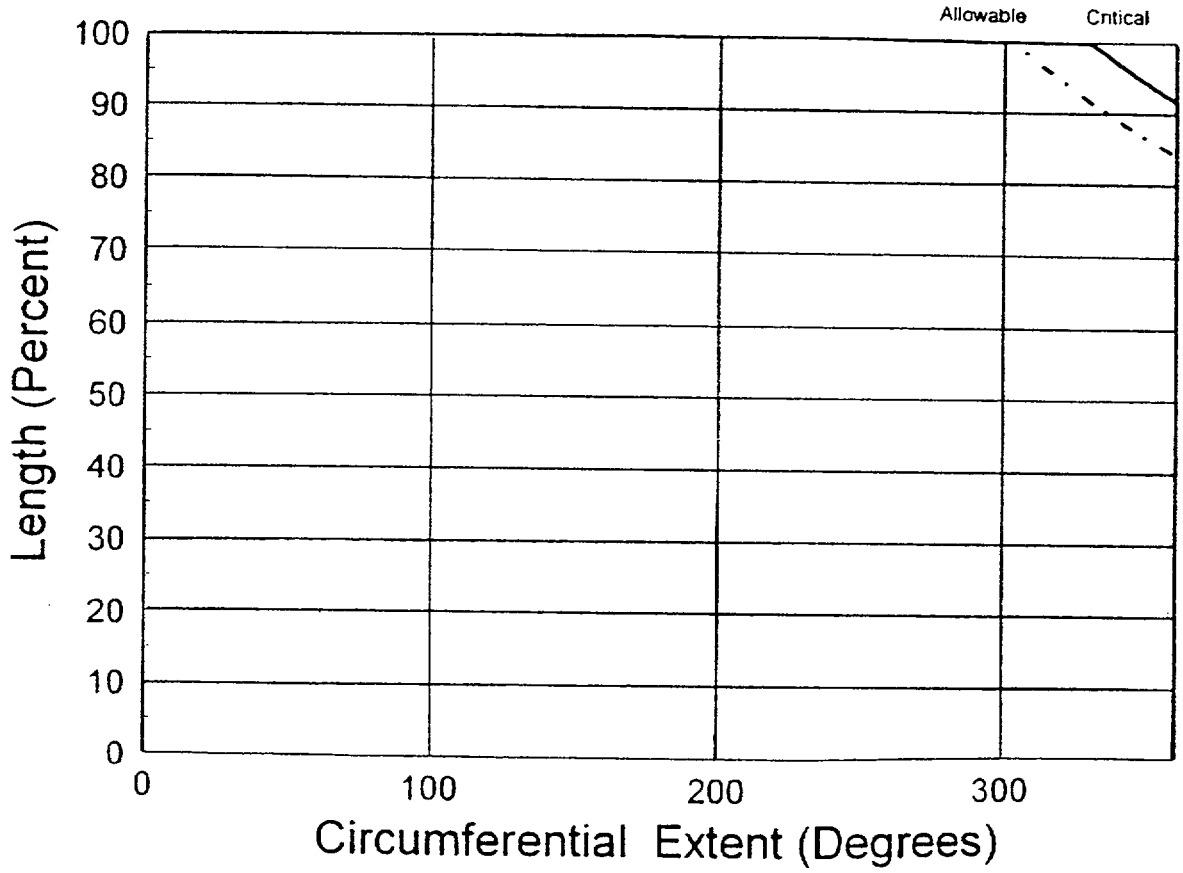

Figure A-3 Allowable Regions of Lack of Fusion for the Outermost Penetration Tube to Weld Fusion Zone.

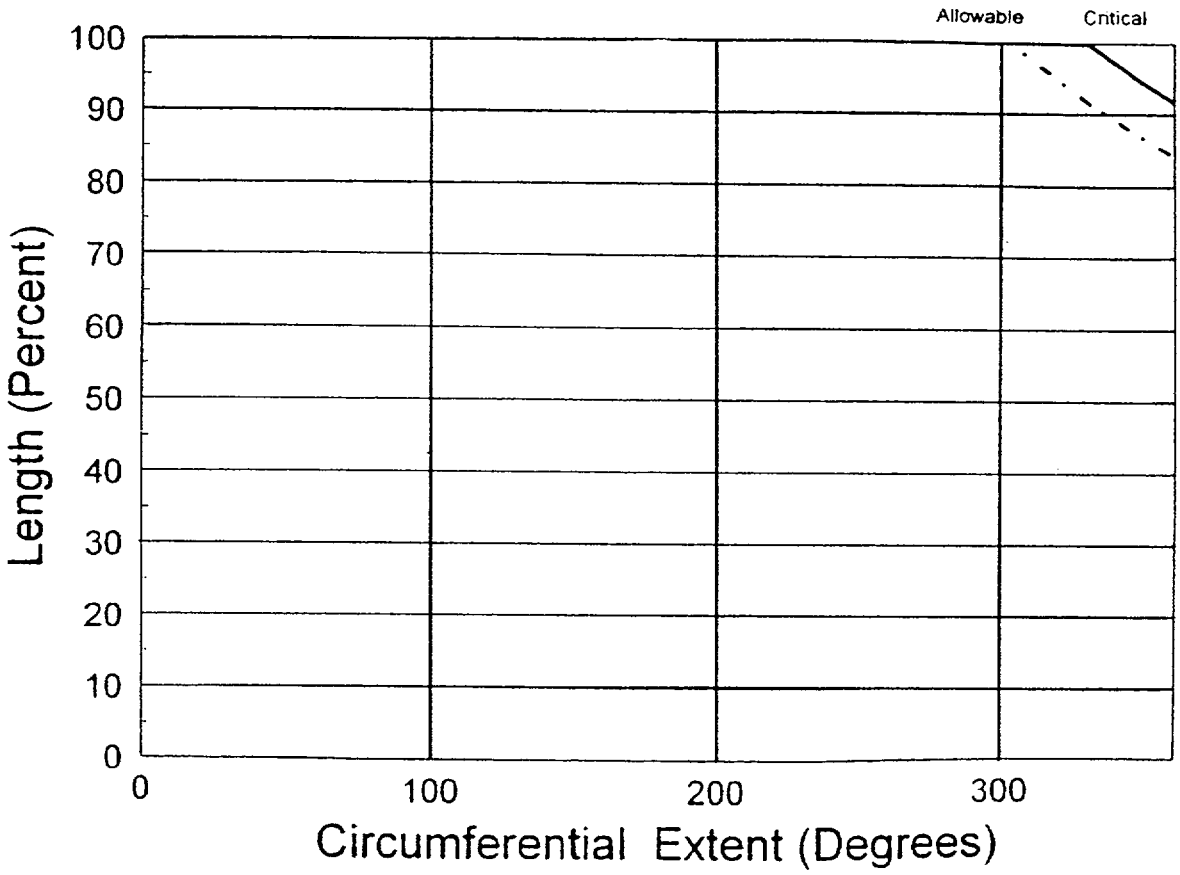

Figure A-4 Allowable Regions of Lack of Fusion for All Penetrations: Weld to Vessel Fusion Zone.

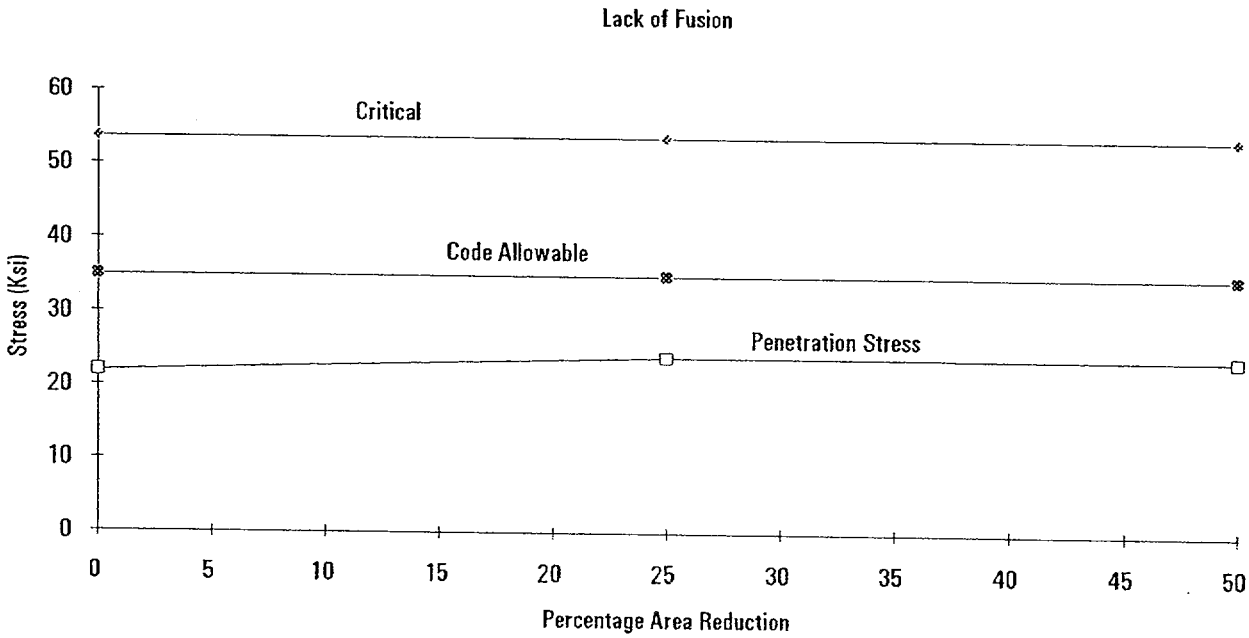

Figure A-5. Allowable Regions of Lack of Fusion for the Weld to Vessel Fusion Zone.